

COMITÉ DE RÉDACTION

Rédacteur en chef:

EUGEN A. PORA, membre de l'Académie de la République Socialiste de Roumanie

Rédacteur en chef adjoint:

RADU CODREANU, membre de l'Académie de la République Socialiste de Roumanie

Membres:

MIHAI BĂCESCU, NICOLAE BOTNARIUC, TEODOR BUȘNIȚĂ, membres correspondants de l'Académie de la République Socialiste de Roumanie; P<sup>r</sup> ILIE DICULESCU; GR. ELIESCU, M. A. IONESCU, membres correspondants de l'Académie de la République Socialiste de Roumanie; P. JITARIU, membre de l'Académie de la République Socialiste de Roumanie; OLGA NECRASOV, membre correspondant de l'Académie de la République Socialiste de Roumanie; VICTOR PREDA, membre de l'Académie de la République Socialiste de Roumanie; GH. V. RADU, LUDOVIC RUDESCU, membres correspondants de l'Académie de la République Socialiste de Roumanie; GRIGORE STRUNCARU; RADU MEȘTER, secrétaire de rédaction.

Le «Revue Roumaine de Biologie» paraît quatre fois par an. Toute commande de l'étranger (fascicules ou abonnements) sera adressée à ILEXIM, Département d'exportation-importation (Presse), Boîte postale 2001, Calea Griviței 64-66, Bucarest 12, Roumanie, ou à ses représentants à l'étranger.

Les manuscrits, les livres et les publications proposés en échange, ainsi que toute correspondance seront envoyés à la rédaction.

REVUE ROUMAINE DE BIOLOGIE  
Calea Victoriei 125, Sector I  
București, Românie, Tel. 50.76.80

EDITURA ACADEMIEI  
REPUBLICII SOCIALISTE ROMÂNIA  
Calea Victoriei 125, Sector I  
București, Românie, Tel. 50.76.80

REVUE ROUMAINE DE  
BIOLOGIE

SÉRIE DE BIOLOGIE ANIMALE

TOME 20

1975

N° 4

SOMMAIRE

Z. FEIDER, Une nouvelle larve de <i>Trombidia</i> : <i>Atractothromboides danubialis</i> n.g., n.sp. . . . .	223
IONEL P. PETCU and VIORICA HONCIUC, Contributions to the study of the female external genital complex in Ophionidae (Hym. Ichneumonidae) . . . . .	229
CONSTANTINA SORESCU, Osteological studies in some Cyprinid fishes in relation to their phylogeny (Pisces, Cyprinidae) . . . . .	237
ELENA CHIRIAC, ȘTEFANIA BOLDOR et ELENA VĂDINEANU, Un cas d'hyperparasitisme chez la perche ( <i>Perca fluviatilis</i> L.) . . . . .	241
ELENA TRACIUC, Les glandes séricigènes chez certaines araignées «Haplogynes» . . . . .	245
ROLAND BAUCHOT, MARIA CALOIANU-IORDĂCHEL, MONIQUE DIAGNE et JEAN-MARC RIDET, L'encéphale d' <i>Acipenser ruthenus</i> Linné 1758 (Pisces, Chondrostei, Acipenseridae). Étude quantitative préliminaire . . . . .	249
A. GOPALAKRISHNA and K. B. KARIM, Development of the foetal membranes in the Indian leaf-nosed bat, <i>Hipposideros fulvus fulvus</i> (Gray) II. Morphogenesis of the foetal membranes and placentation. . . . .	257
MATILDA JITARIU, ELENA CHERA, ECATERINA DUCA, GABRIELA LINCK, PINCU ROTIMBERG and ISTVÁN SZILAGYI, Lipido-carotenoid metabolism in <i>Salmo gairdneri</i> during embryogenesis . . . . .	269
CORNELIA GEORMĂNEANU, The karyotype of urodele amphibian <i>Triturus montandoni</i> . . . . .	275
MARGARETA MANOLACHE, Chromosome complement characterization by G-banding in <i>Gallus domesticus</i> . . . . .	281
MIHAI CRUCE et ION RĂDUCAN, Cycle d'activité chez la tortue terrestre ( <i>Testudo hermanni hermanni</i> Gmel.) . . . . .	285
COMPTE RENDU . . . . .	291
INDEX ALPHABÉTIQUE . . . . .	293

REVUE ROUMAINE DE  
BIOLOGIE

REVUE DE BIOLOGIE ANIMALE

TOME 20

SOMMAIRE

UNE NOUVELLE LARVE DE TROMBIDIA :  
*ATRACTOTHROMBOIDES DANUBIALIS* n.g., n.sp.

PAR  
Z. FEIDER

The author describes a new genus and a new species *Atractothromboides danubialis* characterized by the shield and the number of the claws of the legs.

Parmi les acariens de la famille *Microtrombidiidae* Feider, 1959 nous avons décrit, dans les stades adulte et larvaire, le genre *Atractothrombium* Feider, 1952 avec deux espèces *A. fusicomum* (Berlese, 1910) et *A. transsylvanicum* Feider, 1950.

Dans une collection d'acariens, obtenue par l'amabilité de N. Vasiliu, nous avons trouvé plusieurs spécimens d'une larve qui par plusieurs caractères, à savoir l'écusson du prodorsum (scutum), la forme des coxes et la pilosité des coxes et de l'idiosome, ressemble au genre *Atractothrombidium*. Toutefois, par deux caractères importants, la forme de l'écusson du prodorsum (scutum) et le nombre réduit des griffes des deux premières paires de pattes, la nouvelle larve en diffère. Le scutum, au lieu d'être entier, comme dans le genre mentionné, est divisé par une ligne chitineuse transversale qui passe en arrière des poils AA. D'autre part, au lieu d'avoir deux griffes et un empodium à chaque patte des trois paires, comme le genre *Atractothrombium*, la larve possède seulement deux griffes dépourvues d'empodium aux deux premières paires de pattes. La troisième paire de pattes présente deux griffes et un empodium.

Nous considérons que par ces différences l'espèce nouvelle appartient à un nouvel genre *Atractothromboides* n.g. nommé ainsi pour rappeler la ressemblance avec le genre *Atractothrombium*, et à une nouvelle espèce *Atractothromboides danubialis* n.sp., collectée dans une localité du voisinage du Danube.

Espèce type *Atractothromboides danubialis* n.g.n.sp.

Les dimensions du corps et des parties du corps sont notées dans le tableau 1.

L'idiosome est elliptique fusiforme, arrondie à ses deux extrémités (Pl. I, fig. 1).

L'écusson antérieur ou scutum, plus large au niveau de son milieu, a les bords latéraux excavés dans le tiers postérieur. L'extrémité antérieure, où sont fixés les poils AA, est séparée du reste par une ligne transversale.

Le second écusson, ou scutellum, est elliptique.

Les dimensions des poils et les dimensions des intervalles entre les poils de deux écussons sont les suivantes :

AA	AW	SB	PW	ASB	PSB	MA	AP	SD	AM	AL	PL	S	LSS	SH	SS	SL
35	68	44	76	95	29	52	55	124	35	61	52	73	90	25	37	64

Tableau 1

Dimensions, en microns, de *A. danubialis*

Organe	Dimensions		Organe	Dimensions	
1. Idiosome	L	247	9. Membrane buccale	D	23
	l	116		H	87
2. Scutum	L	104	10. Distance inter-strobiliaire	L	11
	l	96			
3. Scutellum	L	90	11. Palpe	L	49
	l	52		l	23
4. Écusson oculaire	L	29	12. Palpotarse	L	8,7
	l	15		l	5,8
5. Lentille I	D	12	13. Poil long du palpotarse	L	35
	D	6			
6. Poils dorsaux	L	29-63	14. Chélicère	Total	L 78
	L	21-43		Griffe	L 17
	L	46		Appendice	L 15
7. Gnathosome	L	79	15. Patte	I	L 267
	l	58		II	L 244
8. Anneau buccal	D	20		III	L 264
	H	4			

Abréviations : L = longueur, l = largeur, D = diamètre, H = hauteur.

Sur la partie dorsale les poils, barbelés, fixés sur un écusson ovalaire, sont disposés en cinq rangées contenant 6, 4, 6, 6, et 2 poils.

Les écussons des yeux, fixés au niveau des poils postérieurs du cutum, sont plus larges en avant.

Sur la face ventrale on observe les prolongements inférieurs triangulaires du scutum. Autour de l'uropore sont fixées trois paires de poils barbelés, dont la dernière est fixée sur des écussons (Fig. 2).

Le gnathosome présente un anneau chitineux festonné et concentriquement à l'anneau une membrane caractéristique au genre (Pl. II, fig. 3, 4). Sur la face ventrale on observe une paire de poils galeux lisses et une paire de poils élargis digités, les strobili.

Les chélicères ont le corps plus large en arrière. Le doigt mobile est mince et courbé, tandis que le doigt fixe est tronqué (Fig. 5). L'appendice, ou apodème, est courbé.

Fig. 1. — Corps, vue dorsale ; fig. 2. — corps, vue ventrale.

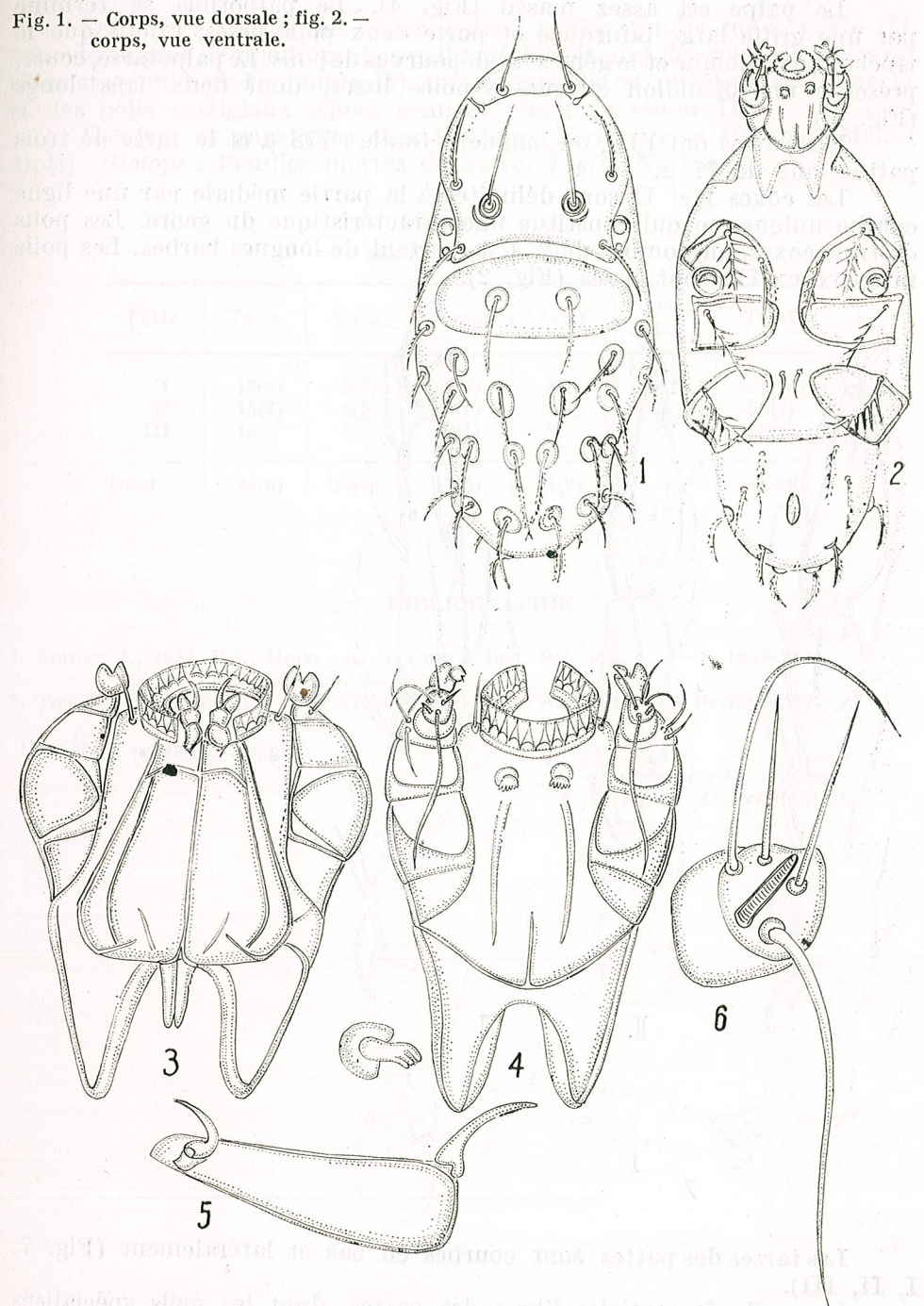


Fig. 3. — Gnathosome, vue dorsale ; fig. 4. — gnathosome, vue ventrale ; fig. 5. — chélicères ; fig. 6. — palpotarse.

Le palpe est assez massif (Fig. 4). Le palpotibia se termine par une griffe large bifurquée et porte deux poils lisses, tandis que le trochanter, le fémur et le génu sont dépourvus de poils. Le palpotarse, court, présente un solénidion et quatre poils lisses, dont deux très longs (Fig. 6.)

Les pattes ont l'IP, ou longueur totale : 778  $\mu$  et le tarse de trois pattes long de 77  $\mu$ .

Les coxes I et II sont délimitées à la partie médiale par une ligne courbe unique, ce qui constitue une caractéristique du genre. Les poils de trois coxes, en nombre de 2, 1, 1, portent de longues barbes. Les poils intercoxaux III sont lisses (Fig. 2).

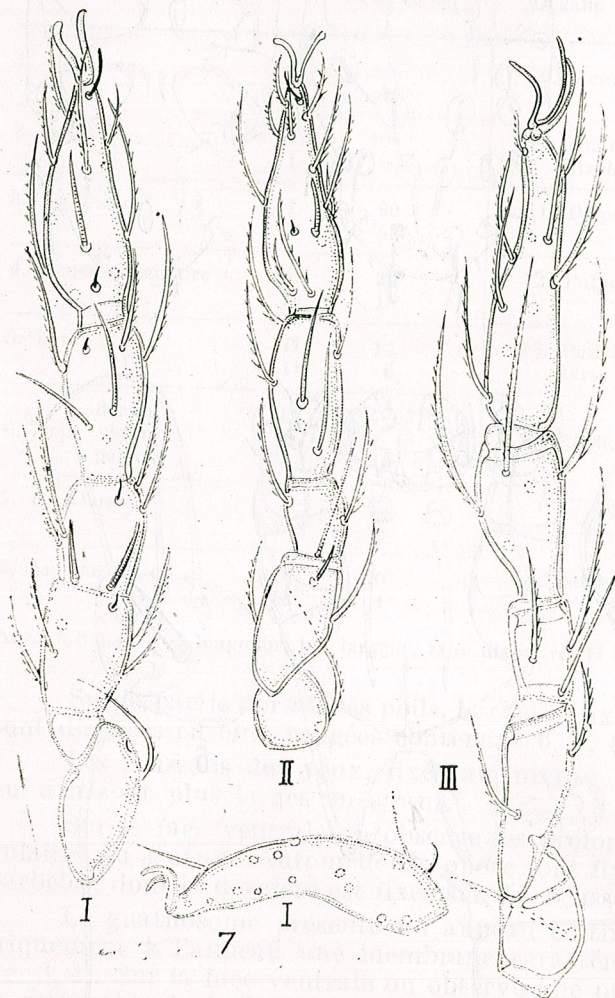


Fig. 7. — Pattes I, II, III.

Les tarsi des pattes sont courbés en bas et latéralement (Fig. 7, I, II, III).

Les poils des articles libres des pattes, dont les poils spécialisés sont en parenthèse, sont notés dans le tableau 2.

Les pattes I et II ont chacune deux griffes, tandis que le patte III possède en plus l'empodium. Les poils spécialisés sont des solénidions (tars, tibia et génu I et II, fémur II), une eupathidie et un famulus (tarse I) et des poils vestigiaux (tibia, génu et fémur I; fémur II).

*Holotype* et paratypes chez l'auteur. *Terra typica* Dubova (Mehe-dinți). *Biotope* : Feuilles mortes de hêtre. *Legit* : N. Vasiliu.

Tableau 2

Nombre des poils des pattes

Patte	Tarse	Tibia	Génu	Fémur	Trochan-ter	Total
I	18(3)	9(3)	7(3)	6(1)	1	41(10)
II	15(3)	6(2)	3(1)	3(1)	1	28(7)
III	12	5	3(1)	2	1	23(1)
Total	45(6)	20(5)	13(5)	11(2)	3	92(18)

#### BIBLIOGRAPHIE

1. FEIDER Z., 1954, Rev. Univ. « Al. I. Cuza », Inst. Pol. Iași, 1, 1-2, 195-210.
2. — Zool. Zh., 1959, 384, 537-549.
3. THOR S., WILLMANN C., 1947, *Trombitidae*, Tierr. Walt. Gruy. C., Berlin, 3, 71.

Reçu le 8 avril 1975

Université « Al. I. Cuza »  
Iași, str. Universității 16

CONTRIBUTIONS TO THE STUDY OF THE FEMALE  
EXTERNAL GENITAL COMPLEX IN OPHIONIDAE  
(HYM. ICHNEUMONIDAE)

BY

IONEL P. PETCU and VIORICA HONCIUC

In this paper the authors analyse for the first time the parts of the female external genital complex from 14 species of Ophionidae, as well as from the species *Devorgilla canescens* Grav. which was described by Franco Frilli. The morphological parts show specific differentiations, which, together with the other morphostructural characters, complete the diagnosis of the species.

The specialty literature offers few detailed data on the female external genital complex in Ichneumonidae and especially in Ophionidae [3].

Such studies were carried out by Frilli [1] and Petcu [2], who minutely examined this complex in *Devorgilla canescens* Grav. and respectively *Agrypnon flaveolatum* Grav., indicating in the latter some new morphological components.

Considering that this morphological complex presents a special value in delimiting the specific characters, we suggested the investigation of 15 species in which we can notice after a close investigation the morphological components which prove specific differentiations and which, besides other morphostructural characters, complete the diagnosis of the species.

These distinct characters are :

In species *Devorgilla canescens* Grav., *Sinophorus fuscicarpus* Thoms., *Cremastus schoenobius* Thoms., the stylets are far thinner and larger as concerns the rest of the genital complex.

In species *Trichonotus tenuicornis* Grav., *Anomalon foliator* Fabricius, *Cymodusa petulans* Holmgr. the teeth are sharper as compared to the round edges of the other species. In *Dusona bucculeata* Grav. the stylet has 7 teeth against the other species which have 5—4 teeth.

In species *Anomalon foliator* Fabricius, *Devorgilla canescens* Grav., *Sinophorus fuscicarpus* Thoms., *Cremastus schoenobius* Thoms., *Demophorus similis* Brischke the genital valvae are longer than T. IX.

In species *Ophion luteus* L., *Casinaria orbitalis* Grav., *Casinaria tenuiventris* Grav., *Diadegma monospila* Thoms., *Dusona bucculeata* Grav., *Hyposoter ebeninus* Grav. the genital valvae are smaller than T. IX.

In species *Ophion luteus* L., *Trichonotus tenuicornis* Grav. *Anomalon foliator* Fabricius, *Campoletis raptor* Zett., *Campoletis zonatus* Grav. the

appendix styli is formed of two distinct lobes at the anterior edge, against the other species where it is formed of only one lobe slightly undulated at the anterior edge.

Excepting the external genital complex in *Devorgilla canescens*, previously analysed [1], in the other 14 species it is described for the first time by the authors of this paper.

In order to understand the way in which the whole complex functions, we investigated the articulation of the ovipositor pieces, respectively of the sheath and stylets, at whose level a whole system of muscles act. It results that the stylets are articulated by the valvifer 1 (fig. 12,  $vf_1$ ), while the sheath is articulated at the valvifer 1 and 2 (fig. 12.)

In order to materialize these morphological criteria we shall refer only to the description of the female external genital complex in species *Ophion luteus* L., while in the other species the specific differences will be inferred from the same morphostructural criteria, accompanied by the comparative analysis which results from the figures (figs 1–16) annexed to the paper.

### 1. *Ophion luteus* L. (figs 1, 2)

The tergite IX is about twice longer than wide. The anterior and posterior edges are curved, the lateral ones are straight. The hairs are present only in the posterior part. The valvifer 2 is narrowed in the posterior part, presenting an evident prolongation; in the inferior half it is covered by T.IX. Its length is equal with that of T.IX. The sheath and stylets have the same length, a little longer than T.IX and the valvifer 2 taken together. The stylets have five teeth. The genital valves are thick and short, about 3 times longer than wide and shorter than the complex T.IX — valvifer 2. The cerci are about four times longer than wide. The appendix styli has the form of blades, sinuous at the superior edge.

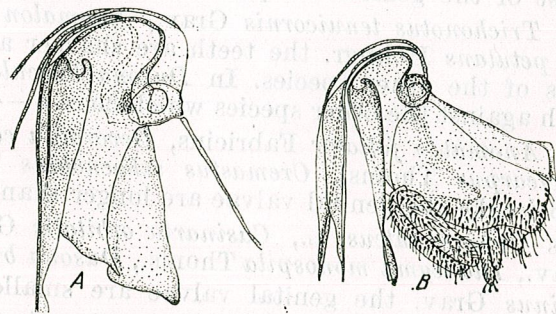


Fig. 1. — *Ophion luteus* L., ♀: A, the external genital complex — lateral section; B, general view of the external genital complex, laterally seen.

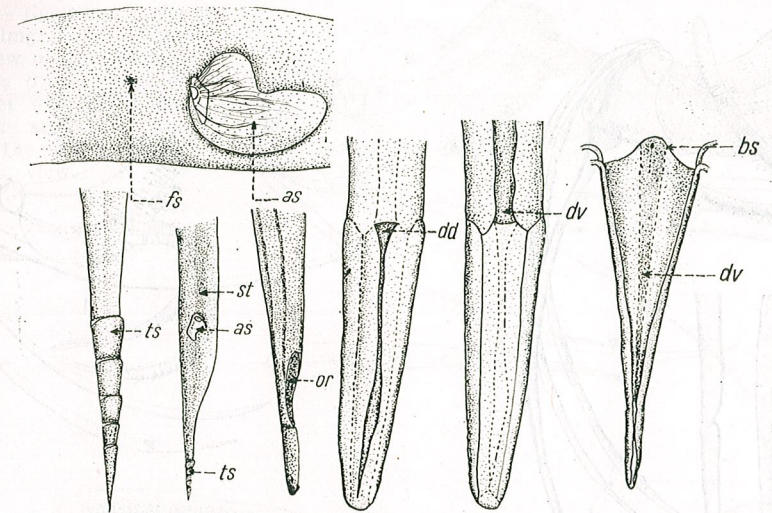


Fig. 2. — *Ophion luteus* L., ♀: *ts*, the teeth of the stylet; *dv*, ventral ditch of the sheath; *dd*, dorsal ditch of the sheath; *bs*, the basis of the sheath; *st*, stylet; *or*, dorsal orifice of the sheath; *as*, appendix styli; *fs*, foramen styli.

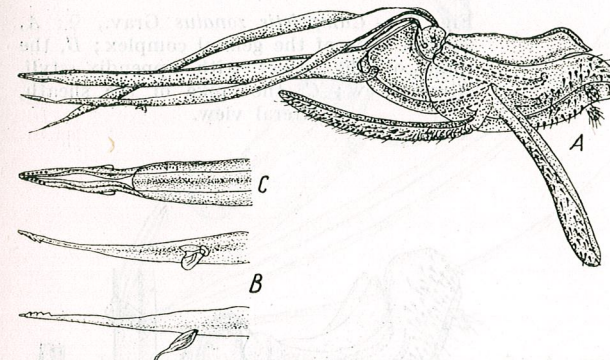


Fig. 3. — *Trichonotus tenuicornis* Grav., ♀: A, general view of the genital complex; B, the spike of the stylet with the teeth and appendix styli; C, the spike of the sheath, dorsal view.

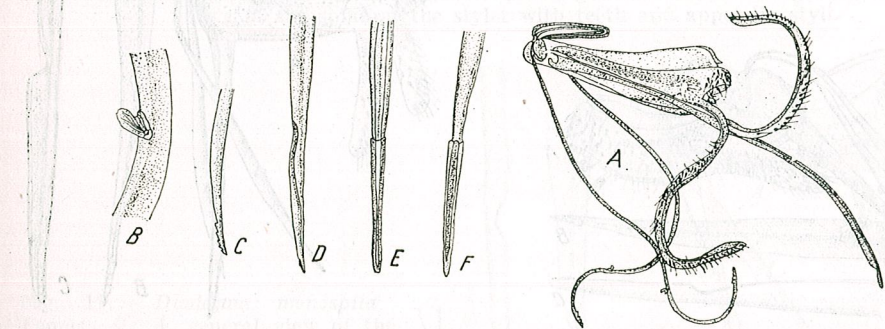


Fig. 4. — *Anomalon foliator* Fabricius, ♀: A, general view of the genital complex; B, fragment of stylet with appendix styli; C, the spike of the stylet; D, the spike of the sheath, lateral view; E, the spike of the sheath, ventral view; F, the spike of the sheath, dorsal view.

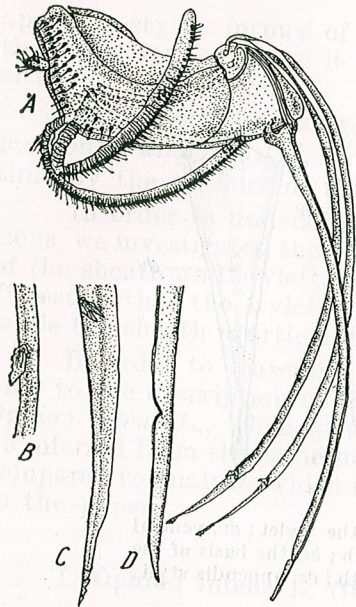


Fig. 5. — *Campoletis raptor* Zett., ♀: A, general view of the genital complex; B, fragment of stylet with appendix styli; C, the spike of the stylet; D, the spike of the sheath, lateral view.

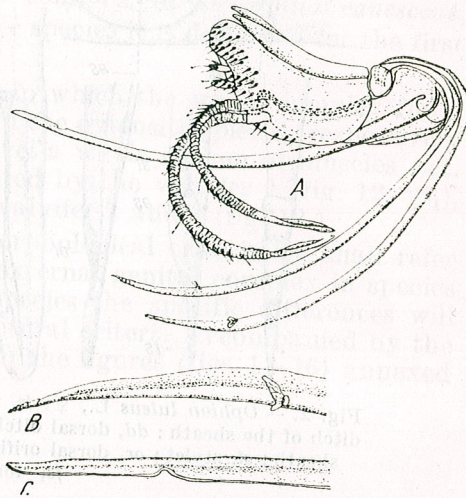


Fig. 6. — *Campoletis zonatus* Grav., ♀: A, general view of the genital complex; B, the spike of the stylet with appendix styli, lateral view; C, the spike of the sheath, lateral view.

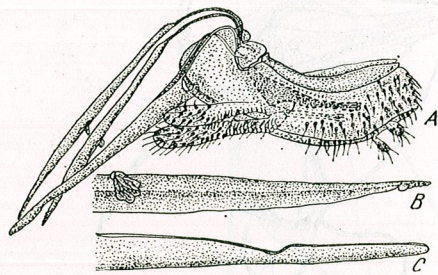


Fig. 7. — *Casinaria orbitalis* Grav., ♀: A, general view of the genital complex; B, the spike of the stylet with teeth and appendix styli, lateral view; C, the spike of the sheath, lateral view.

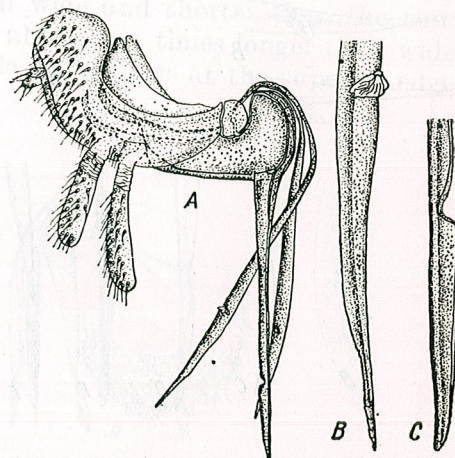


Fig. 8. — *Casinaria tenuiventris* Grav., ♀: A, general view of the genital complex; B, the spike of the stylet with teeth and appendix styli; C, the spike of the sheath, lateral view.

Fig. 9. — *Cymodusa petulans* Holmgr., ♀: A, general view of the genital complex; B, the spike of the stylet with teeth and appendix styli; C, the spike of the sheath, lateral view.

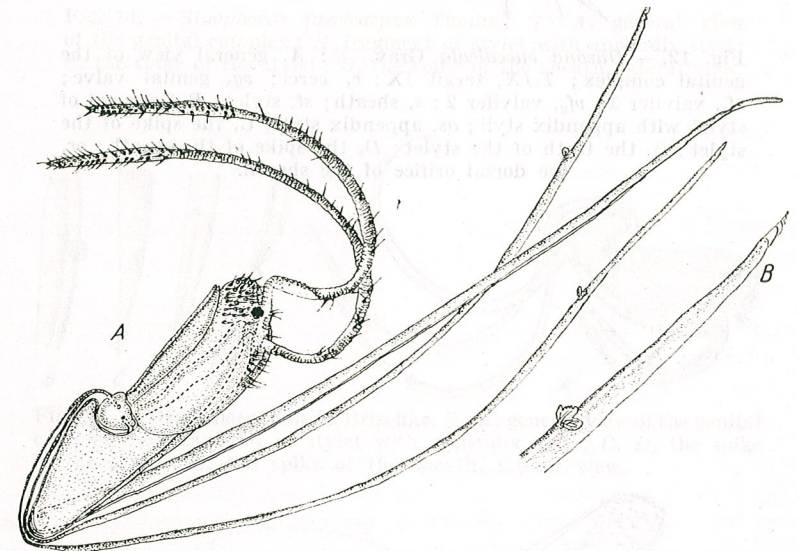
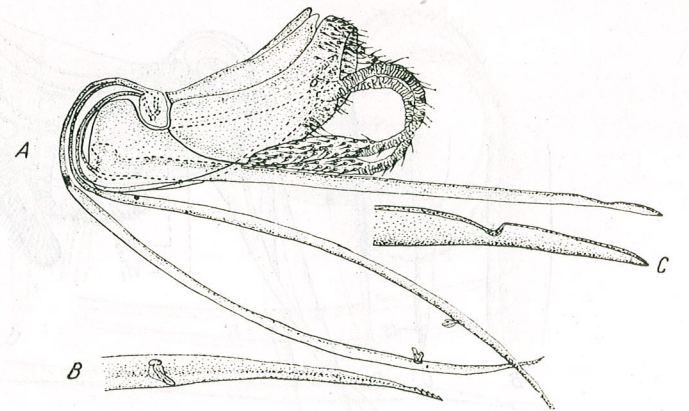
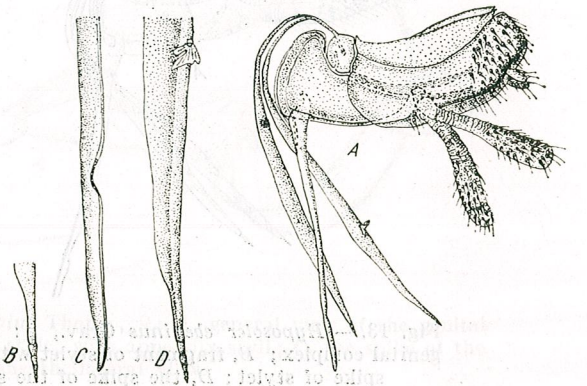


Fig. 10. — *Devorgilla canescens* Grav., ♀: A, general view of the genital complex; B, the spike of the stylet with teeth and appendix styli.

Fig. 11. — *Diadegma monospila* Thoms., ♀: A, general view of the genital complex; B, the spike of the stylet; C, the spike of the sheath, lateral view; D, the spike of the stylet with teeth and appendix styli.



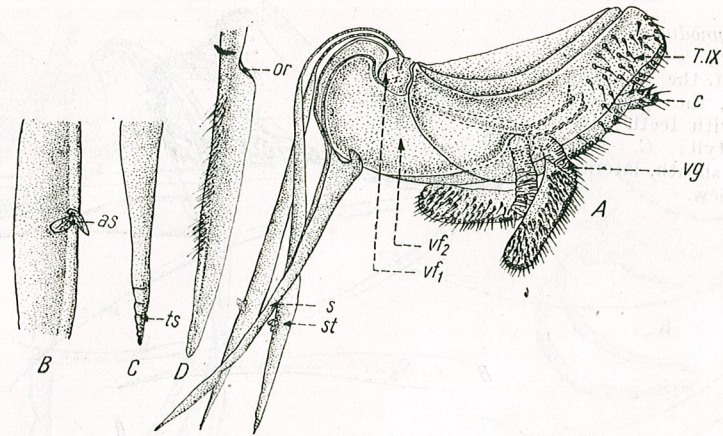


Fig. 12. — *Disona bucculeata* Grav., ♀: A, general view of the genital complex; T.IX, tergite IX; c, cerci; vg, genital valve;  $vf_1$ , valvifer 1;  $vf_2$ , valvifer 2; s, sheath; st, stylet; B, fragment of stylet with appendix styli; as, appendix styli; C, the spike of the stylet; ts, the teeth of the stylet; D, the spike of the sheath; or, the dorsal orifice of the sheath.

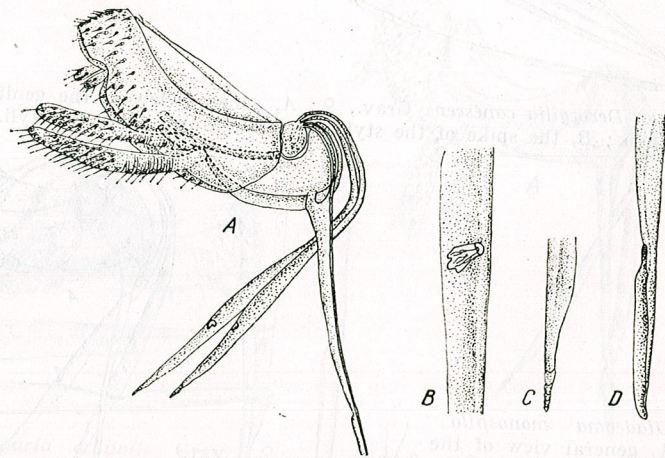


Fig. 13. — *Hyposoter ebeninus* Grav., ♀: A, general view of the genital complex; B, fragment of stylet with appendix styli; C, the spike of stylet; D, the spike of the sheath, lateral view.

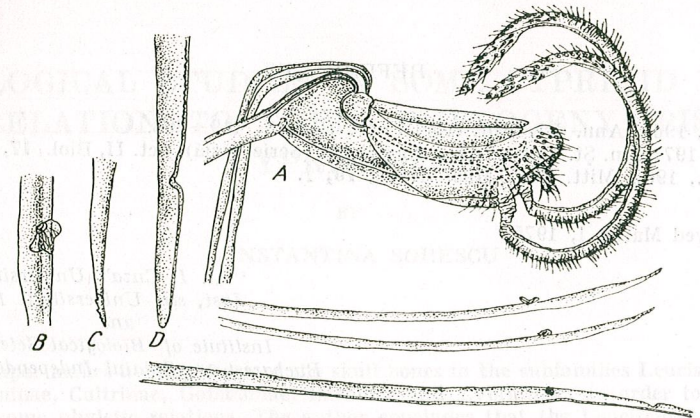


Fig. 14. — *Sinophorus fuscicarpus* Thoms., ♀: A, general view of the genital complex; B, fragment of stylet with appendix styli; C, the spike of the stylet; D, the spike of the sheath, lateral view.

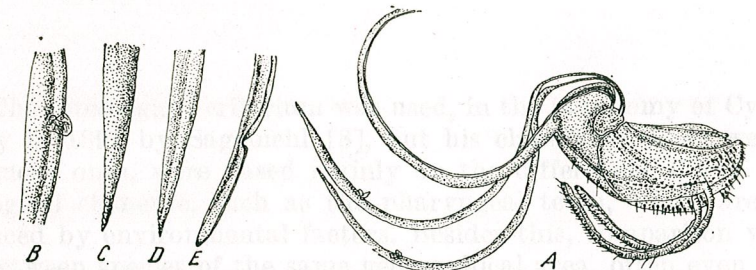


Fig. 15. — *Demophorus similis* Brischke, ♀: A, general view of the genital complex; B, fragment of stylet with appendix styli; C, D, the spike of the stylet; E, the spike of the sheath, lateral view.

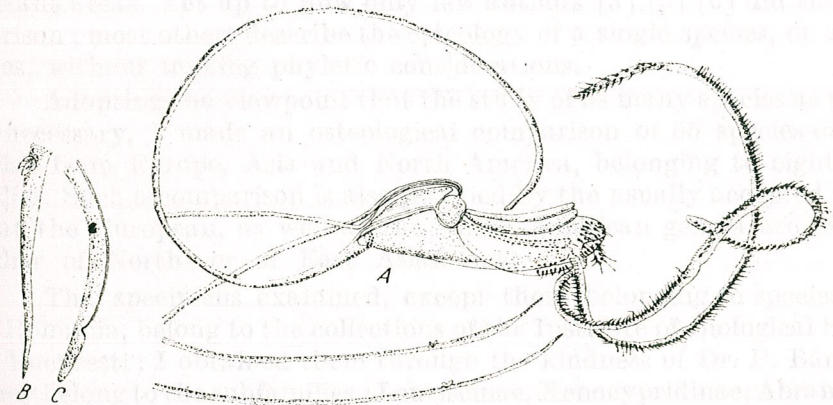


Fig. 16. — *Cremastus schoenobius* Thoms., ♀: A, general view of the genital complex; B, the spike of the stylet with appendix styli; C, the spike of the sheath, lateral view.



## REFERENCES

1. FRILLI F., 1965, Ann. Ist. Ent. Agr. Univ. Bari, 1, 119-208.
2. PETCU I., 1971, An. Șt. Univ. "Al. I. Cuza" Iași (Serie Nouă), Sct. II, Biol., 17, 2, 241-248.
3. OESER R., 1961, Mitt. Zool. Mus. Berlin, 73, 1.

Received March 1, 1975

"Al. I. Cuza" University  
Iași, str. Universității 16  
and  
Institute of Biological Sciences  
Bucharest 17, Splaiul Independenței 296

## OSTEOLOGICAL STUDIES IN SOME CYPRINID FISHES IN RELATION TO THEIR PHYLOGENY (PISCES, CYPRINIDAE)

BY

CONSTANTINA SORESCU

The paper makes a comparison of the skull bones in the subfamilies Leuciscinae, Danioninae, Cultrinae, Gobioninae, Barbinae and Cyprininae, in order to establish some phyletic relations. The author concludes that the Leuciscinae are a primitive subfamily and that the Xenocypridinae and Abramidinae are their offshoots. The Danioninae are primitive, too; the Gobioninae, Barbinae and Cyprininae descend from them. Within the Barbinae, one can distinguish primitive species, whose skull bears some similarity with that of the Danioninae (their presumed ancestors) and evolved species, better adapted to benthonic life.

The osteological criterium was used, in the taxonomy of Cyprinidae, already in 1891 by Sagemehl [8], but his classification, as well as the subsequent ones, were based mainly on the differences shown by some osteological elements, such as the pharyngeal teeth, which are directly influenced by environmental factors. Besides this, comparison was made only between species of the same geographical area, often even from the same biotope. These cannot therefore be considered as conclusive.

The osteological criterium is actually valid only if the comparison is made between very many species, from various biotopes and from distant areas. Yet up to now only few authors [3] [5] [6] did such comparison; most others describe the osteology of a single species, or of a few ones, without making phyletic considerations.

Adopting the viewpoint that the study of as many species as possible is necessary, I made an osteological comparison of 55 species of Cyprinidae from Europe, Asia and North America, belonging to eight subfamilies. Such a comparison is also justified by the usually accepted opinion that the European, as well as the North American genera are offshoots either of North- or of East Asian ones.

The specimens examined, except those belonging to species living in Romania, belong to the collections of the Institute of Biological Sciences in București; I obtained them through the kindness of Dr. P. Bănărescu. They belong to the subfamilies: Leuciscinae, Xenocypridinae, Abramidinae, Danioninae, Cultrinae, Gobioninae, Barbinae, and Cyprininae.

REV. ROUM. BIOL. - BIOL. ANIM., TOME 20, No 4, p. 237-240, BUCAREST, 1975

I consider that only those osteological characters have a phyletic significance which remain constant within the subfamily, without changing according to the manner of life of the species. The only skull bones satisfying this condition are the supraethmoid, frontals, dermopterotics, prevomer and parasphenoid. They are all dermal bones, being the first which appear during the ontogenetic development. This fact confirms the modern viewpoint according to which the larval stage, not the adults represent the source of evolution.

This paper deals with the variability (within the eight subfamilies of Cyprinidae) of only two bones of the skull: the supraethmoid and the parasphenoid. Based mainly on the study of these two bones, but also on the others, as well as on the pectoral girdle and on the Weberian apparatus [11–18], the author proposes a phyletic scheme of the Cyprinidae (fig. 1).

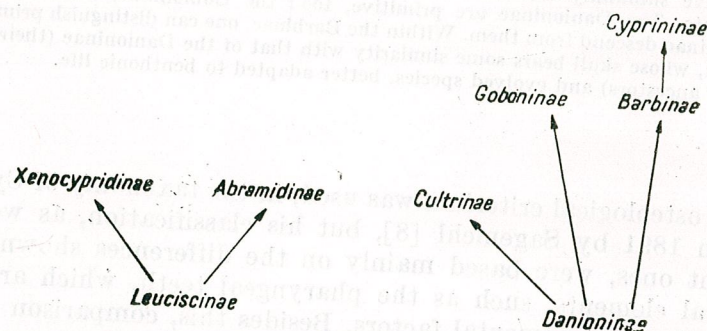


Fig. 1

In the European, Asian and North American species belonging to the subfamilies here considered as primitive (Leuciscinae and Danioninae), the supraethmoid has a small anterior concavity [13] [14]. From them started two independent evolutionary directions. In one of them the anterior concavity of the supraethmoid became deeper and is bordered by two long antero-lateral expansions (Abramidinae and Xenocypridinae [13]). In the Gobioninae [16], Barbinae, and Cyprininae [14] the anterior concavity is replaced by an osseous rostral process. These modifications of the supraethmoid are correlated with the improvement of the feeding mechanism of the fishes, through the accentuation of the protractility of the mouth. In the Cyprinidae the protractility of the mouth is realized by a suspensorium apparatus allowing the forward movement of the upper jaw. It consists of a rostral bone (which connects the praemaxilla to the neurocranium) and of a pair of preethmoids II (located at the articulation of the maxilla with the preethmoid [14]).

In all species of the primitive subfamilies (Leuciscinae and Danioninae), irrespective of their habitat or feeding habits, the mouth is but slightly protractile, the rostral rudimentary and the preethmoids II are cartilaginous capsules; the supraethmoid has a slight anterior concavity.

According as evolution goes on, the trend towards the accentuation of the protractility of the mouth is realized in two ways, also determining adequate modifications of the supraethmoid:

1. In the Abramidinae and Xenocypridinae the connection of the rostral to the skull becomes longer through the development of the two antero-lateral expansions of the supraethmoid [13].

2. In the Gobioninae, Barbinae and Cyprininae, the protractility of the mouth becomes stronger through the development of a well developed suspensorium apparatus and of a bony rostral process of the supraethmoid, which extends the connection of the rostral with the skull and hence also the articulation of the upper jaw to the skull [14].

The steps in the realization of this evolution in the three above-named subfamilies are evident in some of their rather primitive species, whose skull is somewhat intermediate between that of their presumed Danion ancestors and the more advanced species of the same subfamily. A single example will be mentioned: in *Puntius sophore*, a primitive Indian Barbin, the rostral process of the supraethmoid is in an incipient stage, in spite of the fact that this species is related to and has similar feeding habits as the European *Barbus barbus* [14] in which the rostral process of the supraethmoid is well developed and the mouth strongly protractile.

Interesting differences are shown also by the parasphenoid. In some species of Leuciscinae this bone undergoes a strong invagination in the pharyngeal region, because of the excessive development of the pharyngeal teeth; nevertheless, it retains the typical shape of the Leuciscinae, differing from the parasphenoid of the Gobioninae [16] or of the Barbinae [14].

Correlating the observations made on all bones of the skull, on the pectoral girdle and on the Weberian apparatus, whose detailed description was done in former papers [11–18], it is concluded that the phyletic relations within the Cyprinidae are those shown in figure 1.

#### CONCLUSIONS

1. Comparative osteological investigations have shown that only the supraethmoid, frontals, dermopterotics, prevomer and parasphenoid are skull bones which remain constant within the subfamilies and can be used for phyletic conclusions.

2. The trend towards an improvement of the feeding mechanisms determines an accentuation of the protractility of the mouth in evolved subfamilies of Cyprinidae: Gobioninae, Barbinae and Cyprininae.

3. It is suggested that the Leuciscinae and Danioninae are primitive and from them have evolved the other subfamilies: Abramidinae and Xenocypridinae from the Leuciscinae, Cultrinae; Gobioninae, Barbinae, and Cyprininae from the Danioninae. Within the evolved subfamilies, different evolution steps can be recognized. The specialization is evident in the Cultrinae, many of which are pelagic.

4. The evolution of the subfamilies of Cyprinidae went on parallelly.

## REFERENCES

1. BĂNĂRESCU P., 1964, *Fauna R.P.R., Pisces, Osteichthyes*, Ed. Academiei, București, vol. XIII.
2. BENDE S., 1949, *Acta hung. Biol.*, **1**, 4, 127-156.
3. GREENWOOD P. H., JUBB R. A., 1967, *Ann. Cape Prov. Mus. Sth. Afr.*, **6**, 17-36.
4. JARVIK E., 1960, *Théories de l'évolution des vertébrés*, Masson, Paris.
5. RĂMASWAMI L. S., 1952, *Proc. nat. Inst. Sci. India*, **18**, 6, 495-536.
6. — 1957, *Proc. zool. Soc. Calcutta*, **303**, 293-303.
7. REGAN C. T., 1911, *Ann. Mag. nat. Hist.*, **8**, 13-32.
8. SAGEMEHL M., 1891, *Morph. Jahrb.*, **17**, 489-595.
9. SAXENA P. K., 1966, *Zool. Anz.*, **179**, 5, 366-378.
10. SINHA H. M., 1959, *J. Asia Soc. Bengal*, **1**, 1-14.
11. SORESCU C., 1968, *Senckenberg. Biol.*, **49**, 5, 387-397.
12. — 1968, *Bul. șt. Craiova*, **10**, 713-720.
13. — 1969, *Anal. Univ. Craiova*, **11**, 495-505.
14. — 1970, *Rev. roum. Biol. - Zool.*, **15**, 4, 239-245.
15. — 1970, *Rev. roum. Biol. - Zool.*, **15**, 6, 403-408.
16. — 1970, *St. Cerc. Biol. - Zool.*, **22**, 5, 437-441.
17. — 1971, *St. Cerc. Biol. - Zool.*, **23**, 4, 319-329.
18. — 1972, *Rev. roum. Biol. - Zool.*, **17**, 6, 391-398.

Received February 22, 1975

University of Craiova  
Faculty of Biology  
Craiova, 13, str. A.I. Cuza

## UN CAS D'HYPERPARASITISME CHEZ LA PERCHE (*PERCA FLUVIATILIS* L.)

PAR

ELENA CHIRIAC, ȘTEFANIA BOLDOR et ELENA VĂDINEANU

In the paper is recorded, for the first time in literature, a hyperparasitism case observed at the perch (*Perca fluviatilis* L.). The massive infestation of the parasite *Ligula intestinalis* with the *Tetracotyle variegata* hyperparasite (over 350 specimens) is also remarked.

Parmi quatre perches (*Perca fluviatilis* L.) provenant de la mare de Baghea en mai 1964, nous avons trouvé un exemplaire parasité par *Ligula intestinalis*. En l'examinant de près, nous avons observé à la surface du cestode de nombreuses petites protubérances, plus ou moins ovales (fig. 1), qui renfermaient des métacercaires de Strigéidés du type *Tetracotyle*. Nous les avons attribuées à *Tetracotyle variegata*, dont l'adulte est *Cotylurus pileatus* (Rudolphi, 1802).

Les cas d'hyperparasitisme ne sont pas rares chez les vers, mais ils ont un caractère sporadique, c'est pourquoi on les a rarement retrouvés et la plupart ne furent jamais identifiés. Il s'agissait surtout de larves de nématodes trouvées dans des cestodes ou dans des trématodes et de métacercaires progénétiques infestant des crustacés parasites, etc.

Dubinina [1] a été la première à signaler des métacercaires de *Tetracotyle variegata* (Creplin, 1925) dans les *Ligula colymbi* Zeder, 1803, de *Cobitis taenia* L. et de *Gobio gobio* L. Ultérieurement, Dubinina, en étudiant des *Ligula* des poissons de toutes les régions de l'U.R.S.S., constate l'hyperparasitisme des métacercaires de *Tetracotyle variegata* chez *Ligula colymbi* parasite de *Cobitis taenia* et de *Gobio gobio*, alors qu'il



Fig. 1. — *Ligula intestinalis* L. (d'une perche) avec des protubérances renfermant des métacercaires de *Tetracotyle variegata*.

est extrêmement rare chez *Ligula intestinalis* et *Digramma interrupta* d'*Abramis brama*. En effet, dans tout son matériel, une seule *Ligula intestinalis* provenant d'une brème portait deux *Tetracotyle variegata*, dont un dégénéré.

Dans le delta du Volga, sur de nombreux adultes de *Ligula colymbi* provenant des oiseaux ichthyophages, hôtes non spécifiques (*Ardea alba*, *Phalacrocorax carbo* et *Podiceps cristatus*), Dubinina n'y trouva qu'un seul exemplaire parasité par *T. variegata*. Vraisemblablement la métacercaire, aboutissant dans un hôte non spécifique, se fixe à la *Ligule* et y dégénère, tandis que dans les hôtes spécifiques (Lariformes) elle quitte le cestode (continuant à vivre dans la lumière intestinale de l'oiseau hôte). C'est ainsi que Dubinina a souvent observé des cicatrices dans le tégument des ligules adultes, provenant de Lariformes, parasités en même temps par des adultes de *T. variegata*, c'est-à-dire de *Cotylurus pileatus*.

*Ligula intestinalis* examinée par nous présentait plus de 350 métacercaires localisées superficiellement sous le tégument, d'où on pouvait les détacher aisément parce-qu'elles n'avaient pas de membranes kystiques, semblant être libres parmi les fibres musculaires ou les cellules parenchymateuses (fig. 2).

Sur les coupes microscopiques, on observait les métacercaires pénétrant très profondément dans le parenchyme du cestode, jusqu'aux ébauches des organes génitaux placés au centre. Immédiatement sous le tégument de la *Ligula*, les métacercaires étaient disposées le long des fibres musculaires longitudinales, alors que dans le parenchyme elles étaient sans ordre apparent. L'absence d'une membrane kystique dénote qu'il n'y aurait aucune réaction de défense réciproque entre *Ligula* et *Tetracotyle*.

*T. variegata* est un parasite commun des poissons Cyprinidés [2] se trouvant habituellement dans des kystes à paroi mince formés à la surface de différents organes internes. Dans notre cas, il n'y avait aucune métacercaire dans le corps de la perche. Tous les *Tetracotyle* étaient attirés par la *Ligula* (comme par un tactisme chimique), qui leur offrait des conditions favorables à leur développement, sans réactions antagonistes de défense. La perche apparaît ici comme un hôte non spécifique du *T. variegata*.

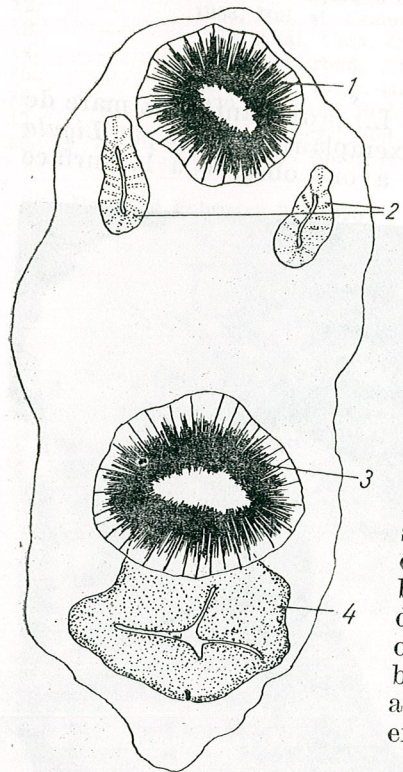


Fig. 2. — *Tetracotyle variegata* (Creplin, 1925) 1, ventouse buccale; 2, pseudoventroses; 3, ventouse ventrale; 4, organe de Brandes.

## BIBLIOGRAPHIE

1. DUBININA M. N., 1956, Zool. jurnal, 35, 8, 1139—1144.
2. ROMAN ELENA, 1955, Cercetări asupra parazitofaunei peștilor din Dunăre, Ed. Acad. R.P.R. București, 36—37.

Reçu le 13 janvier 1975

Faculté de Biologie  
Chaire de biologie animale  
Bucarest 35, Splaiul Independenței 93—95

# LES GLANDES SÉRICIGÈNES CHEZ CERTAINES ARAIGNÉES « HAPLOGYNES »

PAR

ELENA TRACIUC

The paper presents the results of the comparative study of the silk glands in four species of primitive spiders, belonging to different families. A much smaller number of types of glands was found in these families, comparatively to those already mentioned in the literature. This can be explained by the life history of these spiders.

Les premiers travaux sur les glandes séricigènes des araignées se rapportent aux espèces les plus communes, c'est-à-dire les plus accessibles, qui construisent des toiles volantes. Ce sont justement les espèces dont l'appareil séricigène est le plus complexe. Il s'agit des travaux de Meckel [19], Oeffinger [20], Buchholz-Landois [5], Bertkau [3], Schimkewitsch [27], Warburton [30], Apstein [1], Bonnet [4], Kiesow-Stark [8].

D'autres travaux ont complété nos connaissances sur la structure du tissu glandulaire séricigène; citons ceux de Johannson [8], Millot [14-18] et Helmuth et Mahler [7].

Le premier, et jusqu'à présent le seul travail plus complet sur les glandes séricigènes, concernant les aspects aussi bien anatomiques que cytologiques chez un grand nombre d'espèces appartenant à plusieurs familles, est celui de Margareta Atanasiu-Dumitresco [2]. Signalons encore les travaux de biochimie, histochimie, ultrastructure, physiologie et écologie de Glatz [6], Legendre [10], Mikulska [12] [13], Peakall [21] [22], Richter [23-26], Traciuc [28], Wasowska [31-34], Wilson [35-37], Witt et collab. [38].

Nous présentons des données sur l'appareil séricigène de quatre espèces d'Araignées Haplogynes, formes primitives qui ne tissent pas de toile et mènent un genre de vie particulier, indiqué ci-après.

## MATÉRIEL ET TECHNIQUE

Nos recherches portent sur des femelles adultes et juvéniles de :

*Archaea vadoni*, famille Archaeidae, provenant d'arbustes de la forêt Anamalazoatra, région Périnet, Madagascar.

*Segestria senoculata*, famille Dysderidae, capturée sous l'écorce, dans le massif montagneux de Gîrbova, Sinaia, Roumanie.

*Nemesia pannonica coheni*, famille Ctenizidae, et *Proatipus muralis*, famille Atypidae (Mygalomorphae), capturée dans la forêt de Hagieni, Dobrogea du Sud, Roumanie, des galeries dont elles tapissent les parois avec une toile spéciale.

Les animaux ont été fixés dans un mélange de Bouin et Duboscq-Brasil; *Archaea* a été inclus dans la céloïdine-paraffine, les autres seulement dans de la paraffine. Les coupes de 7  $\mu$  épaisseur furent colorées au hémalum-éosine et d'après la méthode trichromique de Mallory.

## OBSERVATIONS

La complexité de l'appareil séricigène est due d'une part au nombre élevé des glandes, d'autre part à leur forme extrêmement variable.

Il y a deux classifications basées exclusivement sur la forme des glandes, celle de Apstein [1] et celle de Millot [16]. Margareta Atanasiu-Dumitresco [2] introduit la structure de l'épithélium sécréteur, un caractère bien plus significatif que la forme des glandes, qu'elle réunit en trois grandes catégories.

Nos observations sur les quatre espèces primitives d'araignées portent sur l'anatomie des glandes séricigènes et les observations histologiques nous ont servi pour des précisions supplémentaires.

Les glandes séricigènes sont situées dans la partie ventrale de l'abdomen, depuis les filières jusqu'au niveau de la fente génitale.

Chez *Archaea vadoni* nous avons constaté quatre types de glandes : ampulacées, tubulaires, acineuses et piriformes.

Les glandes ampulacées sont au nombre de quatre, dont deux latérales grandes et deux médianes de taille moyenne. Les glandes latérales dépassent antérieurement la fente génitale, atteignant la région des phyllo-trachées. La partie distale se continue par un long canal d'évacuation, pelotonné, qui s'ouvre par des macrofusules sur les filières antérieures. Les canaux des glandes ampulacées médianes sont courts et s'ouvrent toujours par des macrofusules au sommet des filières médianes. Les canaux de ces glandes sont plus larges que ceux des autres types.

Les glandes tubulaires, au nombre de deux paires, ont une position antéro-latérale. Le corps glandulaire cylindrique, long et ondulé, se continue par un canal court s'ouvrant par des macrofusules sur les filières médianes. Nous n'avons pas trouvé ces glandes chez les nymphes au stade II, mais seulement chez les femelles adultes après accouplement.

Les glandes acineuses, au nombre de quatre paires, forment une agglomération au-dessus des filières antérieures, tout près de la paroi ventrale de l'abdomen (Pl. I, fig. 1). Leur canal est court, sinueux et rigide; il s'ouvre par des microfusules sur les filières antérieures.

Les glandes piriformes, au nombre de trois paires, sont situées derrière les glandes acineuses. Elles ont un canal plus long et plus large que celui des glandes acineuses et sont disposées en ligne droite (Pl. I, fig. 1). Selon notre opinion (qui concorde avec celle de Millot), ces glandes sont en réalité des mini-ampulacées, ayant tous les traits caractéristiques des glandes ampulacées : forme du corps glandulaire, type de l'épithélium, affinités pour les colorants, type du canal. Elles ne diffèrent des glandes ampulacées que par les anses des canaux qui ne sont pas contournées. M. Atanasiu-Dumitresco décrit des glandes ampulacées médianes dont les canaux ne forment pas de vraies anses.

Chez *Segestria senoculata* nous avons constaté une paire de glandes ampulacées latérales et une paire médiane (glandes A, selon Millot). Les premières s'ouvrent sur les filières antérieures et les secondes sur les filières médianes, par des macrofusules.

Glandes acineuses : 10 paires, disposées en deux longues grappes d'un côté et de l'autre de la gonade (Pl. I, fig. 2); toutes ces glandes s'ouvrent sur les filières antérieures par des microfusules.

Il y a chez cette espèce 9 paires de glandes piriformes, formant deux grappes symétriques avec les glandes acineuses, mais ayant une position dorsale par rapport à celles-ci. La longueur des canaux de ces glandes varie beaucoup, en fonction de leur position dans les grappes (Pl. I, fig. 2, 3). Chez cette espèce il n'y a pas de glandes tubulaires.

Une particularité topographique de toutes les glandes séricigènes chez *Nemesia pannonica coheni* est leur localisation dans la partie postérieure de l'abdomen, dans la région des filières. Il s'y ajoute l'existence d'un seul type de glandes acineuses de grande taille, très larges (Pl. II, fig. 4) et de glandes piriformes de type commun (Pl. II, fig. 5). Les canaux des glandes acineuses sont typiques, de même leur épithélium glandulaire.

Chez *Proatypus muralis*, il y a également deux types de glandes, ampulacées, et piriformes, en très grand nombre, plus de 30, situées entre la base des filières et le milieu de l'abdomen (Pl. II, fig. 6). Étant disposées à différents niveaux, tant latéralement qu'en position médiane par rapport à la base des filières, la longueur de leurs canaux varie beaucoup. Elles s'ouvrent par un seul type de fusules, situées sur toutes les filières.

Nos observations nous ont permis de constater que *Archaea* a quatre types de glandes séricigènes, *Segestria* trois, *Nemesia* et *Proatypus* n'en ont chacun que deux. Toutes les glandes, excepté les tubulaires, fonctionnent depuis le premier stade nymphal. À l'exception des glandes tubulaires, toutes les autres ont deux parties distinctes : une partie antérieure, dont la sécrétion est filante et a une certaine affinité pour les colorants, et une partie basale, toujours à sécrétion filante mais à affinités tinctoriales différentes. L'épithélium de ces glandes est prismatique. Les glandes tubulaires ont un épithélium cubique qui devient pavimenteux dans la période d'activité sécrétrice.

En conclusion, nos observations montrent chez les quatre espèces étudiées un appareil séricigène plus simple, comprenant un nombre réduit de types de glandes, contrairement aux araignées solitaires construisant de vraies toiles volantes.

La simplicité de leur appareil séricigène confirme leur primitivité, en corrélation aussi avec leur mode de vie.

## Remerciements

Notre gratitude va à Mme le Prof. Margareta Dumitresco pour ses précieux conseils, à M. le Prof. R. Legendre pour l'envoi d'araignées primitives difficiles à obtenir et à M. Fuhr pour ses renseignements arachnologiques.

## BIBLIOGRAPHIE

1. APSTEIN C., 1889, Arch. f. Naturg., **55**, 1, 29-74.
2. ATANASIU-DUMITRESCO M., 1941, Ann. Acad. Roum., **16**, mém. 19, 1-67, 1-81.
3. BERTKAU, PH., 1882, Arch. f. Naturg., **48**, 316-359.
4. BONNET P., 1929-1930, Bull. Soc. Zool. Fr., **54**, 501-523; **55**, 53-77, 118-136.
5. BUCHOLZ R., LANDOIS L., 1868, Arch. Anat. Physiol., 240-255.
6. GLATZ L., 1972, Z. Morph. Tiere, **72**, 1-25.
7. JOHANSSON B., 1914, Act. Univ. Lund., **10**, 5, 1-12.
8. KIESOW-STARK J., 1932-1933, Z. Naturwiss. Jena, **66**, 1, 1-40.
9. KOVOOR J., ZYLBERBERG L., 1974, Ann. Sci. Nat., Zool. Paris, 12 sér., **16**, 1-26.
10. LEGENDRE R., 1960, XVème Congrès Entomologie, Vienne, 412-413.
11. MAHLER H., 1938, Zeitschr. f. Morph. ökol. Tiere, **34**, 439-498.
12. MIKULSKA I., 1967, Zool. Poloniae, **17**, 4, 357-365.
13. - 1969, Zool. Poloniae, **19**, 2, 279-291.
14. MILLOT J., 1926, C.R. Soc. Biol. Paris, **94**, 10-11.
15. - 1929, Bull. Soc. Zool. Fr., **54**, 3, 194-206.
16. - 1930, Bull. Soc. Zool. Fr., **55**, 2, 150-175.
17. - 1931, Bull. Soc. Zool. Fr., **56**, 1, 75-83.
18. - 1931, Arch. Zool. Exp. et Gén., **71**, 38-45.
19. MECKEL H., 1846, Arch. Anat. Physiol., 1-73.
20. OEFFINGER H., 1886, Arch. Micr. Anat., **2**, 1-12.
21. PEAKALL D. B., 1964, Comp. Biochem. Physiol., **12**, 465-470.
22. - 1966, Comp. Biochem. Physiol., **19**, 253-258.
23. RICHTER C. J. J., 1970, Z. Morph. Tiere, **68**, 37-68.
24. - 1970, Oecologia (Berl.), **5**, 185-199.
25. - 1970, Oecologia (Berl.), **5**, 200-214.
26. - 1970, Netherlands J. Zool., **20**, 3, 392-400.
27. SCHIMKEWITSCH W., 1884, Ann. Sci. Nat., Zool., **17**, 6, 1-94.
28. TRACTUC E., 1971, Rev. Roum. Biol.-Zool., **16**, 3, 365-374.
29. TURCHIND J., MILLOT J., 1926, C.R. Soc. Biol. Paris, **94**, 171-173.
30. WARBURTON C., 1890, Quart. J. Micr. Sci., **31**, 29-39.
31. WASOWSKA S., 1966, Zool. Poloniae, **16**, 1, 9-30.
32. - 1967, Zool. Poloniae, **17**, 1-2, 3-13.
33. - 1969, Zool. Poloniae, **19**, 4, 505, 515.
34. - 1970, Zool. Poloniae, **20**, 2, 257-267.
35. WILSON R. S., 1962, Quart. J. Micr. Sci., **103**, 4, 549-555.
36. - 1962, Quart. J. Micr. Sci., **104**, 4, 557-571.
37. - 1969, Am. Zoologist, **9**, 103-111.
38. WITT P. N., REED CH. F., PEAKALL D. B., 1968, *Problems in Regulatory Biology*, Springer Verlag, Berlin, Heidelberg, New York.

Reçu le 6 mai 1974

Institut de Recherches Biologiques  
Laboratoire de Bio'ogic cellulaire  
Bucarest 17, Splaiul Independenței 296

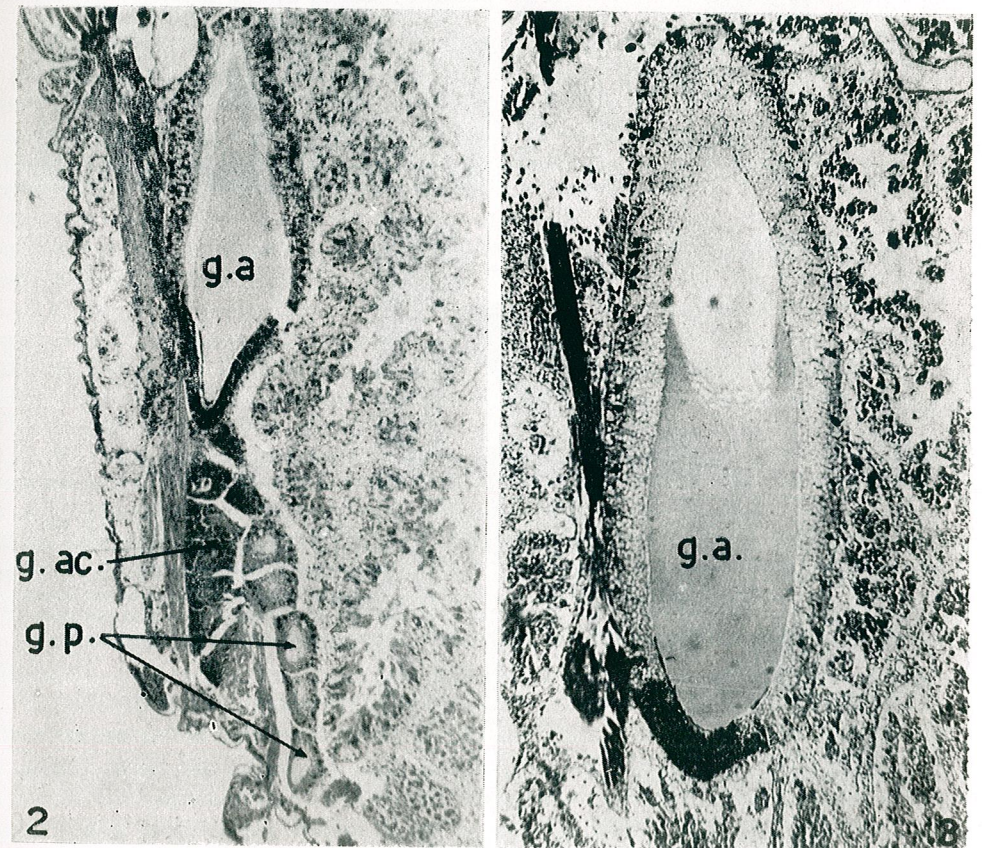
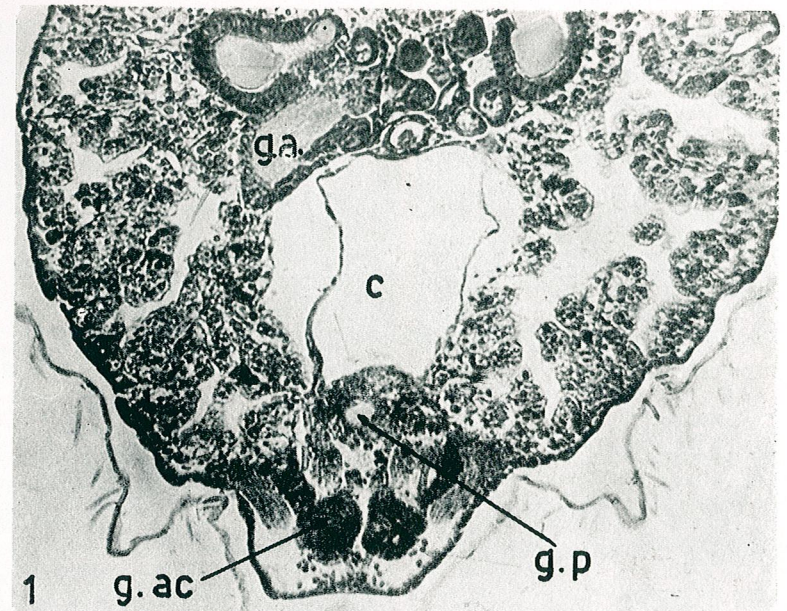


PLANCHE I

Fig. 1. — *Archaea vadoni*, coupe transversale; fig. 2, 3. — *Segestria senoculata*, coupe sagittale.

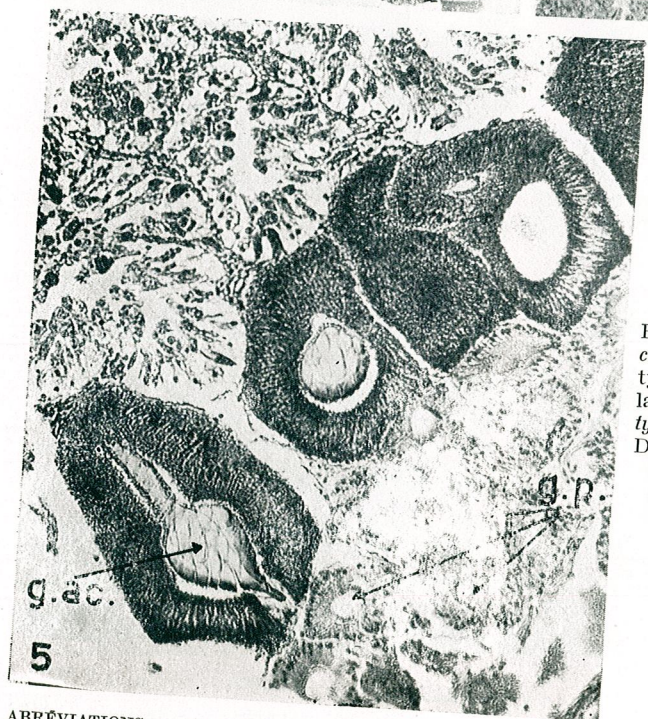
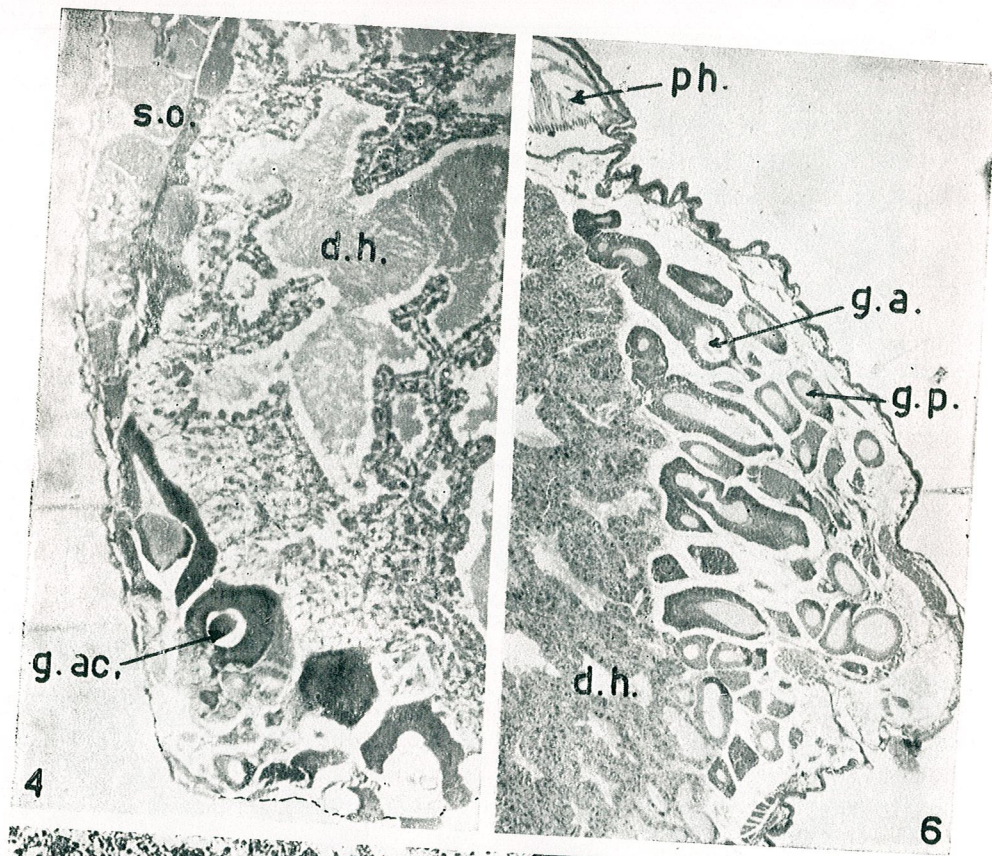


PLANCHE II

Fig. 4, 5. — *Nemesia pannonica coheni*, coupe sagittale. Les deux types de glandes ne dépassent pas la zone des filières; fig. 6. — *Proatypus muralis*, coupe sagittale. Dans l'abdomen les glandes aboutissent aux phyllotrachées.

ABRÉVIATIONS : c., cloaque; d.h., diverticule hépatique; g.a., glandes ampullacées; g.ac., glandes aciniformes; g.p., glandes piriformes; ph., phyllotrachée; s.o., sac ovarien.

L'ENCÉPHALE D'*ACIPENSER RUTHENUS* LINNÉ 1758  
(PISCES, CHONDROSTEI, ACIPENSERIDAE). ÉTUDE  
QUANTITATIVE PRÉLIMINAIRE

PAR

ROLAND BAUCHOT, MARIA CALOIANU-IORDĂCHEL, MONIQUE DIAGNE et  
JEAN-MARC RIDET

We studied the brain-body weight relationships as well as the relative volumes of different encephalic structures in *Acipenser ruthenus* L. The value of the intra-specific brain-body weight allometry was established at 0,50, a value very close to that of Selacians and at the limit of variation of the Teleosteans. The relative volumes of the main encephalic structures are interpreted and discussed in comparison with other Teleostean species.

Chondrostéens, Holostéens et Brachioptérygiens forment ensemble le groupe des Ganoïdes qui se situe, tant paléontologiquement que phylogénétiquement, dans la lignée pré-téléostéenne. Un tel groupe n'a pas manqué d'attirer l'attention des neuroanatomistes, dès la fin même du XIX<sup>ème</sup> siècle, et les études qui ont été réalisées ont résolu l'essentiel des problèmes d'interprétation de l'architecture encéphalique de ces poissons. L'analyse quantitative des structures encéphaliques chez les Téléostéens, que nous avons entreprise, nous a donc conduits à envisager aussi l'étude quantitative de ces formes ganoïdes.

C'est N. Goronowitsch [3] qui a fourni la première étude approfondie de l'encéphale d'*Acipenser ruthenus*, espèce européenne confinée aux eaux douces. F. Theunissen [17] y a ajouté quelques précisions sur les noyaux des nerfs moteurs encéphaliques, tandis que Z. Grodzinski [4] [5] étudiait l'irrigation encéphalique. Plus récemment, R. Nieuwenhuys [9] [10] en a donné quelques images dans une étude plus générale sur le prosencéphale des Actinoptérygiens. Les autres espèces du genre *Acipenser* ou les autres Chondrostéens, ont été étudiés par J. B. Johnston [6-8], qui a essentiellement travaillé sur *Acipenser rubicundus*, autre nom de l'espèce *A. flavescens* Rafinesque, de l'est de l'Amérique du Nord, et plus récemment par I. N. Sbikin [16], qui a consacré une courte note à la morphologie externe de l'encéphale des Esturgeons européens amphibiotes.

Les autres publications sur les Esturgeons concernent essentiellement l'hypophyse ou le système neurosécrétoire hypothalamo-hypophysaire et ne seront donc pas citées ici. Les documents fournis par N. Goronowitsch et par J. B. Johnston sur l'architecture de l'encéphale des Esturgeons sont assez précis pour nous éviter d'en reprendre l'étude chez *A. ruthenus*.



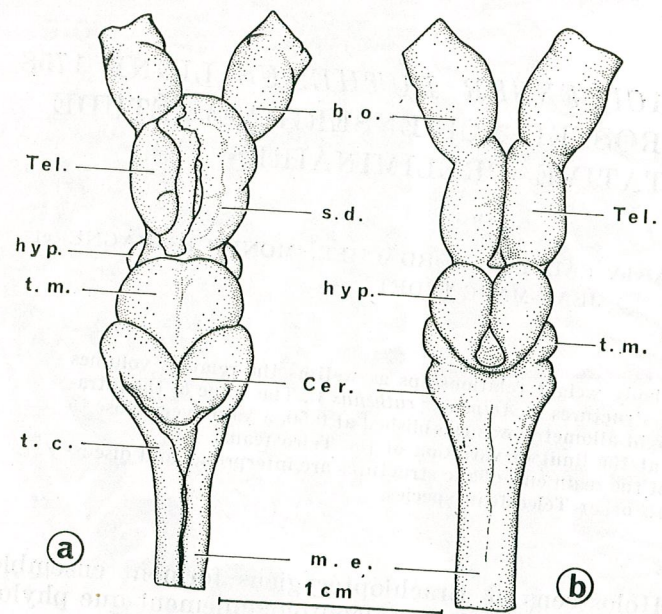


Fig. 1. — Encéphale d'*Acipenser ruthenus* en vues dorsale et ventrale.

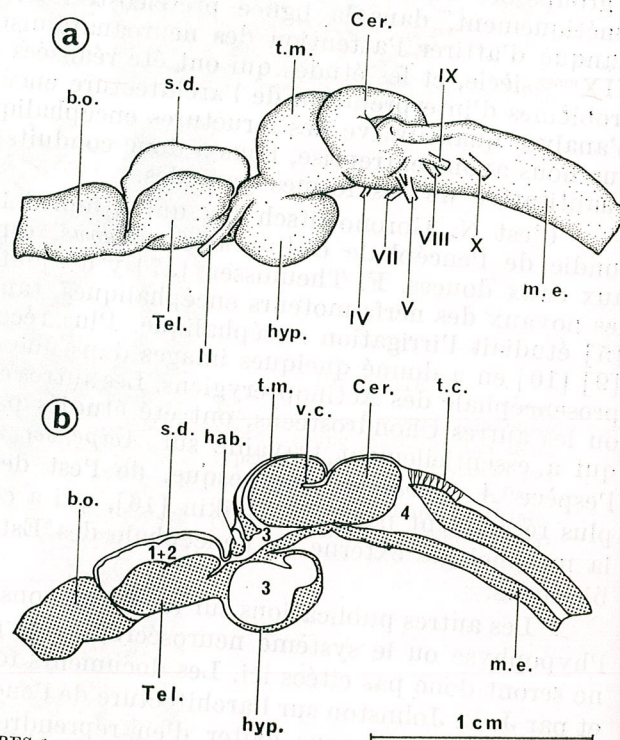


Fig. 2. — Encéphale d'*Acipenser ruthenus* en vue latérale et reconstitution du plan sagittal médian.

ABRÉVIATIONS COMMUNES AUX FIGURES 1 et 2. : b.o. : bulbe olfactif; Cer. : cervelet; hab. : habenula; hyp. : hypothalamus; m.e. : moelle épinière; s.d. : sac dorsal; t.c. : toile choroiidienne du 4<sup>ème</sup> ventricule; Tel. : télencéphale; t.m. : toit mésencéphalique; v.c. : valvule cérébelleuse; II à X : nerfs crâniens; 1 à 4 : ventricules.

MATÉRIEL ET MÉTHODE

Les échanges culturels entre la France et la Roumanie ont permis à l'un d'entre nous, au cours d'un bref séjour à Bucarest en octobre 1974, de participer à la pêche d'un certain nombre d'individus d'*Acipenser ruthenus* Linné 1758, dans le Danube (Fetești). Les poids somatiques (Ps.) ont été mesurés sur place, sur une balance fournie par les pêcheurs, et dont la sensibilité explique les valeurs arrondies de ces poids. Les poids encéphaliques (Pe) ont été mesurés à Paris, après préparation des encéphales et correction, pour tenir compte de la diminution de poids due à l'action du liquide de Bouin utilisé comme fixateur. Le tableau 1 fournit ces valeurs pour les 9 exemplaires récoltés et fixés.

Tableau 1

Ex. n°	Ps (en g)	Pe (en g)
1	600	0,672
2	720	0,805
3	650	0,613
4	90	0,236
5	80	0,223
6	210	0,533
7	45	0,185
8	1 200	0,895
9	920	0,723

Les fig. 1 et 2 fournissent les aspects dorsal, ventral et latéral de l'encéphale d'*Acipenser ruthenus*, ainsi qu'une reconstitution du plan sagittal médian. Pour les raisons exposées ci-dessus, nous ne croyons pas utile de décrire ces illustrations.

RÉSULTATS

Relations pondérales encéphalo-somatiques

Les valeurs du tableau 1 nous ont permis de tracer le graphique de la fig. 3, qui fournit, en doubles coordonnées logarithmiques, la position des 9 exemplaires mesurés. L'étude de la corrélation correspondante fournit un coefficient  $r = 0,9746$  et un coefficient d'allométrie (mesuré par l'axe majeur réduit)  $a = 0,501$ . Cette dernière valeur se situe dans les limites de variation calculées par l'un d'entre nous chez les Téléostéens (0,42 à 0,50) (J. M. Ridet [13]).

Cette valeur du coefficient d'allométrie de croissance de l'encéphale devra être vérifiée par celles qu'on pourra déterminer à partir d'autres espèces de Chondrostéens. Actuellement, elle s'inscrit à une place qui semble logique entre les Sélaciens (valeur moyenne : 0,50. Cf R. Bauchot, R. Platel, J. M. Ridet [2]) et les Téléostéens (valeur moyenne : 0,46), mais bien au-dessus des Amphibiens Urodèles (valeur moyenne : 0,44. Cf M. Thireau [18]), des Reptiles Sauriens (valeur moyenne : 0,43. Cf R. Platel [12]), des Oiseaux (valeur moyenne : 0,365. Cf R. Platel, R. Bauchot et C. Delfini [11]), ou des Mammifères Insectivores (valeur moyenne : 0,23. Cf R. Bauchot et H. Stephan [1]). Des études analogues chez les Holostéens ou les Polyptères permettraient de vérifier cette tendance à la diminution du coefficient d'allométrie de croissance encéphalique quand on va des Vertébrés primitifs vers les Vertébrés évolués.

Le plus gros exemplaire d'*Acipenser ruthenus* récolté pèse 1 200 g environ. L'espèce peut atteindre des poids bien supérieurs et certains individus dépassent 5 000 g. A partir de la formule :

$$Pe = 2,267 Ps^{0,502}$$

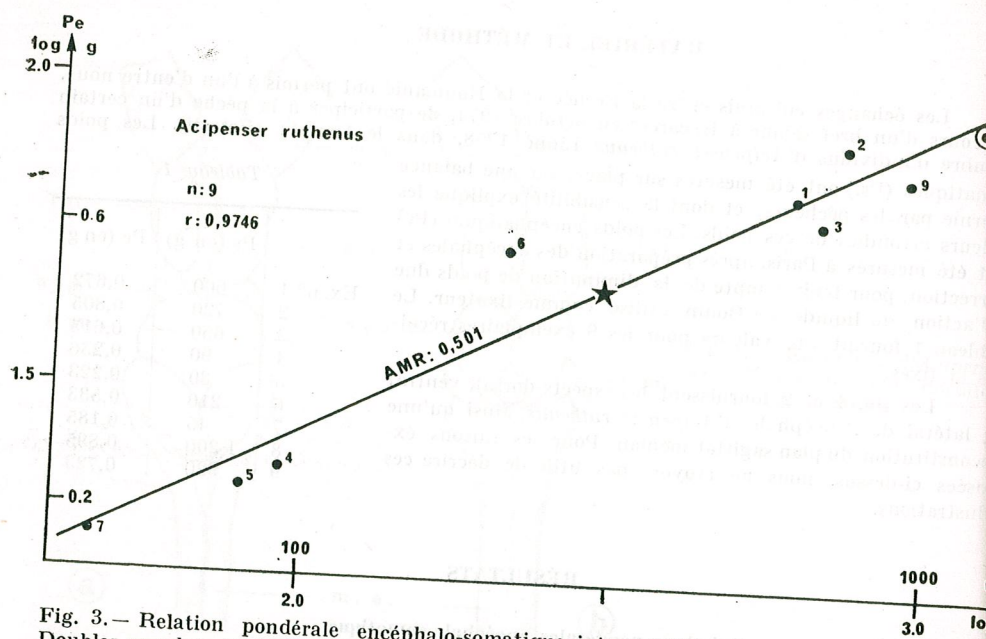


Fig. 3. — Relation pondérale encéphalo-somatique intraspécifique chez *Acipenser ruthenus*. Doubles coordonnées logarithmiques. L'étoile représente le centre de gravité de la distribution. Le point noir cerclé représente l'individu qui a servi aux découpages. AMR = axe majeur réduit (coefficient d'allométrie). n = nombre d'individus. r = coefficient de corrélation.

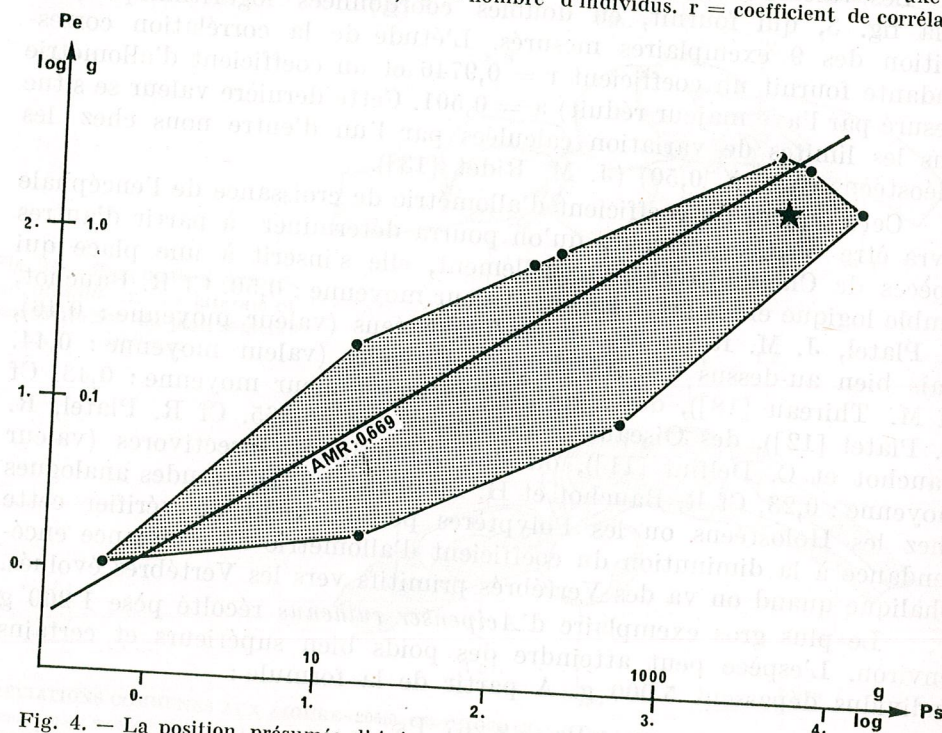


Fig. 4. — La position présumée d'*Acipenser ruthenus* par rapport aux Téléostéens, dans la relation pondérale encéphalo-somatique interspécifique. Doubles coordonnées logarithmiques. L'espèce est figurée par une étoile.

fournie par la corrélation ci-dessus, nous avons calculé ce que serait le poids encéphalique d'un individu de 4 500 g. Le calcul fournit la valeur  $Pe = 1,824$  g. Cette couple de valeur 4 500/1,824 nous a alors servi à situer l'espèce *Acipenser ruthenus* par rapport au polygone de distribution des Poissons Téléostéens (fig. 4). La valeur 4 500/1,824 est figurée par une étoile. On constate que cette espèce d'Esturgeon se situe en dessous de la droite d'équilibre de l'ensemble des Téléostéens, mais qu'elle est loin de figurer parmi les espèces les plus primitives. La valeur  $a = 0,669$  du coefficient d'allométrie de filiation encéphalique provient de l'étude de 118 espèces de Téléostéens, tant européennes que réunionnaises (J. M. Ridet, P. Gueze, R. Platel et R. Bauchot [14]).

#### Volume des principales subdivisions encéphaliques

Nous avons utilisé le plus gros de nos exemplaires (N° 8) pour faire l'analyse volumétrique des principales subdivisions encéphaliques. Ce choix est dicté par le souci de se rapprocher le plus possible de l'architecture de l'adulte, car l'on sait que les taux de croissance ontogénétique peuvent varier dans des proportions assez importantes d'une formation encéphalique à l'autre. Si l'on admet que l'exemplaire N° 8 ( $Ps = 1\ 200$  g) est un adulte, dont l'essentiel de la différenciation encéphalique est effectué, notre choix est alors parfaitement justifié.

L'encéphale a un poids frais de 0,895 g, ce qui correspond à un volume frais de 859,42 mm<sup>3</sup>. Après inclusion, l'encéphale a été coupé à une épaisseur de 20 μm puis coloré au violet de crésyl. Nous avons alors photographié 50 niveaux, équidistants de 0,68 mm, pour couvrir l'ensemble de l'encéphale, puis reconstitué le volume sur coupe par la méthode des pesées; ce dernier est de 388,806 mm<sup>3</sup>, ce qui correspond à un coefficient de rétraction de 2,21 voisin de ceux qui ont été calculés chez les autres vertébrés.

Ce volume sur coupe, rapporté à l'état frais, comporte 11,536 mm<sup>3</sup> de substance qui appartient à la moelle épinière (soit 1,34 %) et 173,003 mm<sup>3</sup> de structures diverses (portions proximales des nerfs crâniens, portions de pie-mère restées sur place lors de la dissection, etc... soit 20,13 %), si bien que les structures purement encéphaliques ne mesurent plus que 674,722 mm<sup>3</sup><sup>1</sup>. De cette dernière valeur, il faut encore soustraire le volume des ventricules, qui est particulièrement important chez les Esturgeons par suite de la grande taille du sac dorsal, qu'il est très difficile de délimiter, sinon arbitrairement, des ventricules proprement dits. Ce volume « ventricules + sac dorsal » atteint 237,973 mm<sup>3</sup>, soit 35,27 % du volume encéphalique proprement dit. Le volume de tissu nerveux n'est donc plus que de 436,749 mm<sup>3</sup>, et c'est sur cette valeur qu'ont été établis les pourcentages qui figurent dans le tableau 2. Nous avons fait figurer, sur ce même tableau, pour d'éventuelles comparaisons, les pourcentages établis strictement de la même façon sur trois espèces de Téléostéens des eaux françaises : la Truite, *Salmo gairdneri*, la Carpe, *Cyprinus carpio*,

<sup>1</sup> C'est pour cette raison que nous n'avons pas analysé l'indice d'encéphalisation de cette espèce. Nous en attendons confirmation à partir d'un matériel complémentaire.

et la Vieille ou Labre, *Labrus bergylta*, dont les résultats ont été fournis par l'un d'entre nous (J. M. Ridet [15]).

Nous avons fourni les grandes subdivisions encéphaliques. Sous la dénomination de lobe gustatif, nous comprenons ce que N. Goronowitsch appelle lobe vagal, mais dans lequel F. Theunissen a montré que parvenaient également des afférences d'origine faciale. La fonction essentiellement gustative de ce centre semble ne pas faire de doute, et nous devons le comparer à l'ensemble des lobes facial et vagal des Cyprinidae.

Tableau 2

Structure encéphal.	<i>Acipenser ruthenus</i>			<i>Salmo</i> Volume %	<i>Cyprinus</i> Volume %	<i>Labrus</i> Volume %
	Nombre de niveaux	Volume frais	Volume %			
Télesc.	13	83,956	19,22	12,37		
Hémisph.	6	46,355	10,61	10,12	10,70	23,41
Bulbes olf.	7	37,601	8,61	2,26	6,51	22,84
Diencephale	7	33,612	7,70	14,11	4,19	0,58
Tractus opt.	5	3,470	0,794	2,72	9,48	19,98
Toit optique	7	24,465	5,60	23,10	0,91	2,74
Métencéphale	22	116,975	26,80	24,65	8,03	26,19
Cervelet	16	88,727	20,32	21,70	31,46	19,28
Valvule	6	28,248	6,48	2,95	14,69	16,08
Tronc céréb.	27	174,271	39,90	22,09	16,77	3,20
Lobe gust.	15	13,516	3,09	—	38,72	12,42
Tronc s.s.	27	160,755	36,81	22,09	19,27	—
					19,45	12,42

Les quelques points remarquables que l'on peut tirer de la comparaison des volumes et des diverses formations encéphaliques de l'Esturgeon avec ceux de la Truite, de la Carpe et de la Vieille peuvent être résumés ainsi :

- Les bulbes olfactifs sont très développés, le double en volume relatif de ceux de la Carpe, la mieux pourvue des 3 Téléostéens étudiés ;
- les structures plus ou moins étroitement liées à la vision (tractus optiques, diencephale, toit optique) sont peu développées, même par rapport à la Carpe, qui est la moins bien pourvue ;
- les structures plus ou moins étroitement liées à la gustation (lobe gustatif, valvule) sont plus volumineuses que chez la Truite ou la Vieille, mais moins développées que chez la Carpe ;
- le cervelet au sens strict a une importance relative comparable à celle de la Truite, mais est bien plus développé que celui de la Carpe ou de la Vieille ;
- enfin le tronc cérébral sensu stricto diminue en taille relative quand on suit la série *Acipenser* — *Salmo* — *Cyprinus* — *Labrus*.

On peut déduire des remarques ci-dessus qu'*Acipenser ruthenus* est une espèce à vision faible (microptique), à olfaction très importante (macrosomatique), à gustation importante (présence de barbillons gustatifs), à mouvements locomoteurs complexes (cervelet important). La prise en considération des volumes relatifs des hémisphères cérébraux d'une part, du tronc au sens strict de l'autre semble de plus être en accord avec

la position systématique de ces poissons : l'Esturgeon, espèce pré-téléostéenne, a un tronc cérébral bien plus volumineux relativement que celui de la Truite ou de la Carpe, espèces malacoptérygiennes, lequel est à son tour bien plus volumineux que celui de la Vieille, espèce acanthoptérygienne.

## CONCLUSIONS

L'allométrie pondérale encéphalo-somatique interspécifique chez *Acipenser ruthenus* est de 0,50, valeur très proche de celle des Sélaciens et à la limite de variation des Téléostéens. Par rapport aux autres Poissons osseux, cette espèce se situe en dessous de la droite d'équilibre interspécifique, sans être pour autant parmi les moins encéphalisées.

L'analyse des volumes relatifs de diverses structures encéphaliques et leur comparaison avec les volumes chez la Truite, la Carpe et la Vieille, montrent un bon accord général entre les valeurs obtenues et ce que l'on sait de la biologie de cette espèce : elle est microptique, macrosomatique, pourvue de barbillons gustatifs et vraisemblablement assez mobile dans son milieu. Les volumes relatifs des hémisphères cérébraux et du tronc cérébral sont dans des proportions conformes à la place qu'assigne la systématique à ces diverses espèces.

## BIBLIOGRAPHIE

1. BAUCHOT R. et H. STEPHAN, 1964, Acta Zool., 45, 63-75.
2. BAUCHOT R., PLATEL R. et J. M. RIDET, 1975, Copeia.
3. GORONOWITSCH N., 1888, Morphol. Jb., 13, 427-574.
4. GRODZINSKI Z., 1945, C.R. Acad. Cracovie, 1-7, 13.
5. —, 1948, Bull. Int. Acad. Cracovie, B II, 1-6, 61-81.
6. JOHNSTON J. B., 1898, Zool. Bull., 26, 221-241.
7. —, 1901, Zool. Jb., 15, 59-260.
8. —, 1911, J. Comp. Neurol., 21, 6, 489-591.
9. NIEUWENHUYNS R., 1962, J. Morphol., 111, 1, 69-88.
10. —, 1964, Acta Morphol. Neerl-Scand., 6, 1, 65-79.
11. PLATEL R., BAUCHOT R. et C. DELFINI, 1973, Z. wiss. Zool., 185, 88-104.
12. PLATEL R., 1974, Zool. Anz., 192, 332-382.
13. RIDET J. M., 1973, C.R. Acad. Sci., Paris, Série D., 276, 1437-1440.
14. RIDET J. M., GUEZE P., PLATEL R. et R. BAUCHOT, 1975, C.R. Acad. Sci., Paris, Série D., 280, 109-112.
15. RIDET J. M., 1975, Bull. Mus. Nat. Hist. Nat., 3<sup>e</sup> série.
16. SBIKIN I. N., 1973, Voprosy Ichtiol. Akad. Nauk., 13, 5, 945-948.
17. THEUNISSEN F., 1914, Kon. Akad. Wet. Amsterdam Proc. Sect., Sci., 16, 1032-1045.
18. THIREAU M., 1973, Bull. Mus. Nat. Hist. Natur., 3<sup>e</sup> série, 188, 1947-1513.

Reçu le 18 avril 1975

Université de Paris  
Laboratoire d'Anatomie comparée  
Paris 7, 2 Place Jussieu  
et  
Institut de Science Biologiques  
Bucarest 17, Splaiul Independenței 296

DEVELOPMENT OF THE FOETAL MEMBRANES IN THE  
INDIAN LEAF-NOSED BAT, *HIPPOSIDEROS FULVUS*  
*FULVUS* (GRAY)

II. MORPHOGENESIS OF THE FOETAL MEMBRANES  
AND PLACENTATION

BY

A. GOPALAKRISHNA and K. B. KARIM

The development of the yolk sac, allantois and the histogenesis of the placenta of *Hipposideros fulvus fulvus* are described. While the yolk sac is large and forms an extensive chorio-vitelline placenta during early stages of development, the yolk-sac splanchnopleure becomes separated from the chorion during advanced stages, and undergoes collapse and folding accompanied by a hypertrophy of the endodermal cells resulting in its assuming a gland-like appearance with the lumen reduced to streak-like spaces during the final stages of gestation.

The allantoic vesicle is large until mid-pregnancy but becomes obliterated during the final stages of gestation. A narrow allantoic duct, however, remains in the umbilical cord.

The final allantoic placenta is mesometrially located, double discoidal, labyrinthine and vasodichorial. A conical accessory haemochorial placenta is present in the gap between the two placental discs near the maternal border of the placenta.

The early development, implantation of the blastocyst and the development of the embryo and the extra-embryonic structures until the embryo of *Hipposideros fulvus fulvus* reaches the neural groove stage of development were described by one of the present authors (Karim, in press) in the first part of this series of papers. The author also reviewed the literature on the embryology of the bats belonging to the family Hipposideridae and described the material and methods employed in these studies. The present paper embodies the development of the foetal membranes and placentation in this bat.

OBSERVATIONS

1. Stage of free allantoic diverticulum

Figures 5 and 6 illustrate the arrangement of the foetal membranes at an early stage of development of the allantois, which has not yet established contact with the placenta but lies as a free diverticulum with an enlarged vesicle at its extremity. The allantoic duct and the vesicle are lined by a distinct squamous epithelium. The amnion occurs as a thin bilaminar membrane bounding a large amniotic cavity. Although the placenta appears to be present on all the sides of the uterus in the figures, the examination of the entire series of sections reveals that the placenta is actually in the form of a spherical cup with a thick base on the mesometrial side, progressively thinning sides on the lateral sides of the uterus

and the mouth of the cup towards the antimesometrial side. Hence, there is no placenta on the antimesometrial side where a small area of the abembryonic nonvascular segment of the yolk-sac wall is in contact with the uterine endometrium, the uterine epithelium having been lost from the region at an earlier stage of pregnancy.

The placenta can be recognized into two kinds: the chorionic placenta on the mesometrial aspect of the uterus (that is, the base of the placental cup), and the chorio-vitelline placenta in the rest of the regions of the placental cup where the vascularized yolk-sac wall is in contact with the placenta (fig. 7). The histological structure of the placenta is similar to what was noticed during the neural groove stage of development (Karim, in press). The placenta consists near its foetal border of numerous placental tubules, each of which is composed of a central maternal blood capillary with hypertrophied endothelial lining surrounded by a layer of syncytiotrophoblast and a layer of cytotrophoblast. In the deeper regions of the placenta there is a continuous mantle of syncytiotrophoblast in which a network of maternal blood capillaries occur. The endometrial tissue bordering the maternal margin of the placenta has a loose texture and contains numerous fluid-filled intercellular spaces.

## 2. Early limb-bud stage

The foetus has developed one pair of limb-buds. The general arrangement of the foetal membranes at this stage of development is given in figures 1 and 8. The amnion is a uniformly thin bilaminar membrane enveloping the foetus, and is closely adherent to the allantois at several places.

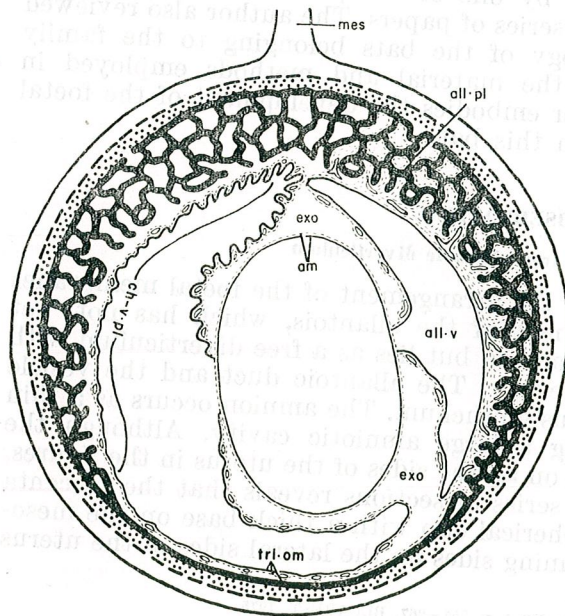


Fig. 1. — Semischematic drawing to illustrate the arrangement of the foetal membranes at the early limb-bud stage of development of the embryo. *all. pl*, allantoic placenta; *all. v*, allantoic vesicle; *am*, amnion; *ch-v. pl*, chorio-vitelline placenta; *exo*, exocoelom; *mes*, mesometrium; *tri. om*, trilaminar omphalopleure.

The yolk sac is large and appears in sections as a roughly crescentic bag attached by its abembryonic surface to the antimesometrial and a part of the lateral wall of the uterus. The entire yolk-sac wall is vascularized. The roof of the yolk sac on the embryonic region is separated from the chorion and lies freely in the exocoelom. The endodermal cells of the yolk sac are cuboidal in the free segment and in the region of the chorio-vitelline placenta on the lateral sides of the uterus, while they are squamous in the abembryonic segment where there is no placenta.

The allantois carries foetal vessels to the placenta on the mesial and part of the mesometrial side of the uterus, and has a large vesicle which has spread fan-wise at the foetal border of the placenta. The allantoic mesenchyme and foetal blood vessels have entered the hollows of the cytotrophoblastic villi.

Two types of placenta can be recognized at this stage, the chorio-vitelline placenta on the lateral sides of the uterus, and the chorio-allantoic placenta on part of the mesometrial side and the mesial side of the uterus. There is a fundamental difference between the chorio-allantoic placenta and the chorio-vitelline placenta. While the allantoic mesenchyme and foetal blood vessels actually enter the placental complex in the chorio-allantoic placenta, the vitelline vessels do not enter the placental complex but remain on the foetal border of the chorio-vitelline placenta. Hence, the chorio-vitelline placenta does not reach the structural complexity attained by the chorio-allantoic placenta.

Histologically the major portions of the placenta consists of numerous "placental tubules" hanging from the uterine wall (fig. 10). On the mesometrial side the placental tubules are more widely separated than at other regions, and allantoic mesenchyme and capillaries and the part of the yolk sac adjacent to the allantoic stalk lie in the space thus created on the mesometrial side of the uterus. The cytotrophoblastic villi are broad and extend almost to the maternal border of the syncytiotrophoblastic shell leaving a thin strip of the syncytiotrophoblast at the periphery. Each placental tubule (fig. 11) consists of a central maternal blood capillary with hypertrophied endothelial cells surrounded by two layers of trophoblast — an inner syncytiotrophoblast with lightly staining nuclei and an outer cytotrophoblast containing darkly staining nuclei. In sections stained by the PAS procedure a dark scarlet coloured membrane becomes apparent between the endothelial lining of the maternal vascular channels and the syncytiotrophoblast.

An interesting feature of this stage of development is that some of the placental tubules at the base of the placental cup near the mesometrial side of the uterus have broken down and maternal blood has become extravasated into large spaces surrounded by a layer of cytotrophoblast (fig. 9).

The deciduo-placental junction is loose and spongy, and remnants of a few uterine glands containing an eosinophilic secretion in the lumina are present near the myometrium.

## 3. Late limb-bud stage

The foetus has developed two pairs of limb-buds. The arrangement of the foetal membranes during this stage is illustrated in figures 2 and 12. The thin bilaminar amnion is in contact with the vascularized foetal wall of the allantoic vesicle in many places.

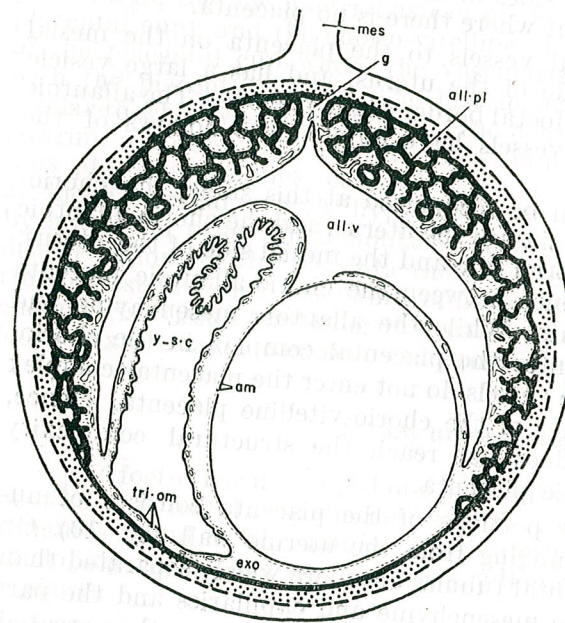


Fig. 2. — Semischematic drawing to illustrate the general arrangement of the foetal membranes at the late limb-bud stage of development of the embryo. *g*, placental gap; *y-s.c.*, yolk-sac cavity. Other labelling as in figure 1.

Exocoelom has extended to the region where the chorio-vitelline placenta was present during the previous stage. Consequently the vascular splanchnopleure of the yolk sac is separated from its contact with the placenta. Hence, the chorio-vitelline placenta is abolished. However, the exocoelom has not yet extended to the abembryonic region, where the vascular trilaminar segment persists and lies abutting against the uterine wall. Hence, the yolk-sac splanchnopleure is free on all the sides except on the abembryonic side. The endodermal cells are cubical to columnar and contain considerable amounts of PAS-positive material. The mesodermal cells form an investment of fusiform cells on the exocoelomic surface of the splanchnopleure.

The placenta which is entirely chorio-allantoic is still cup-shaped. The allantois has spread fan-wise on the foetal surface of the placental cup and contains an extensive allantoic vesicle which almost completely surrounds the amniotic cavity except on the antimesometrial side. The placenta is incompletely divided into two moieties due to the presence of a shallow gap at the base of the placental cup on the mesometrial side of the uterus. Histologically the placenta has undergone a considerable change over the previous stage. The placental tubules have undergone

branching and the branches of adjacent tubules have become anastomosed (fig. 13) resulting in the establishment of the labyrinthine placenta. The endothelial cells of the maternal capillary in the tubule have hypertrophied and contain darkly staining spherical nuclei. A thick zone of eosinophilic cytoplasm belonging to the syncytiotrophoblast surrounds the endothelium (fig. 14). In sections stained by PAS procedure a dark scarlet nonfibrous membrane (fig. 15) appears to be present in the middle of this zone of cytoplasm. A layer of cytotrophoblast surrounds the syncytiotrophoblast. The intertubular regions are occupied by allantoic mesenchyme and foetal blood capillaries.

The junctional zone is intensely PAS-positive. The entire zone is loose and spongy and tears off easily during the fixing and staining procedures.

## 4. Mid-pregnancy

The general arrangement of the foetal membranes at this stage of development is illustrated in figure 3. The foetus has considerably enlarged, and occupies the major volume of the gestation sac. Exocoelom has extended into the yolk-sac wall on all the sides so that the yolk-sac splanchnopleure has become completely separated from the chorion. The richly vascularized yolk-sac splanchnopleure has undergone further collapse and lies as a partly shrivelled structure between the amnion and the placenta. The endodermal lining (fig. 16) of the yolk sac has been thrown into numerous folds, and the cells are cubical to columnar, each containing a large centrally placed vesicular nucleus with darkly staining chromatin granules (fig. 17). The mesodermal investment does not exhibit any change over that in the previous stage.

The allantoic vesicle is large and almost completely surrounds the amniotic cavity except for a small region on the antimesometrial side. The foetal wall of the allantoic vesicle, that is, the wall adjacent to the amnion, is closely adherent to the amnion in several places so that a vascular amnio-allantoic membrane is formed. However, the amnion lies as a thin bilaminar membrane in other regions where the yolk sac intervenes between the amnion and the allantoic vesicle.

Histologically, the chorio-allantoic placenta has become more compact so that the intertubular areas in the placenta have become reduced. The placenta is still cup-shaped and is distinctly double discoidal, but the placental tubules are in the process of destruction at the margin of the cup where the cytotrophoblast has lost its cell boundaries, and along with the syncytiotrophoblast, occurs as large masses of cytoplasm in which numerous pycnotic nuclei lie scattered irregularly (Fig. 18). The cup-shaped chorio-allantoic placenta is progressively converted into a discoid structure on the mesometrial side. The placenta consists of a

closely approximated three dimensional network of placental tubules which have the same structure as in the previous stage of development. The deciduo-placental junction is loose and spongy.

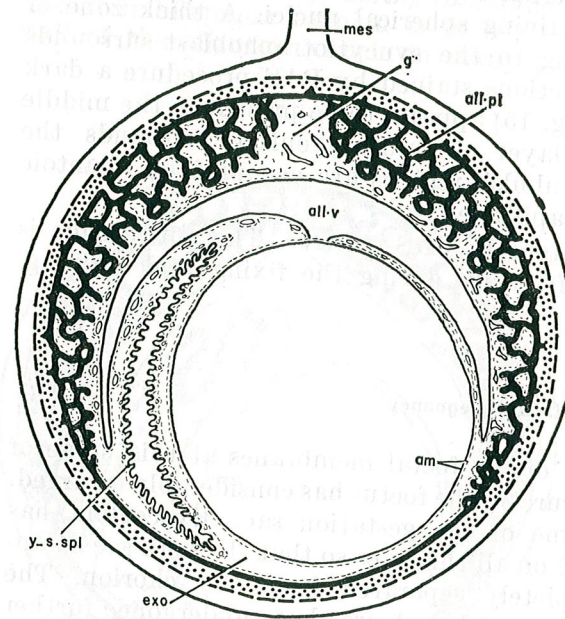


Fig. 3. — Semischematic representation of the arrangement of the foetal membranes at mid-pregnancy. *y-s.spl*, yolk-sac splanchnopleure. Other labels as in figure 2.

#### 5. Full term

Figure 4 illustrates the general topography of the foetal membranes at full term. The foetus has undergone enormous enlargement and almost completely fills the gestation sac. The long bones of the foetus are in the process of ossification and the petagia have been completely formed. The foetus is enclosed in a thin bilaminar amnion which is closely adherent to the body of the foetus and the allanto-chorion on the entire foetal surface of the placenta.

The yolk sac lies adjacent to the chorio-allantoic placenta on the mesometrial side of the uterus, and its lumen is considerably reduced due to the collapse and intense folding of the yolk-sac splanchnopleure (fig. 19). The remnants of the yolk-sac cavity contains an eosinophilic secretion. The endodermal cells of the yolk sac have undergone enormous hypertrophy and have become columnar. Large vacuoles are present in the cytoplasm at the bases of the cells, and these seem to have pushed the nuclei towards the distal regions of the cells (fig. 20). In many cells the nuclei are distorted and pycnotic. The apices of many of the endodermal cells have become ruptured, and the cytoplasm of these cells seems to have oozed out into the yolk-sac lumen along with the secretory material. The mesodermal cells form an investment of fusiform cells with darkly staining flat nuclei on the exocoelomic surface of the splanchno-

leure. Thus, the collapse of the yolk sac and the hypertrophy of its endodermal cells impart to it a gland-like appearance. The yolk sac is richly vascularized.

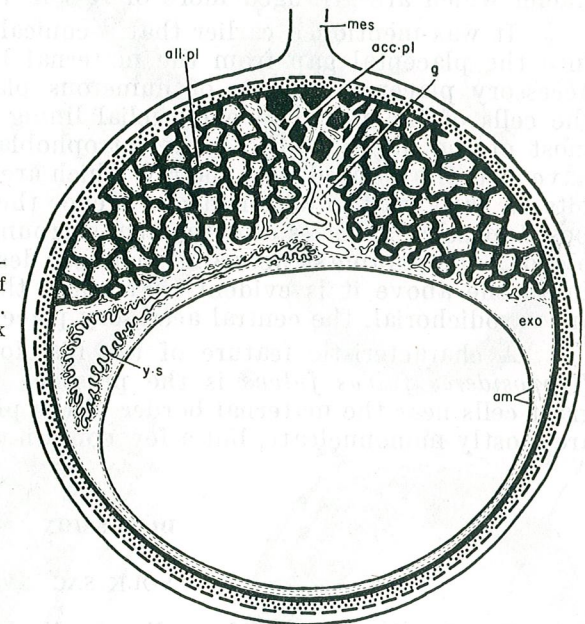


Fig. 4. — Semischematic drawing illustrating the general topography of the foetal membranes at full term. *acc.pl*, accessory placenta; *y.s*, yolk sac. Other labels as in figure 3.

The chorio-allantoic placenta is in the form of a concavo-convex disc separated into two moieties by a deep narrow cleft in its centre, and is located on the mesometrial side of the uterus. At the centre of the disc and projecting into the placental gap from the maternal side is a conical bulb-like structure which is referred to in the following description as the accessory placenta which appears in the form of a lightly stained triangle in stained sections (fig. 21). The allantoic vesicle is completely obliterated, but a small endodermal allantoic duct remains in the umbilical cord which is inserted between the two moieties at the foetal border of the placenta.

Histologically the two main moieties of the placental disc are composed of numerous branching and interconnected placental tubules which have considerably enlarged and which have become closely approximated. Foetal blood capillaries and mesenchyme lie on the walls of the placental tubules. These changes give the placenta a spongy appearance when viewed under low magnification (fig. 22). The distinctive character of the tubules can, however, be noticed at the foetal margin of the placenta. The endothelial cells of the maternal capillaries in the placental tubules have become sparse and depleted of most of the cytoplasm. Hence, in stained sections a few scattered nuclei of the endothelium are noticed in the placental tubules (fig. 23). A thick homogeneous zone of cytoplasm with irregularly distributed lightly staining nuclei surrounds the maternal endothelium. This is remnant of the syncytiotrophoblastic

layer. A dark scarlet nonfibrous PAS-positive membrane lies embedded within this thick zone of cytoplasm (fig. 24). The syncytiotrophoblast zone is surrounded by a layer of cytotrophoblast containing darkly stained nuclei which are arranged more or less in rows.

It was mentioned earlier that a conical accessory placenta projects into the placental gap from the maternal border of the placenta. The accessory placenta consists of numerous placental tubules from which the cells of the maternal endothelial lining have disappeared. Furthermore most of the nuclei of the syncytiotrophoblast and the cytotrophoblast have also disappeared, and the few which are left have broken into small bits on their way to degeneration. Hence the tubules appear to be composed mostly of a mass of cytoplasm surrounding large pools of maternal blood. A comparable structure has not been described in any other mammal. From the above it is evident that while the two main placental discs are vasodichorial, the central accessory placenta is haemochorial.

A characteristic feature of the histology of the ripe placenta of *Hipposideros fulvus fulvus* is the presence of numerous trophoblastic giant cells near the maternal border of the placenta [16]. The giant cells are mostly mononucleate, but a few contain two to four nuclei.

#### DISCUSSION

##### YOLK SAC

The development of the yolk sac displays two main trends in the bats: (i) The abembryonic segment of the yolk sac remains permanently bilaminar or trilaminar as in *Desmodus rotundus murinus* [30], *Noctilio labialis minor* [1], *Glossophaga soricina soricina* [14], *Artibeus jamaicensis parvipes* [34], *Megaderma lyra lyra* [9] [18], and the vespertilionid bats [8] [11] [21] [22] [24] [29]. In Noctilionidae [1], Phyllostomatidae [34], Desmodontidae [30], and Megadermatidae [9] [18] the abembryonic yolk-sac wall remains in contact with the uterine wall, while in Vespertilionidae the abembryonic wall of the yolk sac remains freely hanging in the persistent uterine lumen. (ii) The yolk-sac splanchnopleure becomes completely separated, and the endodermal cells and sometimes the mesodermal elements also undergo hypertrophy, thereby giving it a gland-like appearance. The yolk sac changes its position and ultimately comes to lie adjacent to the placental disc — a location which is opposite to the one it occupied during the earlier stages of development. Whereas the yolk-sac lumen persists as small streaks in some microchiropteran bats such as *Rhinopoma kinneari* [10] [26], *Taphozous longimanus* [10], *Hipposideros bicolor pallidus* [10], and *Rhinolophus rouxi* [2], the yolk sac undergoes complete collapse losing its lumen and becomes converted into a solid, vascular gland-like structure in all Megachiroptera [12] [19] [20] [25] [31], and in *Tadarida brasiliensis cynocephala* [27] among Microchiroptera.

In *Hipposideros fulvus fulvus* the yolk-sac splanchnopleure is completely separated from the chorion, and is thrown into numerous folds

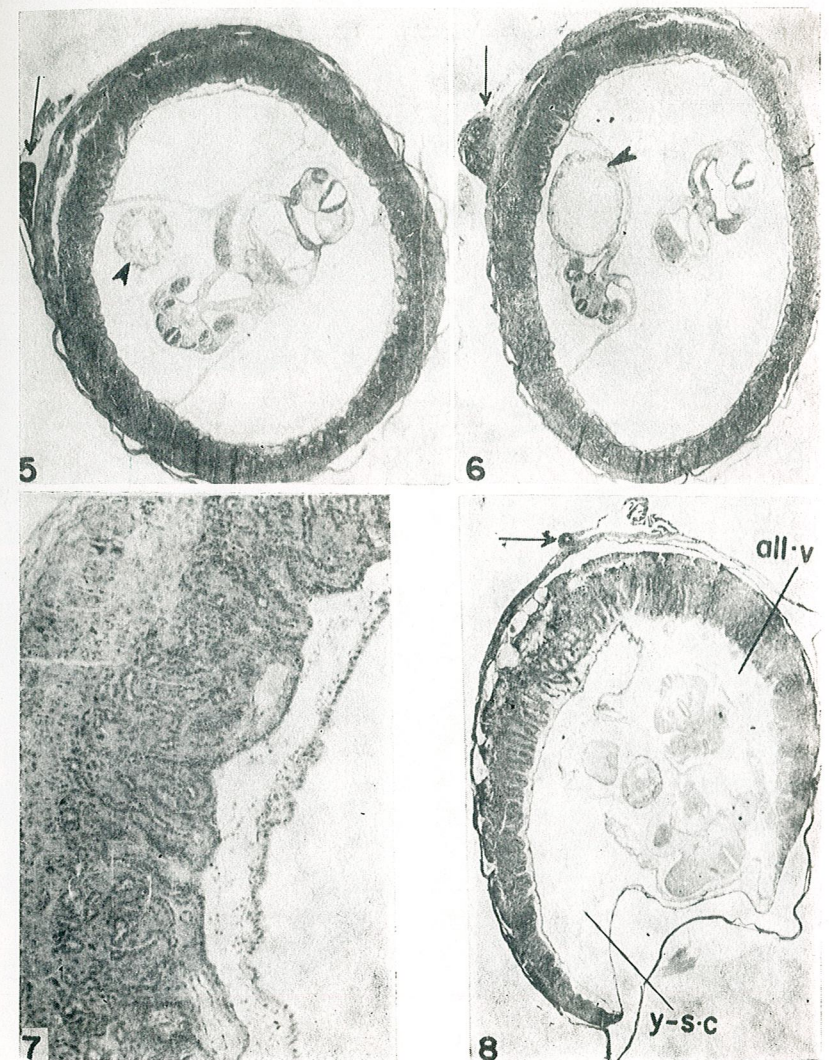


PLATE I

Figs 5 and 6. — Sections passing through two different regions of the uterus containing an embryo at the free allantoic diverticulum stage. Arrow points towards the mesometrium. Note the free allantoic diverticulum (arrow head) with a large vesicle.  $\times 22$ .

Fig. 7. — Part of the chorio-vitelline placenta at the free allantoic diverticulum stage. Note the presence of numerous maternal blood capillaries with enlarged endothelial cells. The placental tubules are distinct near the foetal border of the placenta.  $\times 120$ .

Fig. 8. — Transverse section of the uterus containing an embryo at the early limb-bud stage of development. Arrow points towards the mesometrium. all. v, allantoic vesicle; y-s. c, yolk-sac cavity.  $\times 22$ .



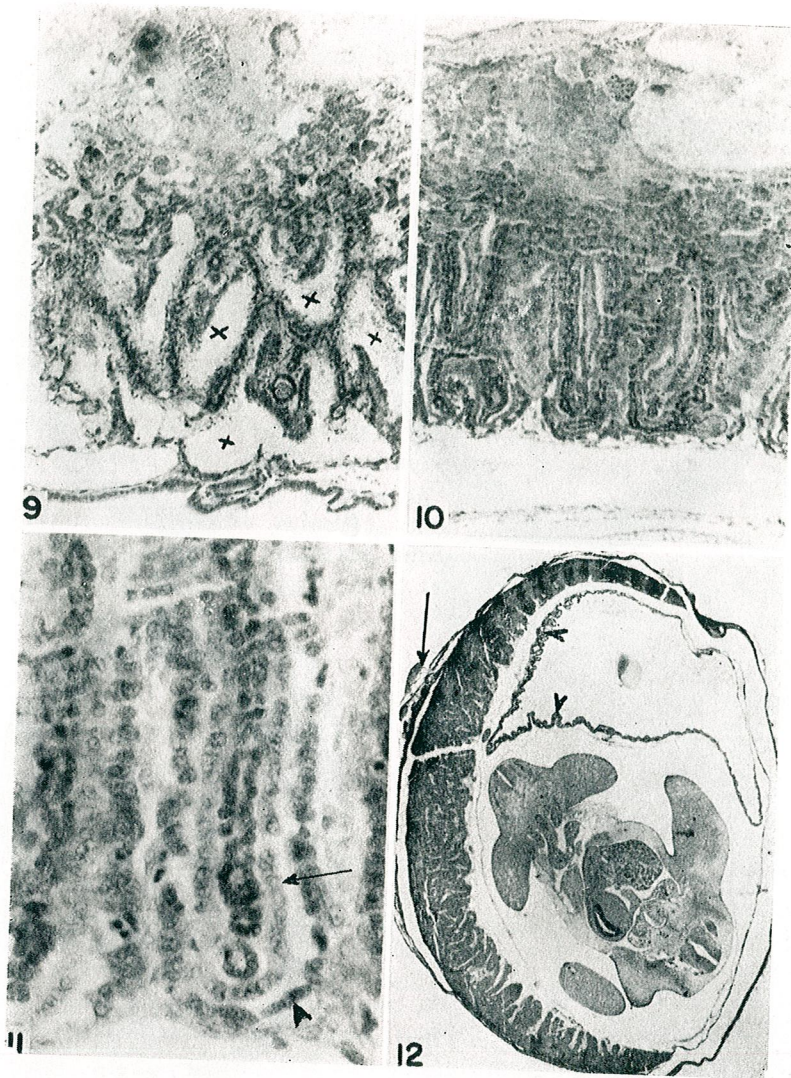


PLATE II

Fig. 9. — Part of the placenta near the mesometrial side of the uterus at the early limb-bud stage. Note the break down of the placental tubules and large spaces (x) into which maternal blood has extravasated and is surrounded by a layer of cytotrophoblast.  $\times 140$ .

Fig. 10. — Part of the chorio-allantoic placenta at the early limb-bud stage.  $\times 140$ .

Fig. 11. — Enlarged placental tubule at early limb-bud stage. Note the presence of a central maternal blood capillary with hypertrophied endothelial cells with darkly staining nuclei surrounded by an inner layer of syncytiotrophoblast (arrow) and an outer layer of cytotrophoblast (arrow head) in the placental tubule.  $\times 450$ .

Fig. 12. — Transverse section of the uterus containing an embryo at the late limb-bud stage of development. Arrow points towards the mesometrium. The arrow head points towards the folded yolk-sac splanchnopleure.  $\times 16$ .

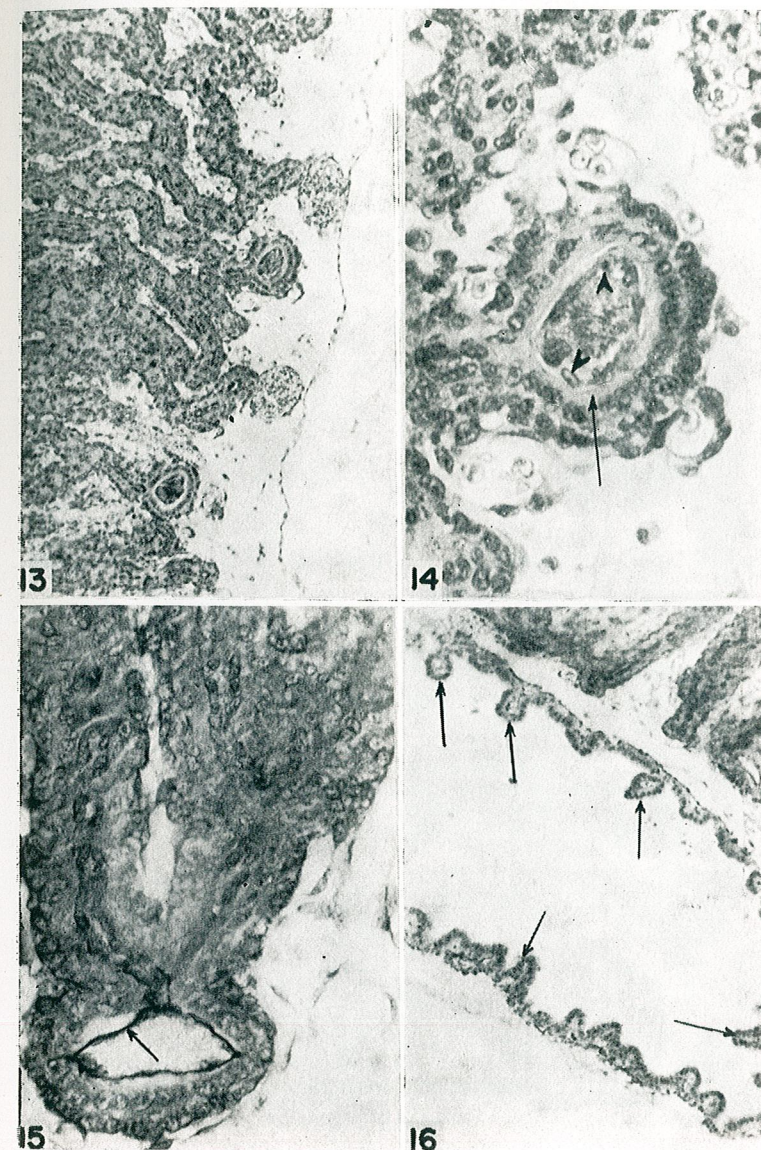


PLATE III

Fig. 13. — Part of the chorio-allantoic placenta at the late limb-bud stage of development of the embryo. Note the labyrinthine condition of the placenta.  $\times 140$ .

Fig. 14. — Enlarged part of a placental tubule shown in figure 13. Note the thick zone of eosinophilic cytoplasm (arrow) belonging to the syncytiotrophoblast surrounding the endothelium (arrow head). The two layers of trophoblast are also distinct.  $\times 480$ .

Fig. 15. — Part of a placental tubule (PAS staining) at late limb-bud stage. Arrow points towards the interstitial membrane.  $\times 480$ .

Fig. 16. — Part of the yolk sac at mid-pregnancy. Many folds of the endodermal lining (arrow) project into the yolk-sac cavity.  $\times 160$ .

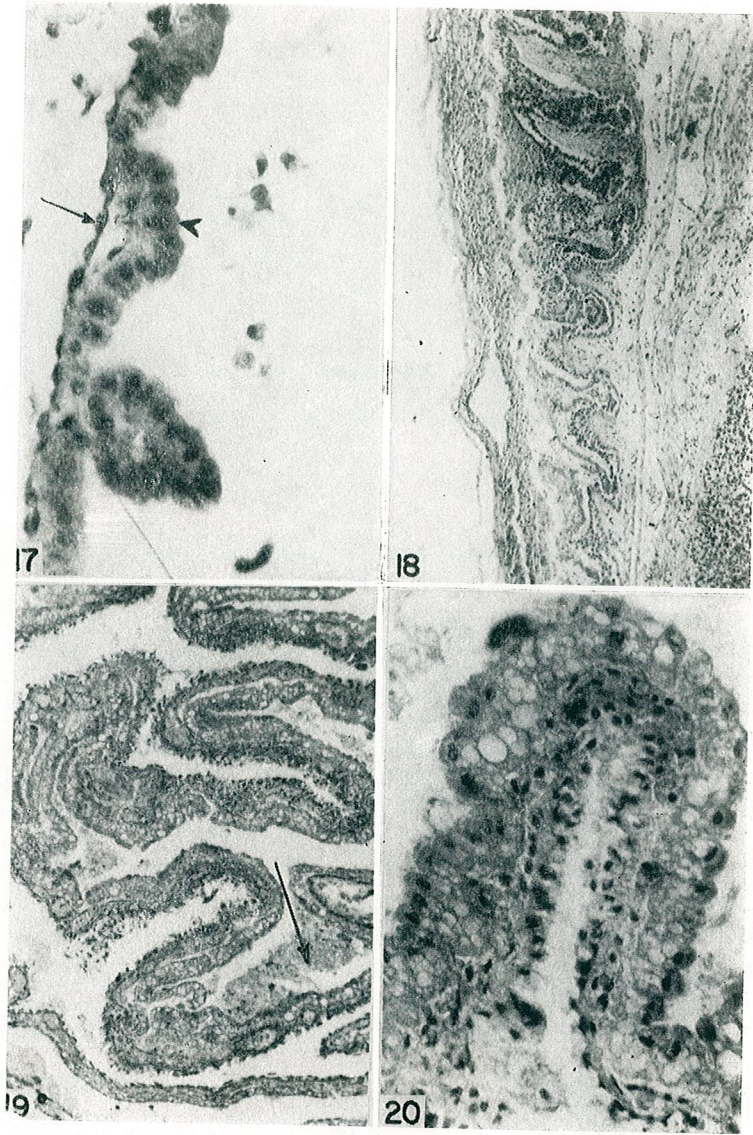


PLATE IV

- Fig. 17. — Enlarged part of the yolk-sac wall shown in figure 16. Note the cubical to columnar endodermal cells (arrow head) and the fusiform mesodermal cells (arrow) forming an investment.  $\times 460$ .
- Fig. 18. — Part of the margin of the placental cup at mid-pregnancy showing the placental tubules in the process of destruction.  $\times 120$ .
- Fig. 19. — Part of the yolk sac at full term. The splanchnopleure has collapsed so that the yolk-sac cavity is reduced to small spaces (arrow).  $\times 140$ .
- Fig. 20. — Part of the yolk-sac wall at full term enlarged. Note the presence of large vacuoles at the bases of the columnar endodermal cells. The nuclei are placed distally, and many of them are pyknotic and distorted in shape.  $\times 460$ .

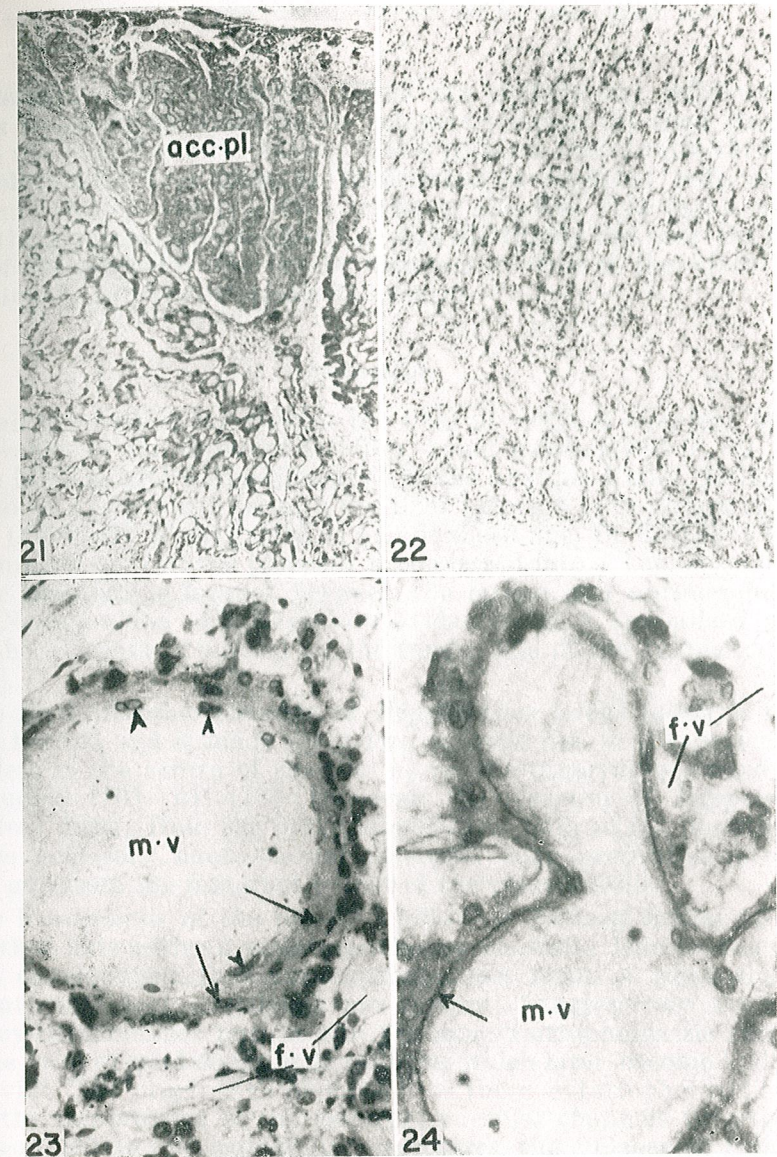


PLATE V

- Fig. 21. — Part of the chorio-allantoic placenta at full term. Note the presence of the accessory placenta (*acc. pl.*) projecting into the gap in the placenta.  $\times 80$ .
- Fig. 22. — Part of the chorio-allantoic placenta at term. The placental tubules have enlarged in size and have become closely approximated, giving the placenta a spongy appearance.  $\times 80$ .
- Fig. 23. — A placental tubule at term (Haematoxylin-eosin staining) from the foetal border of the placenta. The endothelial cells (arrow head) of the maternal vessel (*m.v.*) have become sparse and depleted of most of the cytoplasm. Note the presence of an inner layer of syncytiotrophoblast (arrow) and an outer layer of cytotrophoblast with dark nuclei surrounding the placental tubule. *f.v.*, foetal blood capillary.  $\times 650$ .
- Fig. 24. — Placental tubule (PAS-staining) at term. Note the presence of a dark scarlet PAS-positive membrane (arrow) which lies embedded within the thick zone of cytoplasm. *f.v.*, foetal vessel; *m.v.*, maternal vessel.  $\times 650$ .

and undergoes partial collapse. While the endodermal cells undergo enormous hypertrophy and become columnar during the final stages of gestation the mesodermal elements of the yolk-sac wall do not show any appreciable change and form an investment of fusiform cells on the exocoelomic surface. As gestation advances the free yolk sac is drawn towards the placental disc so that the yolk sac finally lies near the foetal surface of the placental disc on the mesometrial side of the uterus. The yolk-sac lumen persists as streak-like spaces.

#### Placentation

In all the bats so far studied the final placenta is discoidal but its position varies in the different families, being mesometrial in the more primitive families and antimesometrial in the advanced ones. Molossidae appears to be exceptional because the final placenta is mesometrial [27] although the family is recognized as an advanced one. In Emballonuridae the mesometrial part of the placenta is converted into a haematoma [10] [32]. The placenta is located between the lateral and antimesometrial sides in Noctilionidae [1]. Phyllostomatidae forms a specialized group because the placenta is located on the fundic side of the simplex uterus [23] [34].

The final allantoic placenta of *Hipposideros fulvus fulvus* is mesometrially located and is made up of two moieties due to the presence of a deep cleft in the centre of the disc as in the other hipposiderid bats so far studied [10] [13] [15]. However, the placenta of *Hipposideros fulvus fulvus* differs from the other hipposiderid bats so far described in having an accessory haemochorial placental cone projecting into the placental gap from the maternal border of the placental disc.

The histogenesis of the placenta follows a pattern similar to that seen in other bats with an endotheliochorial placenta. During the early stages of development the syncytiotrophoblast forms a thick shell in which maternal blood capillaries are present. Progressively the basal layer of cytotrophoblast pushes into the syncytiotrophoblastic shell, at first in the form of solid columns of cells but which later become hollowed out into villi. The progressive expansion of these cytotrophoblastic villi result in the compression of the maternal vascular channels inverted by syncytiotrophoblast into tubule-like structures, the "placental tubules" [13]. At limb-bud stage each placental tubule is composed of a central maternal blood capillary with a distinct lining of hypertrophied endothelial cells, a homogeneous PAS-positive membrane, a layer of syncytiotrophoblast, a layer of cytotrophoblast and foetal blood vessel wall. The tubules undergo intense branching and anastomosis leading to the establishment of the labyrinthine placenta. After mid-pregnancy the endothelial cells lining the maternal blood vessel walls become progressively attenuated until they become flat and lie scattered in a band of cytoplasm during the final stages of pregnancy. The syncytiotrophoblastic layer also becomes considerably attenuated in the ripe placenta. A patent PAS-positive membrane — the interstitial membrane — [31] forms an integral part of the placental barrier throughout gestation. Wimsatt [31]

indicated that the material of the interstitial membrane may be derived wholly, or in part, from the syncytiotrophoblast. Björkman and Wimsatt [3] have shown that the interstitial membrane in the placenta of *Desmodus rotundus murinus* is never in direct contact with the lumen of the blood space, but is always covered over with a lining of cytoplasm which is continuous with the syncytial trophoblast. They also observed that the interstitial membrane has a dual origin, part of it being the remnant of the basement membrane of the maternal endothelium and part of it being contributed by the trophoblast. Branca [4] and Gérard [7] interpreted the layer of cytoplasm lining the inner surface of the maternal blood vessel wall in the placenta of *Miniopterus schreibersii* as the cytoplasmic remnant of the maternal endothelium. However, recent electron microscopic studies by Enders and Wimsatt [6] on *Myotis lucifugus lucifugus* by Björkman and Wimsatt [3] on *Desmodus rotundus murinus*, and Stephens [28] on *Tadarida brasiliensis cynocephala* have revealed that the endothelial lining is absent from these channels, and that the cytoplasm of the syncytiotrophoblast passes through gaps in the interstitial membrane and forms a continuous lining on the inner surface of the interstitial membrane. Thus, a haemochorial condition is finally established in these bats.

The definitive placenta was described as endotheliochorial in *Rhinopoma kinneari* [26], *Taphozous longimanus* [10], *Noctilio labialis minor* [1], *Megaderma lyra lyra* [10] [18], *Rhinolophus rouxi* [2], *Hipposideros bicolor pallidus* [13], *Hipposideros speoris* [15], and *Scotophilus wroughtoni* [10]. The placenta was described as being haemochorial in most of the vespertilionid bats [6] [11] [21] [24] [29], *Tadarida brasiliensis cynocephala* [27] [28], *Desmodus rotundus murinus* [3]. In *Tadarida brasiliensis cynocephala* [27] [28] the syncytiotrophoblastic layer, and in *Pipistrellus ceylonicus chrysothrix* [21] the cytotrophoblastic layer disappears from the final placenta.

Since both syncytiotrophoblast and cytotrophoblast layers are present in the final placenta of *Hipposideros fulvus fulvus*, the definitive placenta in this bat may be designated as vasodichorial on the basis of the terminology suggested by Wislocki [33] for endotheliochorial placenta and by Enders [5] for haemochorial placenta.

## REFERENCES

1. ANDERSON J. W., WIMSATT W. A., 1963, Amer. J. Anat., **112**, 181-202.
2. BHIWGADE D. A., 1973 (Thesis).
3. BJÖRKMAN N. H., WIMSATT W. A., 1968, Anat. Rec., **162**, 85-97.
4. BRANCA A., 1927, Arch. Zool. exp. gén., **66**, 291-450.
5. ENDERS A. C., 1965, Amer. J. Anat., **116**, 29-68.
6. ENDERS A. C., WIMSATT W. A., 1968, Amer. J. Anat., **122**, 453-489.
7. GÉRARD P., 1928, Arch. Biol., **38**, 327-354.
8. GOPALAKRISHNA A., 1950, Proc. ind. Acad. Sci., **31**, 235-251.
9. —, 1950, Proc. nat. Inst. Sci. India, **16**, 93-98.
10. —, 1958, J. Morph., **102**, 157-197.
11. GOPALAKRISHNA A., KARIM K. B., 1972, Curr. Sci., **41**, 144-146.
12. —, 1972, Curr. Sci., **41**, 639-641.
13. GOPALAKRISHNA A., MOGHE M. A., 1960, Z. Anat. EntwGesch., **122**, 137-149.

14. HAMLETT G. W. D., 1935, Amer. J. Anat., **56**, 327-353.
15. JEEVAJI I. H., 1973 (Thesis).
16. KARIM K. B., 1973, Curr. Sci., **42**, 282-284.
17. —, 1974, Rev. roum. Biol., **19**, 4, 251-256.
18. KHAPARDE M. S., 1971 (Thesis).
19. MOGHE M. A., 1951, Proc. zool. Soc. London, **121**, 703-721.
20. —, 1956, Proc. nat. Inst. Sci. India, **22**, 48-55.
21. PHANSALKAR R. B., 1972 (Thesis).
22. RAMASWAMI L. S., 1933, Half-yearly J. Mysore Univ., **7**, 1-41.
23. RASWEILER J. J., 1972, J. Reprod. Fertil., **31**, 249-262.
24. SAPKAL V. M., 1973 (Thesis).
25. SPRENKEL VAN DER H. B., 1932, Z. mikr.-anat. Forsch., **28**, 185-268.
26. SRIVASTAVA S. C., 1952, Proc. zool. Soc. Bengal, **5**, 105-131.
27. STEPHENS R. J., 1962, Amer. J. Anat., **111**, 259-285.
28. —, 1969, J. Ultrastruct. Res., **28**, 371-398.
29. WIMSATT W. A., 1945, Amer. J. Anat., **77**, 1-51.
30. —, 1954, Acta anat., **21**, 285-341.
31. —, 1958, Acta anat., **32**, 141-186.
32. WIMSATT W. A., GOPALAKRISHNA A., 1958, Amer. J. Anat., **103**, 35-68.
33. WISLOCKI G. B., 1954, in *Gestation. Transactions of the 1st Conference*. The Josiah Macy Jr. Foundation.
34. WISLOCKI G. B., FAWCETT D. W., 1941, Anat. Rec., **81**, 307-317.

Received March 18, 1974

Institute of Science  
Department of Zoology  
Nagpur, India

# LIPIDO-CAROTENOID METABOLISM IN *SALMO GAIARDNERI* DURING EMBRYOGENESIS

BY

MATILDA JITARIU, ELENA CHERA, ECATERINA DUCA, GABRIELA LINCK,  
PINCU ROTIMBERG and ISTVÁN SZILAGYI

It was evidenced the main carotenoid pigments during *Salmo gairdneri*'s embryogenesis. The metabolism of lipid substances during the same period was studied. The participation of both substances in the development of the embryo was ascertained.

Power sources and the sequence of their utilization in fish during embryogenesis has been quite an interesting and most investigated problem [2] [10] [12-14]. As a matter of fact, the material best suited for research has been the roe of salmonides. Nevertheless, the results yielded by these fishes have failed to provide a definite answer to the problem which, for that matter, remains still open.

We have pursued the metabolism of lipids along with the metabolism of carotenoid substances, as it is common knowledge that these substances form complexes with lipids.

## MATERIAL AND METHOD

Roe freshly extracted in order to constitute the *control*, as well as roe taken from the incubator at different intervals from the moment of fertilization were dried up between filter sheets. A portion of this roe served for the determination of total lipids and their fractions, whereas another portion served for the analysis of carotenoid substances.

Total lipids and free fatty acids were determined according to the method presented in [1], total and esterified cholesterol according to [15], phospholipids - to [8].

The material was previously weighed and the carotenoids extracted in light petroleum-acetone (PE-Ac.) 3 : 2. The extracts were kept at 4°C in the dark and in nitrogen atmosphere.

After passing the carotenoid through PE the extinction was read at 450 m $\mu$  on the Beckman D. B. spectrophotometer with a view to calculating the total carotenoid concentration of the respective extract in  $\mu\text{g/g}$  tissue [3].

*Pigment isolation* was carried out by chromatography on a silicagel-celit column 3 : 1 (Silicagel Merck; Celit B. F. Serva) and eluted with increasing concentrations of Ac.-PE.

*Pigment purification* was effected by thin-layer chromatography (TLC) [6] on 35 x 18 and 16 x 9 cm glass plates, 0.25 mm in depth.

The pigments were identified according to the mobility and colour on column and TLC plates, by the following methods :

A reduction of the carbonyl group [7].

Determination of the epoxide group by colour reaction [5].

Absorption spectra in various solvents and the shape of absorption spectra.

An estimation of the partition coefficient [9], when the amount of pigments allow saponification.

An appreciation of the embryonary stage was made according to histological preparation.

### RESULTS AND DISCUSSIONS

In the fresh roe extracted in order to constitute the control, the amount of the total carotenoids is of 0.260  $\mu\text{g/g}$ . After chromatographic separation on silicagel-celit column, four pigmentary fractions are isolated namely, fractions I, II, III, IV.

At TLC, fractions I and II evidenced a single pigment each, in small amount, with  $R_f = 0.97$ . It seems to be  $\beta$ -carotene.

*Fraction III* is eluted from the column in 30% Ac.-PE. It is the richest fraction as to carotenoid forms. At TLC, five pigments emerge *IIIA*, showing on the plate a light-yellow colour with  $R_f = 0.99$ . In PE it has an absorption maximum of 474–443–420  $m\mu$  and in Benzene (Bzn) of 485–455–430  $m\mu$ . The colour reaction is slightly positive. The absorption maxima of both solvents as well as the colour reaction, point to the presence of *taraxanthin*.

*IIIB* has a yellow-greenish colour, with  $R_f = 0.76$  and an absorption maximum of 474–446–425  $m\mu$  in PE, and of 489–459–453  $m\mu$  in Bzn. The partition coefficient after saponification becomes 80% epiphaseous pointing to a *mono-alcohol*. After the absorption maxima of the two solvents as well as the partition coefficient, we may assert that it is  *$\alpha$ -cryptoxanthin*.

*IIIC* has a red-orange colour; after its dissolving in Ac. by decantation there remains fixed on the alkalic paste [6] another pink pigment which dissolves only in acidulated Ac. with 5% glacial acetic acid.

The pigment which dissolves in neutral Ac. has an absorption maximum of 463  $m\mu$  in PE, whose curve shape is symmetrical. The amount of the pigment has been insufficient to allow a reduction. Colour reaction is negative. The colour on the plate TLC, the curve shape and the absorption maximum point to a diketo-carotenoid, most likely *cantaxanthin*.

The pigment dissolved in acidulated Ac. provides an absorption maximum of 468  $m\mu$  in PE with a nice symmetrical curve. It is *astaxanthin*.

*IIID* is yellow-coloured with  $R_f = 0.18$  and an absorption maximum of 477–448–423  $m\mu$  in PE, and 487–456–426  $m\mu$  in  $\text{CH}_3\text{Cl}$ . The reaction towards epoxide is negative. The partition coefficient is 86% hypophasic after saponification [9]. This one as well as the absorption maximum of the two solvents point to the presence of *lutein*.

*IIIE* is an orange pigment with  $R_f = 0.10$  and an absorption maximum of 455–440–427  $m\mu$  in PE and of 492–446–438  $m\mu$  in  $\text{CH}_3\text{Cl}$ . Its amount being small, it was not possible to make any further analyses for its identification.

*Fraction IV* is eluted from the column in 50% Ac.-PE. At TLC, it contains two pigments in small amount, with  $R_f = 0.47$  and 0.07.

After 26 hours from fertilization, the total amount of carotenoid drops. Upon chromatographing on silicagel-celit column, there emerge an equal number of carotenoid fractions, but in reduced concentrations.

From fraction III, cantaxanthin can no longer be evidenced, but astaxanthin, the most highly concentrated pigment in the whole fraction, does appear.

After three days from incubation, the total carotenoid pigment is very small. Only fraction III remains a little more concentrated, at TLC evidencing a yellow-orange coloured pigment, with an absorption maximum of 474–438  $m\mu$  in PE and a straw-yellow coloured pigment with an absorption maximum of 472–442 ~ 428  $m\mu$  in PE. Traces of astaxanthin do still exist. The amount of the remaining pigments from fraction III and IV is too small to allow their analysis.

Starting with the 11th day of fertilization, one can notice an increase of pigment in fraction I, reaching a concentration of 0.0975  $\mu\text{g/g}$  on the 21st day after fertilization. This pigment possesses the same characteristics as those of the control.

On the 21st day of incubation, fraction III gets again rich in various xanthophyllic forms, being likewise much more concentrated. Apart from taraxanthin,  $\alpha$ -cryptoxanthin, lutein, cantaxanthin, and astaxanthin, at TLC a new form is isolated having an absorption maximum of 471–441–418  $m\mu$  in PE and of 485–453–433  $m\mu$  in Bzn. The curve indicates very high peaks of absorption maxima. Reaction towards epoxide is negative. It is not definitive. Another new form is also the carotenoid having an absorption maximum of ~ 467–447  $m\mu$  in PE and of ~ 476–458  $m\mu$  in Bzn. Reduction turns it into a form of 470–445–425  $m\mu$  in PE. It is a *monohydroxy-ketocarotene*. The remaining pigments from fractions III and IV were in very small amount.

When hatching occurs (30 days later), fraction III is rich in epoxides, of which one is *violaxanthin*, identified according to the absorption maximum of 472–442 ~ 419  $m\mu$  in PE and 483–455–430  $m\mu$  in Bzn. The epoxide test is positive. Taraxanthin and  $\alpha$ -cryptoxanthin exist in dosing amounts, whereas cantaxanthin can no longer be evidenced and astaxanthin is present in a rather small amount.

*Fraction IV* contains three pigmentary forms with an absorption maximum of ~ 474–440  $m\mu$ ; 465–385  $m\mu$  and 469–435  $m\mu$  in PE. Their small amount did not allow further analyses.

At the same time, analyses performed on the total lipid and its various forms point to the onset of their metabolism along with the start of fertilization. The total lipid (fig. 1) was followed up starting with the control and up to the egg which contains larvae ready to hatch. It was found to be gradually consumed in the form of phospholipids (fig. 2), of free fatty acids (fig. 5), and cholesterol (fig. 3). We are not going to mention the triglycerides, which were worked upon with an improper method. Our results confirm the general findings of other authors [2] [10] [12–14]. We should like to stress that the consumption of lipids in *Salmo gairdneri* studied by us, is smaller (20%) than 70–80% as indicated by literature [2] and that it is not a continuous consumption, but an intermittent one (figs 2–5). The amount of total lipids in this *Salmo* is three times larger than in *Cyprinus carpio* (data not yet published), which might prove to be the result of its adaptation to life conditions in the fish basin.

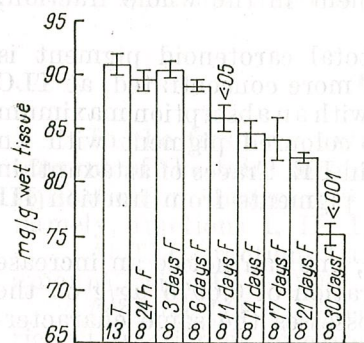


Fig. 1. — The metabolic variations of total lipids during embryogenesis of *Salmo gairdneri*. T, test; F, fertilization.

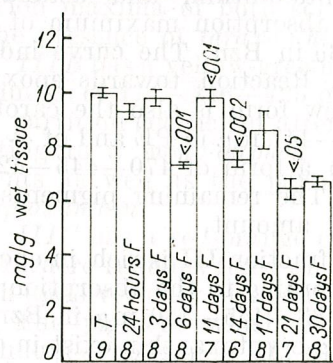


Fig. 3

Figs 3 and 4. — The metabolic variations of total (fig. 3) and esterified (fig. 4) cholesterol in *Salmo gairdneri* during embryogenesis.

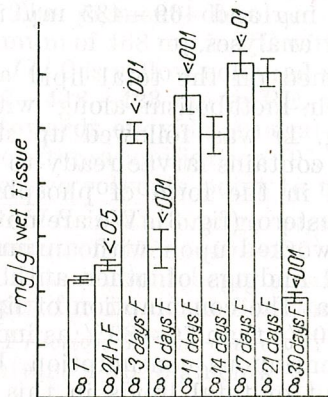


Fig. 5. — The metabolic variations of the free fatty acids in *Salmo gairdneri* during embryogenesis.

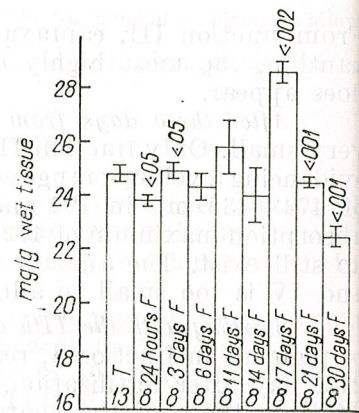


Fig. 2. — The metabolic variations of phospholipids in *Salmo gairdneri* during embryogenesis.

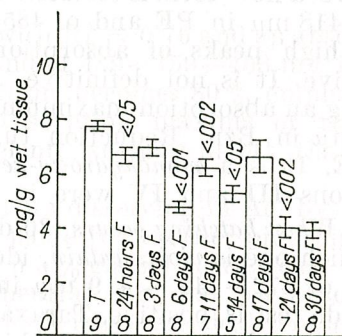


Fig. 4

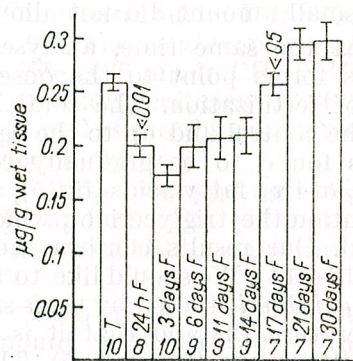


Fig. 6. — The metabolic variations of the total carotenoids in *Salmo gairdneri* during embryogenesis.

Figures 2 and 4 exemplify that phospholipids and esterified cholesterol are involved in the start of embryogenesis, together with carotenoids (fig. 6), demonstrating that both complexes: caroteno-phospholipids and caroteno-cholesterol are involved in the biochemical process brought about by embryogenesis. At the settling of "blastula" (three days' incubation) there occur the lowest carotenoid values and a significant increase of fatty acids (fig. 5).

The embryo with 56 somites (17 days' incubation) is characterized by the highest concentration of free fatty acids and phospholipids during the whole embryogenetic period studied by us, which coincides with a slightly significant increase of carotenoids. Yamagami and Mohri [16] point to the fact that 18 days after fertilization in the egg of *Salmo irideus* an important change, due to the reduction of lecithin and emergence of lysolecithin, has been noticed. The authors do not mention, however, whether this discovery coincides with the quantitative growth of phospholipids.

At the moment of hatching (30 days) the value of all lipid forms is significantly lower than the initial value in non-fecundated egg, thereby clearly demonstrating that they participate as an energetical source in the process of embryogenesis, not only at a certain stage of the embryonic development, but also throughout the whole period until hatching.

The behaviour of the carotenoids is rather peculiar in the initial stage (non-fecundated ovule) yet is shows a significantly high value at the moment of hatching (fig. 6). If we relate the value of total carotenoids, which is  $0.173 \mu\text{g/g}$  three days after fertilization, to that of  $0.294 \mu\text{g/g}$  presented after 30 days, when the larva hatches, we discover that the significance of carotenoid increase is  $p > 0.001$ .

For the time being we are not in a position to explain this fact. We can merely state the possibility of the egg to remake this kind of molecules, well known as excellent donors and acceptors of electrons [11] and serving at the same time as substratums for catabolic processes [4].

#### REFERENCES

1. BARRETTO R. C., MONO D., 1961, Clin. chim. Acta, **6**, 887—889.
2. BLAXTER J., 1969, *Fish Physiology*, Acad. Press, New York — London, vol. III, p. 201.
3. BONALY R., 1967, *Biosynthèse des caroténoïdes cycliques des levures du genre Rhodotorula*, Nancy (Thésis).
4. CHICHESTER C., NAKAYAMA T., 1965, *Chemistry and Biochemistry of Plant Pigments*, Acad. Press, New York — London, p. 446—450.
5. CURL A., BAILEY G., 1961, J. Agric. Food Chem., **9**, 403—405.
6. HAGER A., MEYER-BERTHENRATH T., 1966, Planta (Berl.), **69**, 198—217.
7. KRINSKY N., GOLDSMITH T., 1960, Arch. Biochem. Biophys., **91**, 271—279.
8. OUTHOUSE E., FORBES J., 1957, *Medizinische Chemie*, III<sup>rd</sup> ed., Urban-Schwarzenberg, Berlin — Vienna, p. 468.
9. PETRACECK F., ZECHMEISTER L., 1956, Anal. Chem., **28**, 1484.
10. PREDA V., ȚIU ECATERINA, 1959, St. Cerc. Biol. (Cluj), **5**, 2, 315—318.
11. PULLMAN B., PULLMAN A., 1963, *Quantum Biochemistry*, Interscience Publ., New York—London.

12. SMITH S., 1958, *The Physiology of Fishes*, Acad. Press, New York — London, vol. I, p. 323.
13. TERNER CH., 1968, *Comp. Biochem. Physiol.*, **24**, 933—940.
14. — 1968, *Comp. Biochem. Physiol.*, **24**, 941—947.
15. WOOTTON I. D., 1964, *Microanalyses of Medical Biochemistry*, J. D. Churchill, London, p. 83—86.
16. YAMAGAMI K., MOHRI H., 1967, *The Biochemistry of Animal Development*, Acad. Press, New York — London, p. 372.

Received January 14, 1975

Centre of Biological Researches  
Iasi, str. Karl Marx 47  
and  
Pisciculture Station, Tarcău

## THE KARYOTYPE OF URODELE AMPHIBIAN *TRITURUS MONTANDONI*

BY

CORNELIA GEORMĂNEANU

The chromosomal analysis (the karyotype and the idiogram) was carried out in *Triturus montandoni* species, endemically disseminated throughout the Eastern Carpathian Mountains of Romania. The metaphases of testis obtained from ten adult males of this species were studied. The diploid chromosomes complement is  $2n = 24$  ( $n = 12$ ). The majority of the chromosomes are metacentric. The constant inequality of the homologues from the 8th pair and the small size of the chromosomes in the 12th pair were observed. The secondary constrictions were often seen on the various chromosomes. The bivalents of the spermatocytes in metaphase I are ring-like with terminal or subterminal chiasmata. In some of the metaphases I a pair of univalents is also present. In metaphase II the 12 chromosomes, very contracted, have their chromatids still united by the centromere.

*Triturus montandoni*, an urodele amphibian from the Salamandridae family, lives in the Carpathian Mountains of Romania, between 700 and 1900 m altitude. It is also mentioned in Poland, Czechoslovakia (the Tatra Mountains), and Hungary (Kormobanya). It does not form geographic races, achieving a so-called "Carpathian endemicity".

### MATERIAL AND METHOD

The ten adult males of the *Triturus montandoni* that have been analysed were collected between May and June 1971 in the Eastern Carpathians (the Ceahlău area). The animals received intraperitoneally an amount of 0.2 — 0.4 ml of a 0.5% colchicine solution. The testicles were extracted after three hours, introduced into a hypotonic solution of 0.5% potassium chloride and cut into very small fragments. The obtained suspension was set to rest for 30—45 minutes at room temperature. After centrifugation the supernatant was replaced by a fixative solution containing absolute methyl alcohol and glacial acetic acid (3:1), prepared extemporaneously. Three or four cold fixations were performed. The cell suspension obtained after the last fixation was pipetted on cold slides with the aid of a Pasteur pipette. The slides were flame-dried and stained with Giemsa.

The spermatogonic and the spermatocytic metaphases plates were examined with a 10 × eye-piece and a 90 × objective. To carry out the karyotype the diploid spermatogonial metaphases were photographed with a 60 × objective. After being cut out the chromosomes were paired according to the position of the centromere and not to the strict equality of their size. The chromosomes were measured and the results were tabulated. The idiogram was compiled on the basis of the average length of each chromosome and of the centromeric index.

### RESULTS

The diploid chromosomes number in *Triturus montandoni* is 24. The ratio of the arms ( $r$ ) and the centromeric index ( $i$ ) [7] have been taken as criteria for the chromosome type (table 1).



Table 1  
The nomenclature of chromosome type

Centromere position	Arm ratio (r)	Centromere index (i)*	Chromosome type	Symbol
Median	1.0—1.7	50.0—37.5	metacentric	m
Submedian	1.7—3.0	37.5—25.0	submetacentric	sm
Subterminal	3.0—7.0	25.0—12.5	subtelocentric	st
Terminal	7.0—∞	12.5—0.0	telocentric	t

$$* i = \frac{\text{length of the short arm}}{\text{total length of chromosome}} \times 100$$

Table 2

Chromosome measurements

Group	Chromosome number	Chromosome length (μ)*		Relative length ‰	Arm ratio l/s = r	Centromere index i %	Chromosome type
		Range	mean ± error				
I	1	13.7—18.8	16.3±0.40	116.1	1.09	47	m
	2	14.2—17.6	15.8±0.26	112.6	1.14	46	m
	3	13.3—16.6	15.1±0.24	107.6	1.17	46	m
	4	11.5—15.4	13.6±0.22	96.9	1.40	41	m
II	5	11.3—15.8	13.5±0.25	96.2	1.17	45	m
	6	11.2—15.0	12.9±0.23	91.9	1.30	43	m
	7	9.9—13.4	11.3±0.25	80.5	3.11	24	st
III	8	9.0—12.5	10.4±0.21	74.1	1.34	43	m
	9	7.6—10.0	9.0±0.17	64.1	1.42	40	m
	10	7.6—9.4	8.4±0.15	59.8	2.70	25	sm
	11	7.2—8.7	8.0±0.15	57.0	2.57	29	sm
	12	5.0—6.6	5.8±0.15	41.3	1.10	46	m

\* Total length of the haploid set is 140.3

Measurements carried out on chromosomes of spermatogonial metaphases of *Triturus montandoni* gave the values registered in table 2. On the basis of data presented in table 2 the idiogram was obtained (fig. 1).

The karyotype of this species includes 12 pairs of chromosomes arranged according to the decrease of their size (fig. 2).

Three arbitrary groups of 4 pairs each have been constituted.

**Group I** includes the longest chromosomes of the complement. The 4 pairs have metacentric chromosomes the average length of which varies between 13.6 and 16.3 microns. The chromosomes of the first pair are the longest (average length = 16.3 microns) and the most metacentric ( $r = 1.09$ ). Chromosomes of the second pair are slightly shorter (average length = 15.8 microns) and they are metacentric, too ( $r = 1.14$ ). Chromosomes of the 3rd pair have an average length of 15.1 microns and the arms ratio is 1.17. They are usually difficult to differentiate from pair 2. Chromosomes of pair 4 are significantly shorter than the other components of the group (average length = 13.6 microns) and, although they are metacentric, they have the highest difference between the length of their arms ( $r = 1.40$ ).

**Group II** includes pairs 5 to 8 of which 5, 6, and 8 are metacentric and the pair 7 is subtelocentric. The average length of chromosomes of group II varies between 10.4 and 13.5 microns. Chromosomes of pair 5 have a length of 13.5 microns, very near that of the chromosomes of pair 4, but they are more metacentric than the latter ( $r = 1.17$  as compared with  $r = 1.40$ ) and similar, with regard to the arms ratio, to the chromosomes of pair 3. The chromosomes of pair 6 are slightly smaller (average length = 12.9 microns) and have a median centromere ( $r = 1.30$ ). Chromosomes of pair 7 are very easily recognizable due to their average length (11.3 microns) and to the position of their centromere, which is subterminal ( $r = 3.11$ ). This is the only pair of subtelocentric chromosomes of the complement of *Triturus montandoni* species. In some metaphases the position of the centromere has values near the limit between submedian and subterminal. Length variations have also been observed between homologous of this pair. The chromosomes of pair 8 are the smallest metacentric chromosomes of this group. Their average length is 10.4 microns and  $r = 1.34$ . They have a centromeric index equal to that of chromosomes of pair 6 ( $i = 43\%$ ). A marked inequality of homologous chromosomes of this pair is very characteristic and constantly observed in all the metaphases examined, with a difference of average length of 0.89 microns and limits of 0.26 and 1.91 microns. In some of the metaphases one of the homologous was almost as long as the chromosomes of

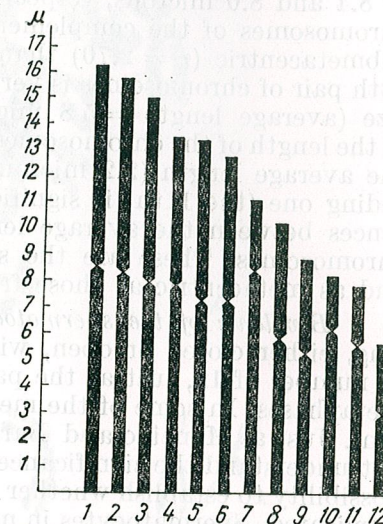


Fig. 1. — *Triturus montandoni* — idiogram.

pair 9. This is a particularity that should be stressed, possibly also in connection with the future studies on the sexual determination, taking into consideration the fact that our studies have been performed only in adult males of this species.

**Group III** includes pairs 9 to 12. The size of chromosomes in this group is smaller than in the preceding two. Pairs 9 and 12 have metacentric chromosomes. In the remaining ones the chromosomes are submetacentric (pairs 10 and 11). The chromosomes of pair 9 are of small size (average length = 9.0 microns) and the arms ratio ( $r$ ) is 1.42. Chromosomes of pair 10 and those of pair 11 are still smaller (average lengths = 8.4 and 8.0 microns, respectively). These are the only submetacentric chromosomes of the complement. The chromosomes of pair 10 are more submetacentric ( $r = 2.70$ ) than those of pair 11 ( $r = 2.57$ ). Finally the 12th pair of chromosomes is very easy to identify because of its very small size (average length = 5.8 microns), just a little more than one third of the length of the chromosomes from the first pair. The difference between the average length (2.2 microns) that sets aside this pair from the preceding one (the 11th) is significantly higher than the mean of the differences between the average lengths of all the other successive pairs of chromosomes. These are the smallest chromosomes of the complement and as metacentric as those from the first pair ( $r = 1.10$ ).

*Bivalents of the spermatocytes in metaphase I* have the form of a ring, either closed or open, with one or two chiasmata (fig. 3) and are in number of 12, just as the pairs of chromosomes in the spermatogonial metaphases. In some of the metaphases I a pair of univalents is also present. Just as Mancino and Barsacchi [9] with *Triturus italicus*, we could not understand the significance of the univalents because we had not the possibility to establish whether the same pair of chromosomes is constantly implicated. Spermatocytes in metaphase II displayed a number of 12 very contracted chromosomes following the action of colchicine (fig. 4) with thickened chromatides, still united by centromere. These 12 chromosomes can be arranged in 3 groups corresponding to those of spermatogonial mitoses.

#### DISCUSSIONS

The present paper reports on the normal cytogenetic aspects observed in the testicles of adult males from the *Triturus montandoni* species. No other cytogenetic analyses have been made up to the present bearing on this species. The chromosomal complement has  $2n = 24$  ( $n = 12$ ) chromosomes, as in other European species of Urodela such as: *Triturus cristatus*; *Triturus alpestris apuanus*; *Triturus vulgaris meridionalis*; *Triturus marmoratus*; *Pleurodeles waltlii*; *Triturus helveticus* and *Salamandra salamandra*. The secondary constrictions were often seen on the various chromosomes. The following observations have been made in other species of Urodela: frequent secondary constrictions on the various chromosomes in *Triturus italicus* [8]; subterminal constrictions on chromosomes no. 10 in the mitotic metaphases of adult tissues in *Triturus marmoratus* [11]; a subterminal constriction on the chromosome no. 1,

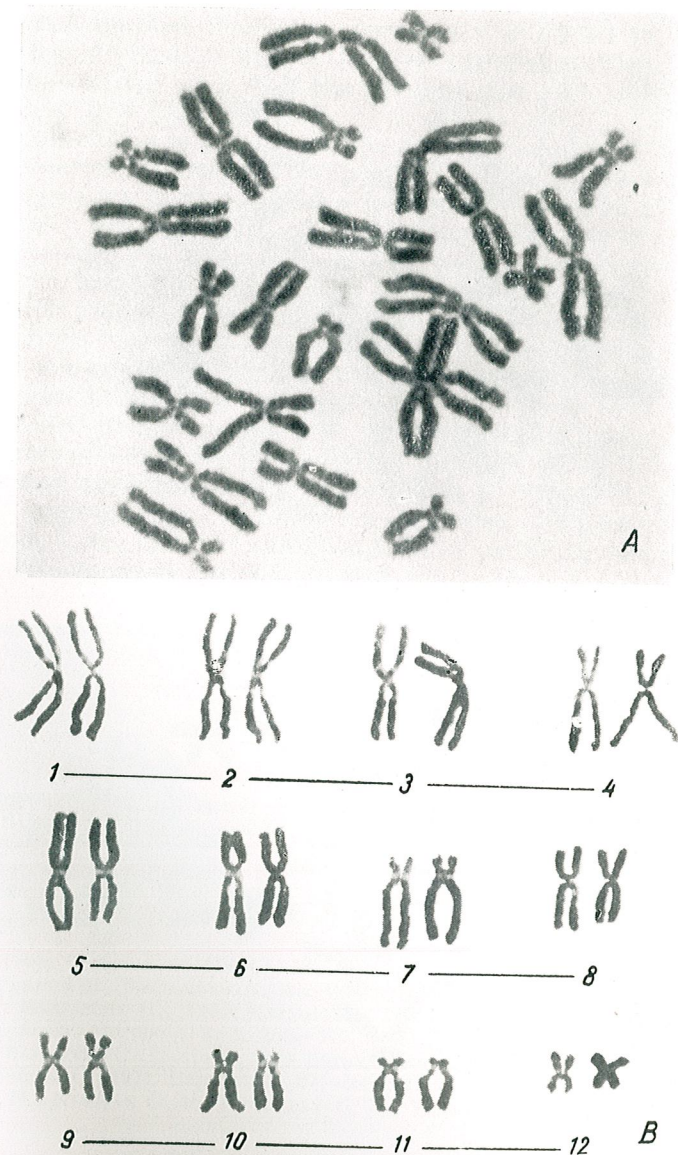


Fig. 2. — Male karyotype from testicle metaphase showing 24 chromosomes: A, metaphase; B, karyotype.

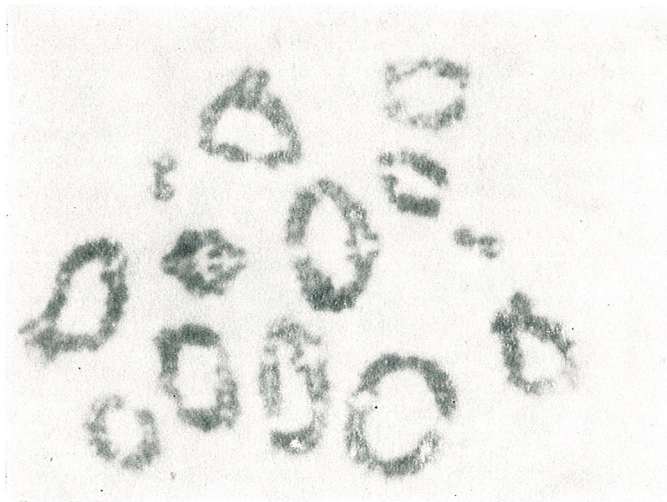


Fig. 3. — First meiotic metaphase showing 12 bivalents.

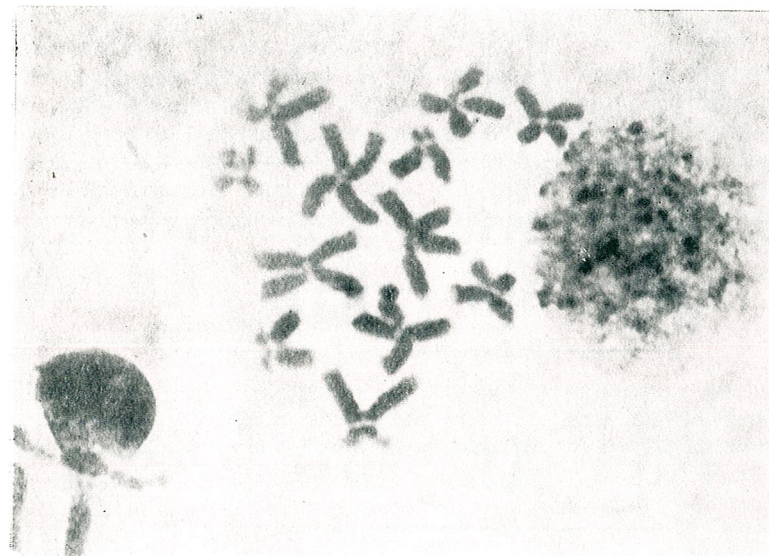


Fig. 4. — Second meiotic metaphase showing 12 dyads.

corresponding to chromosome no. 2 of group I of Callan, and on chromosome no. 11, an intercalary tract occasionally observed on the chromosome no. 5 and the short arm of chromosome no. 6 in *Triturus vulgaris meridionalis*. The marked inequality constantly observed in the homologues of pair 8 is stressed, as well as the great difference of length between the chromosomes of the pair with the smallest size (the 12th) and those of the preceding pair (the 11th).

For the obtention of the karyotype we have employed the decrease in size of the chromosomes and the position of the centromere. In this case the arrangement in three groups is arbitrary since in these groups there are included different types of chromosomes. Thus, in the first group all the chromosomes are metacentric, while in the second group besides the metacentric chromosomes (nos 5, 6, and 8) there is also the only subtelocentric chromosome of the complement (no. 7); group III is made up of two metacentric (nos 9 and 12) and two submetacentric (nos 10 and 11) chromosomes. We could discuss here the more logical approach of taking into account the position of the centromere and only as a secondary parameter the size of the chromosomes, for the grouping operation. In this way the karyotype could be presented as follows: group I — including the large metacentric chromosomes (pairs 1, 2, 3, 4, 5, and 6); group II — including the subtelocentric chromosome and two submetacentric chromosomes (pairs 7, 10, and 11) and group III — including the small-sized metacentric chromosomes (pairs 8, 9, and 12) of table 2.

*Acknowledgements.* We gratefully thank Dr. I. E. Fuhn (from the Institute of Biology, Bucharest) for the identifying of animal species utilized in this work.

#### REFERENCES

1. BARSACCHI G., BUSSOTTI L., MANCINO G., 1970, *Chromosoma (Berl.)*, **31**, 255—279.
2. BEÇAK W., BEÇAK M. L., SCHREIBER G., LAVALLE D., AMORIM F. O., 1970, *Experientia*, **26**, 204—206.
3. BREHM A., 1964, *Lumea animalelor*, Ed. științifică, București.
4. FUHN I.E., 1969, *Broaște, șerpi, șopîrle*, Ed. Științifică, București.
5. GALLIEN L., LABROUSSE M., LACROIX J.C., 1966, *C.R.Acad. Sci. Paris*, **263**, 1984—1987.
6. JAYLET A., 1966, *Chromosoma (Berl.)*, **18**, 79—87.
7. LEVAN A., FREDGA K., SANDBERG A. A., 1964, *Hereditas*, **52**, 201—220.
8. MANCINO G., BARSACCHI G., 1965, *Caryologia*, **18**, 4, 637—665.
9. — 1969, *Ann. Embr. Morphol.*, **2**, 3, 355—377.
10. MANCINO G., BARSACCHI G., NARDI I., 1969, *Chromosoma (Berl.)*, **26**, 365—387.
11. NARDI I., MANCINO G., 1971, *Experientia*, **27**, 424—427.
12. SPARROW A. H., NAUMAN C. H., DONNELLY G. M., WILLIS D. L., 1970, *Radiat. Res.*, **42**, 353—371.

Received November 7, 1974

The "Victor Babeș" Institute  
Laboratory of Cytogenetics  
Bucharest 35, Splaiul Independenței 99—101

# CHROMOSOME COMPLEMENT CHARACTERIZATION BY G-BANDING IN *GALLUS DOMESTICUS*

BY

MARGARETA MANOLACHE

The refinement of the banding techniques allowed the discovery and description of the chromosome bands pattern in many mammalian species. In this context, the homology between the chromosomes of related species became apparent.

In birds, the difficulties generally encountered with the analysis of the chromosome complement itself restricted the applicability of the banding techniques, which were by far less utilized than in mammalian cytogenetics. For comparative cytogenetic studies, however, the band pattern has to be recognized, at least for the species of economic value.

The present paper is concerned with a detailed description of chromosome bands distribution in *Gallus domesticus*, which seems to be a promising field of investigation.

## MATERIAL AND METHODS

Ten normal, one-day-old Cornish chicken, males and females, were used throughout this study; chromosome preparations were obtained from bone marrow by the routine technique described elsewhere [9]. To reveal the band pattern specific to each chromosome pair, either our modification of the Chiarelli trypsin method [10], or the technique described by Schnedl [15] and Chauduri et al. [6] were used. To apply the Giemsa banding technique [6] [15], chromosome preparations underwent a pretreatment for 90 sec. in a NaOH solution, followed by several washings in alcohol 70° and absolute alcohol; the preparations were then incubated for 24 hrs in Soerensen buffer, at 59°C, washed and stained with Giemsa solution. A detailed description of the trypsin technique is given elsewhere [10]; it should be noted however, that the effective exposure to trypsin was, in birds, twice that used in laboratory mammals, while the Giemsa staining time was of about 20–30 minutes.

The International Conference for Standardization in Human Genetics (1971) recommended for any technique revealing the band pattern by Giemsa staining the designation "G-techniques" and for the corresponding patterns the designation "G-bands".

The preparations displaying the most advantageous metaphase plates were photographed and examined by constructing the necessary karyotypes.

## RESULTS AND DISCUSSION

To get precise indications as to the band pattern, karyotypes constructed from preparations undergoing both banding treatments were concomitantly examined. The technique used appeared to give quite comparable results. The trypsin treatment results in clear-cut, well-defined bands, displaying even sub-bands within the main bands. However, the

chromosome swelling observed with this technique, which did not allow the location of centromeres, was removed only by the thermic denaturation procedure, followed by Giemsa staining.

The examination of the 20 karyotypes obtained with chromosomes undergoing the banding treatment, led to the following band pattern, as identified for 15 autosome pairs and the sex chromosomes:

*Pair 1*: submetacentric chromosomes.

*Short arm*: a dark band close to the centromere; a light band separating the proximal third part from a dark band covering the two distal thirds of the short arm.

*Long arm*: four dark bands, of similar breadth, separated from one another by narrow light bands; the trypsin treatment revealed two sub-bands in tandem within each of the dark bands.

*Pair 2*: submetacentric chromosomes.

*Short arm*: one well-marked dark band, located at about the middle of the arm.

*Long arm*: two well-defined dark bands in the median portion, separated from one another by a light band; two additional dark bands of slightly lower staining intensity, of which one is located close to the centromere, while the other at the telomere.

*Pair 3*: acrocentric chromosomes.

Four dark bands, evenly distributed along the chromosomes, the second proximal band showing higher staining intensity.

*Pair 4*: subtelocentric chromosomes.

Two dark bands separated by a light median band, the proximal one being larger and more intense.

*Pair 5*: acrocentric, occasionally short-armed chromosomes.

Two dark bands, separated by a light one.

*Pair 6*: acrocentric chromosomes.

Two dark bands, well-defined in the distal part, separated by a light band.

*Pair 7*: acrocentric chromosomes.

One dark band close to centromere; in the median part a slightly darker zone.

*Pair 8*: meta- or submetacentric chromosomes.

*Short arm*: one dark, distal band.

*Long arm*: one specific, well-defined dark band, located close to the centromere and separated by a light zone from a telomeric dark band.

*Pairs 9, 10, 11, 15*: one distinct, median dark band is characteristic of all these acrocentric chromosome pairs.

*Pair 12*: two dark bands, separated by a light zone are very characteristic of this pair.

*Pair 13*: relatively uniform staining, with no apparent band.

*Pair 14*: subtelocentric chromosomes, occasionally showing one dark band located near the telomere.

*Chromosome Z*: metacentric.

*Short arm*: an intense dark band, generally with no sub-band.

*Long arm*: two dark bands, displaying a characteristic median light zone.

*Chromosome W*: submetacentric.

After thermic denaturation and Giemsa staining, chromosome W showed a zone of higher staining intensity, probably a heterochromatic one, covering the short arm, which makes it easily recognizable in treated metaphase plates (figs. 2 and 3). The long arm is uniformly stained, with no apparent band.

To comply with the chromosome size criterion, as well as with the previous karyotype reports in *Gallus* [1-3] [13] [14] [19], the homogametic sex chromosomes are considered as the 5th pair of the karyotype.

The analysis of the band pattern obtained by trypsinization, as well as by thermic denaturation followed by Giemsa staining, allowed the identification and thorough description of 15 autosomal pairs and sex chromosomes. Due to the difficulties imposed by the constitution itself of the chromosome complement in birds, the banding studies in birds were only occasionally approached (see Nilsson [12] for detailed references concerning the banding studies). In our knowledge, one single description of the band pattern in *Gallus domesticus*, based upon fluorescent staining [16] exists in the literature, which is unfortunately restricted to the 6 macrochromosome pairs. A certain agreement is however apparent between the fluorescences pattern and the Giemsa one, as far as the most characteristic and intense bands are concerned. Nevertheless, our plates allowed a better recognition and characterization of the bands specific to a given chromosome, which, in turn, led to a detailed description of 16 chromosome pairs.

A description and a diagrammatic representation of the pattern obtained by trypsinization for 6 pairs of the chromosome complement in *Gallus domesticus* were recently reported in our country [11]. As our results are in partial disagreement with the above ones, several explanations are necessary: as already mentioned, the trypsinization, in addition to its well-known advantages, causes certain troubles, too, depending mainly upon the conditions and the duration of the treatment; therefore, with advancing degradation, homologous chromosomes displaying different contraction might show apparently different band patterns. Our results, indicating an identical band pattern for homologous chromosomes of pair 1 in all of the metaphase plates so far examined, do not agree with the statement [11] that homologous chromosomes in pair 1 would display a partly heterogeneous band distribution.

In spite of the hypotheses proposed for the nature of the bands, their very origin and real state still remain obscure. One of these hypotheses assumes that while the constitutive heterochromatin blocks generally located close to the centromere are zones of highly repetitive DNA [8], the G-bands spread throughout the genome are families of sequences with a lower number of copies [4] [20].

Drets and Shaw [5] assume that unstained, intermediary zones might consist in unique nucleotide sequences. As to the constitutive heterochromatin distribution in the avian genome, in our knowledge only two reports exist in the literature, one of which being concerned with the heterochromatic nature of chromosome W [17], the other demonstrating the occurrence of heterochromatin in centromeres of most micro-

chromosomes in *Coturnix coturnix japonica* [7]. In this context, further investigation of the heterochromatic pattern in the genome of different bird species is required. At any rate, a detailed and thorough description of the G-bands pattern in a species of high economic value, such as *Gallus domesticus*, seems to be of great interest for further cytogenetic studies.

#### CONCLUSIONS

1. The examination of the band pattern obtained either by trypsinization or by thermic denaturation followed by Giemsa staining allowed the identification and description of 15 autosome pairs and of the sex chromosomes in *Gallus domesticus*.

2. The metacentric chromosome Z displays a rather characteristic band pattern. Chromosome W (in the heterogametic sex) shows an intensely stained, probably heterochromatic zone, which makes it easily recognizable in treated metaphase plates.

Thanks are due to Professor Nicolae Teodoreanu, Ph. D., corresponding member of the Academy of the Socialist Republic of Romania, for valuable discussion and supply of literature references, and to Dr. Ion Voiculescu, from the Department of Cell Biology and Genetics, for the highly qualified advice and valuable criticism.

#### REFERENCES

1. BARJAKTAROVIC N., GARZICIC B., 1972, *Genetika*, **4**, 1, 25-34.
2. BENIRSCHKE K., HSU T. C., 1971, *Chromosome Atlas: Fish, Amphibians, Reptiles and Birds*, **1**, Folio AV-6.
3. BIANCHI N. O., MOLINA J. O., 1967, *Chromosoma*, **21**, 387-397.
4. BRITTON R. J., KOHNE D. E., 1969, *Handbook of Molecular Cytology*, ed. by A. LIMA-DE FARIA, North-Holland Publishing Co., Amsterdam, 21-51.
5. DRETS E. M., SHAW W. M., 1971, *Proc. nat. Acad. Sci. USA*, **68**, 9, 2073-2077.
6. CHAUDURI J. P., VOGEL W., VOICULESCU I., WOLF U., 1971, *Humangenetik*, **14**, 83-84.
7. COMINGS E. D., MATTOCCIA E., 1972, *Exp. Cell. Res.*, **71**, 113-131.
8. FLAMM W. G., 1974, *Int. Rev. Cytol.*
9. MANOLACHE M., 1972, *Lucr. primei Conf. Naț. de Genet. Animală*, 343-347.
10. — 1975, *St. Cerc. Biol. Seria Biol. anim.*, **27**, 4.
11. MATEESCU V., 1973, *St. Cerc. Biol. Seria Zoologie*, **25**, 6, 575-579.
12. NILSSON B., 1973, *Hereditas*, **73**, 259-270.
13. OPRESCU S., CONSTANTINESCU O., VOICULESCU I., 1966, *St. Cerc. Biol. Seria Zoologie*, **18**, 3, 281-284.
14. OWEN J. J. T., 1965, *Chromosoma*, **16**, 601-608.
15. SCHNEDL W., 1971, *Nature New Biol.*, **233**, 93-94.
16. STAHL A., VAGNER-CAPODANO M. A., 1972, *C.R. Acad. Sci.*, **275 D**, 2367-2370.
17. STEFOS K., ARRIGHI F., 1971, *Exp. Cell Biol.*, **68**, 1, 228-231.
18. STEFOS K., 1972, Abstracts Twelfth Annual Meeting American Society for Cell Biology, 249 a.
19. TAKAGI N., MAKINO S., 1966, *Caryologia*, **19**, 4, 443-455.
20. WARING M., BRITTON J. R., 1966, *Science*, **154**, 791.

Received April 29, 1974

Institute of Biological Sciences  
Department of Cell Biology and Genetics  
Bucharest 17, Splaiul Independenței 296

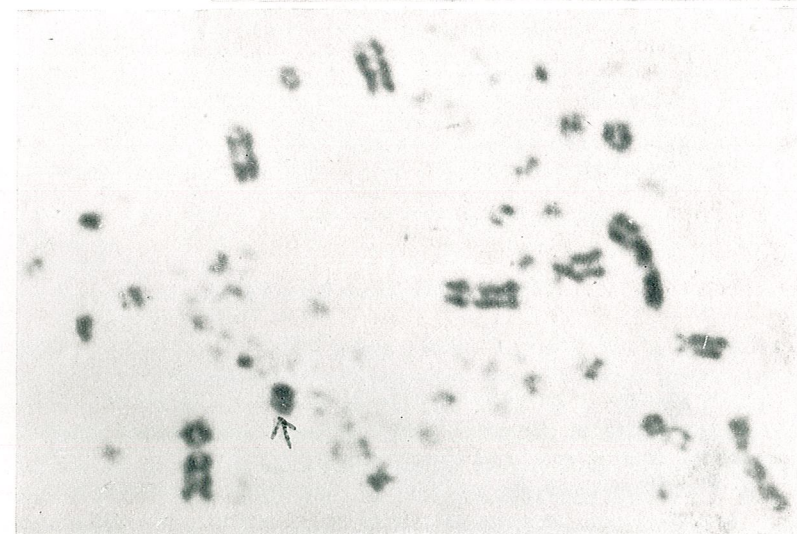
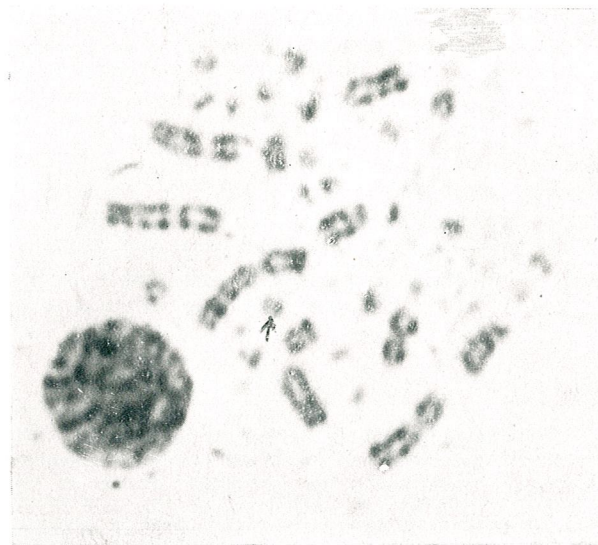
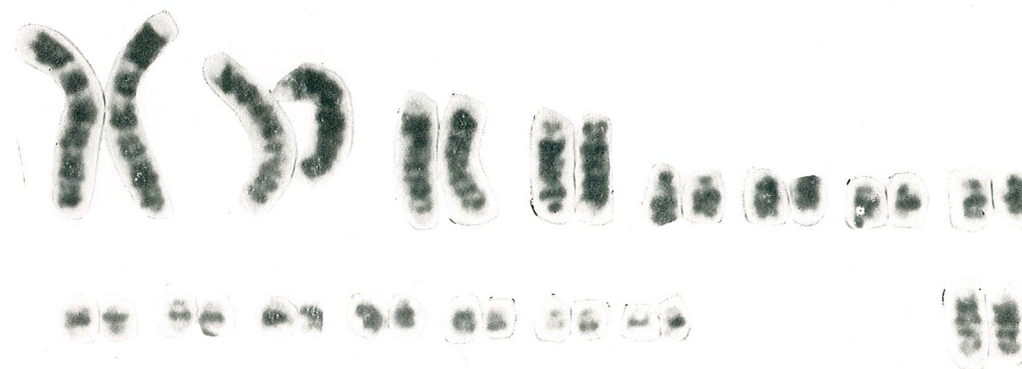


PLATE I. Fig. 1. — The characteristic band pattern of the autosomes (1-15) and of the sex chromosomes, as revealed by trypsinization  
Figs 2. and 3. — Metaphase plates which have undergone the Giemsa-bandig treatment.  
Note chromosome W (arrow).

CYCLE D'ACTIVITÉ CHEZ LA TORTUE TERRESTRE  
(*TESTUDO HERMANNI HERMANNI* GMEL.)

PAR

MIHAI CRUCE et ION RĂDUCAN

The work shows the seasonal activity cycle of *Testudo hermanni* G. and analyses the structure of a population of the acacia forest on the Sișești hills (Mehedinți), by onset and exit of hibernation as well as the modifications of the population density under the influence of some climatic factors.

Il y a peu de recherches dans la littérature concernant l'écologie de la tortue terrestre [1] [2] [5-7]. Dans cet ouvrage, nous présentons le cycle d'activité nictémérale et saisonnière chez *Testudo h. hermanni* Gmel., en analysant la structure d'une population au début et à l'issue de l'hibernation, ainsi que la modification de la densité de la population sous l'influence de certains facteurs climatiques.

MATÉRIEL ET MÉTHODES

Les observations ont été effectuées sur un nombre de 285 exemplaires de *T. hermanni* dans la période mars - novembre 1973-1974, sur les collines de Sișești (départ. Mehedinți). Les tortues capturées ont été doublement marquées: les marginales du côté gauche et du côté droit de la carapace furent d'abord sectionnées avec une scie fine, ensuite nous avons appliqué sur ces mêmes marginales des taches circulaires de peinture. Après avoir été marquées, les tortues ont été mises en liberté et leur activité observée à l'aide d'un binocle, à une distance de 10-15 m. Chaque fois qu'il était nécessaire, les individus ont été recapturés. On a dessiné une esquisse de la station étudiée (2 ha), où l'on marquait à l'occasion des observations hebdomadaires, le nombre et le sexe de chaque individu, la direction de son déplacement, l'heure où les observations étaient faites. L'âge a été apprécié d'après le nombre des anneaux de la plaque abdominale droite ainsi que d'après la longueur de chaque anneau [8]. La densité fut appréciée d'après le nombre total des individus du secteur étudié ou selon le nombre d'individus rencontrés sur la diagonale (= le transect) du secteur. Les données concernant la température de l'air, la  $t^{\circ}$  superficielle du sol, à 5 et à 20 cm profondeur du sol, l'humidité relative de l'air, furent notées à chaque visite de la zone d'étude.

RÉSULTATS ET DISCUSSIONS

Les tortues sortent de l'hibernation à partir de la troisième décennie de mars (fig. 1). Les mâles et les femelles sexuellement mûrs ont fait leur apparition à la surface du sol le 28 III 1973 et le 24 III 1974. A cette époque, dans notre zone d'étude, nous n'avons observé jamais plus de 6 exemplaires. A la sortie de l'hibernacle, le corps a une position presque verticale ou légèrement oblique, la tête est orientée vers le S-E. La sortie de l'hibernacle dure entre 1-2 jours. Dans leur premier jour d'activité,

on reconnaît facilement les individus d'après leur carapace dont la partie antérieure est maculée de sable sec, tandis que celle de la partie postérieure est encore humide. Leurs premiers déplacements sont courts (10–15 m) vers les espaces découverts où elles restent 1–2 heures au soleil.

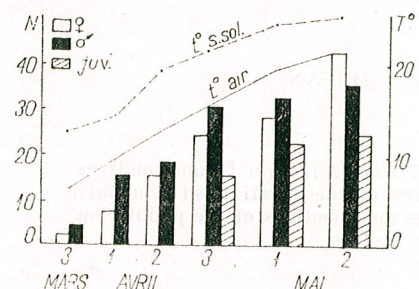


Fig. 1. — Structure d'une population de *T. hermanni* à la sortie de l'hibernation (1974).

nous constatons que leur activité se déroule entre 11–14 h, mais un seul individu n'est en activité que tout au plus 1–2 h par jour. Pendant les deux premières décades d'avril, quand la sortie de l'hibernation continue,

Pendant l'exposition au soleil, le plastron repose directement au sol tandis que la tête, la queue et les membres sont allongés le long de la carapace. Si les conditions sont défavorables — diminution de la température de la surface du sol au dessous de 10°C, accompagnée de l'augmentation de l'humidité relative de l'air de plus de 85% — les tortues regagnent rapidement leurs refuges d'hiver, où elles demeurent 2 ou 3 jours.

En examinant le cycle diurne des adultes sortis de l'hibernation (fig. 2)

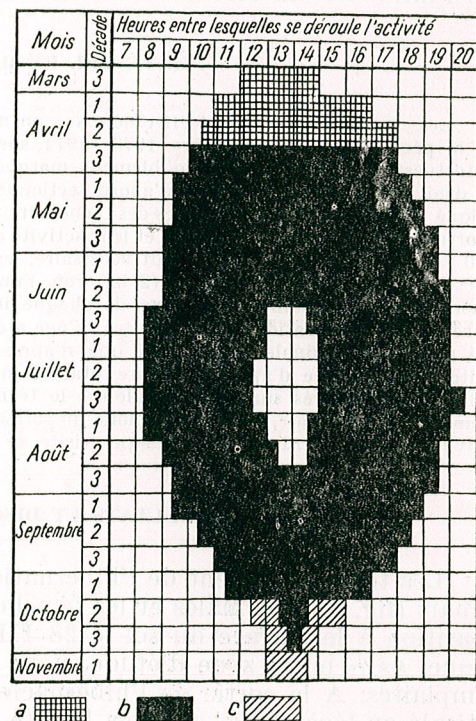


Fig. 2. — Le cycle d'activité diurne et saisonnier chez *T. hermanni*.

a = en activité — seulement les mâles et les femelles  
b = en activité — toute la population  
c = en activité — seulement les jeunes

L'activité est de 6 heures par jour en moyenne, la densité des tortues étant 1 exemplaire par 50 m. Les abris diurnes et nocturnes sont identiques aux hibernacles.

Les jeunes entrent en activité beaucoup plus tard, dans la dernière décade d'avril, quand les températures de l'air et de la surface du sol ne tombent pas sous 15°C. Dans les conditions du microclimat de la forêt d'acacias sur les collines de Sîșești, la 3<sup>e</sup> décade d'avril représente la période où toute la population est active, la densité étant de 1 exemplaire pour 30 m de transect. Les individus en copulation se rencontrent fréquemment.

L'activité est particulièrement intense au cours de la première et de la seconde décade de mai. Les déplacements pour trouver la nourriture ont un grand rayon d'action — parfois même 500 m. L'activité des tortues commence à 8 h 30, la rentrée dans les abris de nuit a lieu à 18–18 h 30. Les femelles sont les plus actives, ensuite les mâles. Les jeunes — surtout ceux éclos l'année précédente — quittent leurs abris seulement après 10 h 30 et sont en activité jusqu'à 18 h 30. Nous signalons que les abris pour la nuit ne sont pas permanents. Parfois une tortue de grande taille est obligée d'élargir un abri trop petit. Dans ce but, elle creuse l'abri avec les membres antérieurs, de droite à gauche, tandis qu'avec les membres postérieurs et la carapace elle l'agrandit légèrement, en exécutant une rotation de 90°. D'habitude, les abris pour la nuit ont une exposition S–E et les individus qui y habitent entrent plus tôt en activité; ou bien S–O, les individus qui y habitent étant les derniers à cesser leur activité.

Dans la dernière décade de mai et la première décade de juin, simultanément avec la floraison des acacias, les femelles commencent à déposer leurs pontes. On observe dans l'intervalle d'une semaine, le groupement des pontes de 6–10, dans des emplacements favorables à la déposition des pontes, à savoir sur les pentes à exposition sud, dont le sol moins tassé est sablonneux ou argileux. C'est pour les femelles la période d'activité maximum (10 heures), pendant laquelle les dépenses d'énergie sont très grandes. Rien que le creusement du nid dure 45 minutes et la déposition de la ponte 30 minutes. Une femelle est obligée de creuser non seulement un seul mais plusieurs nids, à cause des obstacles imprévisibles (racines trop épaisses, gravier, etc.). La densité des individus est la plus grande entre 11–12 et 16–17 h.

Après la seconde décade de juin, quand la majorité des femelles ont déposé leur ponte, on constate une migration de la population le long des vallons vers le village. Les déplacements se font sur 1–1,5 km et sont déterminés principalement par la nourriture (cosses d'haricots, mirabelles, etc.) que les tortues trouvent dans les jardins des paysans. Les déplacements des jeunes ne dépassent pas 250–300 m, en restant à proximité des emplacements d'hibernation, où la réduction de la densité — 1 individu par 60 m — et implicitement celle de la concurrence, font que la nourriture disponible soit en quantité suffisante. L'activité diurne des tortues se réduit à 8–9 heures entre la 3<sup>e</sup> décade de juin et la 3<sup>e</sup> décade de juillet, à cause du repos de midi. Ce repos, qui ne dépasse pas 2 heures pour un individu, n'est total que dans les lieux découverts. Pendant ce temps, les individus de petite taille, surtout les jeunes, sont actifs à l'ombre, sous les taillis de mûriers ou les touffes de fougères. Maintenant, les abris préférés ne sont plus ceux creusés dans les rives, mais les abris superficiels, construits rapidement par l'introduction de la carapace sous les branches sèches et les feuilles mortes.



A la fin de juillet se produit la migration inverse des individus vers le sommet des collines. Le déplacement est très lent, car il est lié aux mûriers, qui mûrissent plus rapidement au pied de la colline que vers les plateaux du sommet. L'ascension des tortues ne se fait pas en direct, mais suivant les courbes à niveau. En août, la majorité des tortues sont de retour sur le sommet des collines. L'activité comprend encore 8-9 heures par jour, car dans la 3<sup>e</sup> décennie d'août et au début de septembre le repos de midi disparaît, les réserves de graisse sont en cours d'accumulation

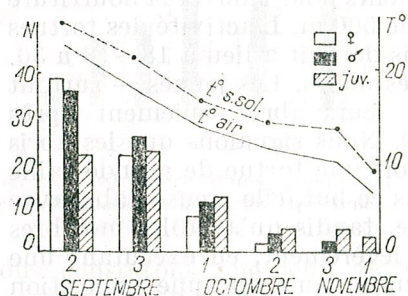


Fig. 3. — Structure d'une population de *T. hermanni* au début de l'hivernation (1974).

chez les adultes et les jeunes se trouvent en pleine croissance [3] [4]. Dans la même période commence aussi l'éclosion des pontes (29.VIII.1973; 5.IX.1974) l'apparition des jeunes nouveaux-nés explique l'augmentation de la densité — 1 individu par 10 m de transect.

L'automne commence dans la deuxième décennie de septembre, en même temps que la baisse de la température et la hausse de l'humidité relative de l'air. Les tortues se préparent à l'hivernation, ce qui se reflète dans la modification de la structure de la population (fig. 3). En même temps, la durée de l'activité diurne se réduit de 6 heures (fin septembre) à 2 heures (fin octobre). En 1973, les premiers individus sont entrés en hibernation le 12 IX, en 1974 seulement le 21 IX. On constate que les femelles entrent plus vite que les mâles et les jeunes en hibernation. La majorité des individus de la population entrent en hibernation au cours de la première décennie d'octobre (1974). Les derniers individus actifs — 3 jeunes — ont été observés le 5.XI.1974. Avant l'hivernation, les tortues s'exposent au soleil et creusent pendant 2 jours un abri d'hivernation.

Les hibernacles sont creusés dans les pentes à sol peu tassé, dont la surface est couverte par des feuilles mortes, des rameaux secs et des fougères. En plus, ces abris sont protégés par les tiges à piquants des mûriers. Ils ne sont pas creusés de haut en bas, mais de biais. Dans certains endroits, les hibernacles sont concentrés, parfois 3 par m<sup>2</sup>, parfois 2, l'un sous l'autre. Un observateur expérimenté peut facilement dépister les abris d'hivernage d'après le petit monticule qu'ils forment à la surface, sans que la couche de feuilles mortes ou le sol paraissent dérangés.

#### DISCUSSIONS

1. La fin de l'hivernation chez *Testudo hermanni hermanni* Gmel. commence dans la 3<sup>e</sup> décennie de mars et continue jusque dans la 3<sup>e</sup> décennie d'avril, quand la majorité des individus de la population sont actifs. La durée de l'activité diurne augmente de 3 à 7 heures. Les jeunes sont les derniers à sortir de l'hivernation.

2. Vers la fin du mois de mai et dans la première décennie de juin, quand commence la ponte, l'activité devient plus intense, arrivant jusqu'à 10 heures par jour à la mi-juin.

3. La migration des tortues le long des vallons, des collines vers le village, qui se produit après la 2<sup>e</sup> décennie de juin, ainsi que la migration en sens contraire qui a lieu fin juillet—début d'août, sont déterminées par la variation saisonnière de la nourriture.

4. L'entrée en hibernation commence dans la 2<sup>e</sup> décennie de septembre et continue jusqu'à la fin de septembre — début d'octobre, quand la majorité des individus ont occupé les hibernacles. La durée de l'activité diurne est réduite de 6 à 2 heures. Les derniers individus actifs (les jeunes) ont été observés le 5.XI.1974. La distribution des hibernacles est groupée.

5. Le preferendum thermique de *Testudo h. hermanni* Gmel. se trouve entre 22-28°C (t° de l'air) et 28-32°C (t° de la surface du sol); l'humidité optimum est 55-75%.

#### BIBLIOGRAPHIE

- BĂCESCU M., 1937, Ann. Sci. Univ. Iassy, 24, 2, 1-10.
- BRATTSTROM B. H., 1965, Am. Midl. Nat., 73, 376-422.
- CARPENTER C. C., 1957, Copeia, 4, 278-282.
- CARR A., GOODMAN D., 1970, Copeia, 4, 783-786.
- CRUCE M., ȘERBAN M., 1970, St. și cerc. Subcom. mon. nat. Dolj, 179-184.
- FUHN I. E., 1956, Ocrotirea naturii, 2, 178-180.
- FUHN I. E., VANCEA Șt., 1971, Reptilia. Fauna R.P.R., Ed. Acad. R.P.E., București.
- SEXTON O. J., 1959, Ecology, 716-718.

Reçu le 23 décembre 1974

Université de Craiova  
Chaire de Biologie  
Craiova, Al. I. Cuza 13

MIRCEA TUFESCU, Populațiile de foraminifere din apele litorale românești (Les populations de foraminifères des eaux littorales roumaines), Ed. Academiei, București, 1974, 176 p., 70 fig.

Le volume comprend les résultats de la recherche des populations de foraminifères des eaux roumaines de la Mer Noire, jusqu'à une profondeur de 20 m, du delta maritime du Danube, ainsi que de la série de lacs littoraux et de lagunes.

Le chapitre I présente l'historique des recherches sur les foraminifères en général et dans le Bassin Pontique, les méthodes utilisées, ainsi que 5 tableaux avec les résultats des analyses quantitatives et qualitatives des prélèvements.

Le chapitre II traite des populations locales de foraminifères et de leur répartition. Parmi les 17 espèces identifiées et incluses dans une clef de détermination, 3 espèces sont nouvelles pour la Mer Noire et seulement 5 espèces sont fréquentes dans les biotopes étudiés. On remarque un programme inédit pour aborder l'étude d'une population en vue de conclusions synthétiques.

Les deux chapitres qui suivent concernent l'organisation des populations étudiées : structure phénotypique et écologique (chap. III), fonctions autoréproductive et évolutive (chap. IV).

Le dernier chapitre présente l'influence des facteurs de milieu sur l'organisation des populations de foraminifères, en soulignant le rôle de la salinité, le principal facteur limitant. À la fin on trouve des renseignements sur la dynamique numérique des principales populations liées au faciès sablonneux.

Le travail bien conçu et écrit, richement illustré, apporte une étude complexe des populations d'un groupe d'animaux de la Mer Noire qui était encore insuffisamment connu. Ce livre s'adresse aux biologistes en leur offrant des matériaux en rapport avec certains aspects théoriques de l'espèce, de l'écologie et de l'évolution dans le domaine marin. Les foraminifères sont également importants comme paléoindicateurs pour les gisements pétrolifères et comme indicateurs de certains aspects du milieu marin actuel.

Stefan Negrea

# REVUE ROUMAINE DE BIOLOGIE

SÉRIE DE BIOLOGIE ANIMALE

TOME 20

1975

## INDEX ALPHABÉTIQUE

	No.	Page.
ABRAHAM AL. D, and MARIA BORȘA, Action of steroid hormones on the <i>de novo</i> synthesis of aminotransferases in the thymus of white rat . . . . .	2	135
APOSTOL GH. v. MATEI-VLĂDESCU CONSTANȚA . . . . .	2	121
BAUCHOT ROLAND, MARIA CALOIANU-IORDĂCHEL, MONIQUE DIAGNE et JEAN-MARC RIDET, L'encéphale d' <i>Acipenser ruthenus</i> Linné 1758 (Pisces, Chondrostei, Acipenseridae). Étude quantitative préliminaire . . . . .	4	249
BĂCESCU MIHAI, Archaic species of Tanaidacea from the Tanzanian waters with the description of a new genus, <i>Tanzanapseudes</i> . . . . .	2	81
BOLDOR ȘTEFANIA v. CHIRIAC ELENA . . . . .	4	241
BORȘA MARIA v. ABRAHAM AL. D. . . . .	2	135
CALOIANU-IORDĂCHEL MARIA v. BAUCHOT ROLAND . . . . .	4	249
CADARIU MARIA, Cerebral ganglia regeneration in <i>Lumbricus terrestris</i> L. . . . .	2	101
CHERA ELENA v. JITARIU MATILDA . . . . .	4	269
CHIRIAC ELENA, ȘTEFANIA BOLDOR et ELENA VĂDINEANU, Un cas d'hyperparasitisme chez la perche ( <i>Perca fluviatilis</i> L.) . . . . .	4	241
CRUCE MIHAI et ION RĂDUCAN, Cycle d'activité chez la tortue terrestre ( <i>Testudo hermanni hermanni</i> Gmel.) . . . . .	4	285
DIAGNE MONIQUE v. BAUCHOT ROLAND . . . . .	4	249
DUCA ECATERINA v. JITARIU MATILDA . . . . .	4	269
FEIDER Z., Une nouvelle larve de Trombidia: <i>Atractothromboides danubialis</i> n.g., n.sp. . . . .	4	223
GEORMĂNEANU CORNELIA, The karyotype of urodele amphibian <i>Triturus montandoni</i> . . . . .	4	275

	No.	Page.
GOPALAKRISHNA A. and K. B. KARIM, Development of the foetal membranes in the Indian leaf-nosed bat, <i>Hipposideros fulvus fulvus</i> (Gray) II-Morphogenesis of the foetal membranes and placentation . . . . .	4	257
GUȚU MODEST, <i>Carpoapseudes bacescui</i> n.sp. and <i>C. menziesi</i> n.sp. (Crustacea-Tanaidacea) from the Peru-Chile trench . . . . .	2	93
HONCIUC VIORICA v. I. P. PETCU . . . . .	4	229
IONESCU ELISABETA v. CONSTANȚA MATEI-VLĂDESCU . . . . .	2	121
JITARIU MATILDA, ELENA CHERA, ECATERINA DUCA, GABRIELA LINCK, PINCU ROTIMBERG and ISTVÁN SZILAGYI, Lipido-carotenoid metabolism in <i>Salmo gairdneri</i> during embryogenesis . . . . .	4	269
KARIM K. B. v. A. GOPALAKRISHNA . . . . .	4	257
KRONELD ROLF, A working model for the synchronization of light in phase shifting burbot, <i>Lota lota</i> L. (Pisces, Gadidae) at the polar circle . . . . .	2	147
LINCK GABRIELA v. MATILDA JITARIU . . . . .	4	269
MADAR J., NINA ȘILDAN and EUGEN A. PORA, Age-dependent anti-insulin effect of hydrocortisone hemisuccinate upon the <i>in vitro</i> glucose uptake of rat epididymal adipose tissue . . . . .	2	131
MANOLACHE MARGARETA, Chromosome complement characterization by G-banding in <i>Gallus domesticus</i> . . . . .	4	281
MATEI-VLĂDESCU CONSTANȚA, GH. APOSTOL, VALERIA RĂDĂCEANU-ARICESCU and ELISABETA IONESCU, Ponderal modifications in chickens with hypothalamic lesions induced by L monosodium glutamate . . . . .	2	121
MEȘTER LOTUS et CĂLIN TESIO, Recherches systématiques basées sur l'électrophorèse, chez certains Blenniidae (Pisces) de la mer Noire . . . . .	2	113
NICÔLAU GRAZIELLA et V. TEODORU, Les variations saisonnières de la fonction thyroïdienne . . . . .	2	141
NICULESCU E. V., Les critères de l'espèce. Le critère morphologique . . . . .	2	73
PETCU IONEL I. and VIORICA HONCIUC, Contributions to the study of the female extern genital complex in Ophionidae (Hym. Ichneumonidae) . . . . .	4	229
PORA E. A. v. J. MADAR . . . . .	2	131
PRUNESCU C. v. PRUNESCU PAULA . . . . .	2	107
PRUNESCU PAULA and C. PRUNESCU, Pigment-bearing multinucleated cells in the liver of malarian rodents during recovery . . . . .	2	107
RĂDĂCEANU-ARICESCU VALERIA v. CONSTANȚA MATEI-VLĂDESCU . . . . .	2	121
RĂDUCAN ION v. MIHAI CRUCE . . . . .	4	285
RIDET JEAN-MARC v. ROLAND BAUCHOT . . . . .	4	249
ROTIMBERG PINCU v. MATILDA JITARIU . . . . .	4	269
SORESCU CONSTANTINA, Osteological studies in some Cyprinid fishes in relation to their phylogeny (Pisces, Cyprinidae) . . . . .	4	237
SZILAGYI ISTVÁN v. MATILDA JITARIU . . . . .	4	269

	No	Page
ȘILDAN NINA v. J. MADAR . . . . .	2	131
TEODORU V. v. GRAZIELLA NICOLAU . . . . .	2	141
TESIO CĂLIN, L'apport de l'électrophorèse en gel d'amidon à la systématique du genre <i>Mesocricetus</i> Nehring (Rodentia, Cricetidae) . . . . .	2	117
TESIO CĂLIN v. LOTUS MEȘTER . . . . .	2	113
TRACIU ELENA, Les glandes séricigènes chez certaines araignées « Haplogynes » . . . . .	4	245
VĂDINEANU ELENA, v. ELENA CHIRIAC . . . . .	4	241